

Optimization of Heterogeneous Wireless Networks with Massive MIMO

by

SHITONG YUAN

Presented to the Faculty of the Graduate School of  
The University of Texas at Arlington in Partial Fulfillment  
of the Requirements  
for the Degree of

DOCTOR OF PHILOSOPHY

THE UNIVERSITY OF TEXAS AT ARLINGTON

April 2016

Copyright © by SHITONG YUAN 2016

All Rights Reserved

To my father Zhengxi Yuan and my mother Hongcheng Sun  
who set the example and who made me who I am.

## ACKNOWLEDGEMENTS

I would like to thank my supervising professor Dr. Qilian Liang for constantly motivating and encouraging me, and also for his invaluable advice during the course of my doctoral studies. I wish to thank my academic advisers Dr. Jonathan Bredow, Dr. Ioannis D. Schizas, Dr. Xuejing Gao and Dr. Yuze Sun for their interest in my research and for taking time to serve in my dissertation committee.

I would also like to extend my appreciation to Dr. Ji Wu, Dr. Xin Wang, Dr. Junjie Chen, Dr. Zhuo Li and Dr. Qiong Wu for their help when I first time came to USA and for the helpful discussions and invaluable comments. I wish to thank Na Wu, Hao Liang, Longwei Wang and Ganlin Zhao for their support and encouragement. I wish also to thank Broadcom Corp. to offer me an internship opportunity during my doctoral studies and also Murali Damiseti, Punit Awatramani, Kamlesh Rath and Dong Zheng for their help and encourage when I working in the company. I wish also to thank who for taking the time to critically evaluate this manuscript.

I am grateful to all the teachers who taught me during the years I spent in school, first in P.R.China finally in the Unites States.

Finally, I would like to express my deep gratitude to my parents who have encouraged and inspired me and sponsored my undergraduate and graduate studies. I am extremely fortunate to be so blessed. I am also extremely grateful to my wife

for her sacrifice, encouragement and patience. I also thank several of my friends who have helped me throughout my career.

April, 2016

## ABSTRACT

Optimization of Heterogeneous Wireless Networks with Massive MIMO

SHITONG YUAN, Ph.D.

The University of Texas at Arlington, 2016

Supervising Professor: Qilian Liang

In the next generation wireless communication system, multi-layers of Heterogeneous Networks (HetNets) are required to provide high efficiency bandwidth usage and high speed data throughput. Users distribution and their quality of service (QoS) request are random, and the number of users may vary through the time. In order to deal with this problem, this thesis builds two games models to optimize the resource allocation corresponding to different situations in the first chapter. The spectrum efficiency is analyzed and compared between two games. By playing those games, cells can serve more users inside one cell, and all users are fair to share the bandwidth according to their requests and locations. The whole system becomes more flexible and performance has been enhanced.

Further, we consider massive MIMO in a two-layer Heterogeneous Cellular Network. The system has a large self-interference and co-channel interference due to full-duplex mode operation. A two-layer HetNets system model is proposed with Massive MIMO in Full-duplex mode. By using Game Theory, an optimized system sum-rate is achieved. We investigate the potential sum-rate before and after the optimization

under the power constraints(both single user power constraint and power constraint at base station). It is shown that after the game theoretical method applied, the system performed a very good access scheduling compare to random access. Compared to non-optimized model, game theoretical method can achieve higher sum-rate.

A novel antenna placement scheme at base station is proposed based on 2-D nested array. We utilize the difference co-array to model and generate all antennas(virtual antennas) in the covariance matrix of channel(virtual channel) coefficients. We also model a Massive MIMO antenna system with nested configuration and list all mathematical procedures to calculate its performance with achievable rate. A zero forcing detector is applied to this Massive MIMO system and the spectral efficiency is given at the end. Given the same number of antennas, the proposed method could achieve higher sum-rate capacity and better spectral efficiency.

The Massive MIMO usually considers the azimuth angle only. However, in a 3D distributed antenna system, the elevation angle cannot be ignored. Nested array as a two dimensional arrays was firstly proposed to perform array processing with increased degree of freedom, using less number of sensors at the same time. A novel 3D MIMO antenna deployment is also proposed based on nested co-array. We model a 3D nested distributed MIMO system and analyze its performance with achievable sum rate.

## TABLE OF CONTENTS

ACKNOWLEDGEMENTS . . . . .	iv
ABSTRACT . . . . .	vi
LIST OF ILLUSTRATIONS . . . . .	xi
LIST OF TABLES . . . . .	xiii
Chapter	Page
1. Resource Allocation in Heterogeneous Network Using Game Theory . . . . .	1
1.1 Introduction . . . . .	1
1.2 Network Structure and Scenarios . . . . .	4
1.3 Non-Cooperative Game . . . . .	6
1.3.1 The Game Model . . . . .	6
1.3.2 The Nash Equilibrium . . . . .	9
1.4 Cooperative Game for Bandwidth Sharing . . . . .	13
1.4.1 The Game Model . . . . .	13
1.4.2 Agreement of Transferable Surplus . . . . .	16
1.4.3 The Benefit Function . . . . .	20
1.5 Performance Analysis . . . . .	21
1.6 Conclusion . . . . .	23
2. Game Theoretical Method for Sum-Rate Maximization in Full-Duplex Mas-	
sive MIMO Heterogeneous Networks . . . . .	25
2.1 Introduction . . . . .	25
2.2 System Model . . . . .	27
2.3 Resource Allocation Game . . . . .	38



2.3.1	The Game model . . . . .	40
2.3.2	An Example . . . . .	42
2.4	Performance Analysis . . . . .	44
2.5	Conclusion . . . . .	46
3.	Massive MIMO with Much Less Antennas Using Nested Placement . . . . .	49
3.1	Introduction . . . . .	49
3.2	Preliminary Work . . . . .	51
3.3	Virtual Channel And System Model . . . . .	53
3.3.1	Virtual Channel . . . . .	53
3.4	Sum-Rate Capacity and Spectral Efficiency of Nested Distributed Massive MIMO . . . . .	57
3.4.1	Model of Nested Distributed Massive MIMO . . . . .	57
3.4.2	Sum-Rate Capacity . . . . .	60
3.4.3	Spectral Efficiency Analysis . . . . .	61
3.5	Numerical Results . . . . .	62
3.6	Introduction of 3D Nested Distributed Massive MIMO . . . . .	64
3.7	System and Channel Model in 3D . . . . .	66
3.7.1	An Example of 3D Nested Massive MIMO System . . . . .	70
3.8	Achievable Rate of 3D Nested Massive MIMO System . . . . .	70
3.8.1	Channel Parameters . . . . .	70
3.8.2	Model of 3D Nested MIMO System . . . . .	73
3.8.3	Achievable Sum Rate Analysis . . . . .	75
3.9	Simulation Results of 3D System . . . . .	77
3.10	Conclusion . . . . .	79
4.	Conclusions and Future Works . . . . .	82
4.1	Conclusions . . . . .	82

4.2 Future Works . . . . .	83
REFERENCES . . . . .	86
BIOGRAPHICAL STATEMENT . . . . .	96

## LIST OF ILLUSTRATIONS

Figure	Page
1.1 Schematic Representation of HetNets . . . . .	4
1.2 Architecture of HetNets . . . . .	7
1.3 Surplus Capacity versus number of users . . . . .	22
1.4 Average capacity of each user as the distance between macrocell and femtocell increases . . . . .	23
2.1 HetNets scenario . . . . .	28
2.2 Full-duplex Massive MIMO Channels . . . . .	30
2.3 Access scheduling by applying game theoretical method . . . . .	44
2.4 Sum-Rate comparison versus signal to noise ratio . . . . .	46
2.5 Sum-Rate versus Self Interference . . . . .	47
2.6 Sum-Rate with different power constraints versus SNR . . . . .	48
3.1 A Virtual Antenna Generated By A Pair of Difference Co-array In Uplink	54
3.2 A Block Diagram for Downlink . . . . .	56
3.3 An Example of Nested-deployed MIMO Antenna Array . . . . .	57
3.4 Spectral efficiency versus number of physical antennas. In this example, nested distributed antenna array could generate a large virtual array more than 800 elements with only 50 physical antennas. Here we assume 30 users are served simultaneously, SNR=2 dB . . . . .	64
3.5 Achievable Sum-Rate versus SNR for physical antenna number fixed to 20 . . . . .	65
3.6 3D Nested Distributed MIMO System in A Building . . . . .	66

3.7	A 3D Virtual Antenna Generated by A Pair of Difference Co-Array . . . . .	68
3.8	An Example of 3D nested Antenna Array . . . . .	71
3.9	3D Large Scale Parameters . . . . .	72
3.10	Achievable sum rate versus antenna tilting angle in different SNR . . . . .	78
3.11	Different number of antennas and placement schemes versus SNR . . . . .	79
3.12	Achievable sum rate of different tilting angle and lower bound . . . . .	80

LIST OF TABLES

Table		Page
2.1	DL users in 5th small cell . . . . .	42
2.2	UL users in 5th small cell . . . . .	43

## CHAPTER 1

### Resource Allocation in Heterogeneous Network Using Game Theory

#### 1.1 Introduction

The wireless communication technology was evolving in the past few decades. The network's capacity and throughput is increasing and spectrum efficiency are getting better with new technologies applied in practice. However, few challenges have been coming in recent years. Firstly, majority of cellular communication users all over the world are still using 2nd or 3rd generation networks. As huge amount of users have started to use 4th generation network service, a larger capacity improvement is needed due to the heavy data traffic. Secondly in some public areas, like airport, school or mall, there is a shortage in wireless resources due to a huge data requirement and interference. Finally it is a market trend that operators need a more efficient and cheaper network. The invention of small cell (like femtocell) based architecture in cellular communication, especially the multi-layers heterogeneous network (HetNets) is an effective solution to the above problems. Small cells have some advantages such as ease of deployment, cheap and can increase the frequency reuse rate.

The interference issue in LTE HetNets is a hot topic in recent years. Different from regular cellular network, HetNets have inter-layer interference. Few solutions have been proposed to this issue such as power control based interference coordination method, base station dynamically coverage range approach. However, for the challenge mentioned above, HetNets need a new method to improve frequency spectrum efficiency. In this research, we propose a new wireless resources allocation method in

multi-layer HetNets based on game theory. Multiple parameters will be introduced to affect the strategies and decision and to find Nash Equilibrium points.

In 3GPP LTE-Advanced release 10 has defined a small cell-delay Node which is located in a macro cell. And Coordinated Multi Point (CoMP) operation is defined in release 11 which allows the set of TX-RX points used in CoMP to be either at different locations, or be co-sited but providing coverage in different sectors and they can also belong to the same or different eNBs. [1] [2] They are both heterogeneous networks (HetNets) in next generation cellular communication system. The research work on HetNets mainly focuses on inter-cell interference, power management, and resources allocation issues. [3] designed distributed utility functions minimum SINR for small cells. A resource management scheme is proposed in [4] [5] [6] [7] based on cognitive radio (CR) technology, which allows small cells to sense the usage of resource in the network. Some hybrid access of small cell method is proposed in [8] [9] which can reduce the co-channel interference with limited user connections.

There are multiple optimization methods for resource allocation. Game theory, as one of these methods, has been applied to this kind of problem for the few years. Game Theory emerged in the early 20th century and was initially used study Chess games. Later, in 1940s, a book on games and economic behaviors was published then it became popular to apply game theory to economic problems. Now days, game theory has been used to study kinds of problem which involve strategic choice making. Like in Petrosjan's book, about 20 applications of game theory were introduced [10]. A basic view of cooperation games and its properties were provided in [11]. [12] made a detail discussion on network and hierarchies with cooperative games. [13] built and analyzed a dynamic spectrum sharing game. [14] built a repeated sharing game for spectrum allocation.

However, the theory and applications of HetNets are rare in next generation and is

reflected in the following aspects:

1. Usually only two layer networks (macro and femto) are considered in HetNets research. In 5G, base stations are dense deployed. Femtocell and picocells are widely deployed by operators especially in densely populated public places.
2. Most access game models are based on non-cooperative or using non-cooperative methods. In game theory, all games must be have a solution that is Nash Equilibrium (NE). But NE is not always the optimal solution for them. In cellular HetNets, base stations are belong to same operator, cooperation is a feasible method to increase the network capacity.

The contributions in this chapter include: a cooperative game model for three layer cellular HetNets is established; Optimized the utility function to maximize the bandwidth allocation surplus; Simulations are displayed to verify the performance improvement.

The rest of this chapter is organized as follows. Section 1.2 introduces the structure of the network then establish a bandwidth sharing game. Some properties are claimed and backwards induction algorithm was used to derive the surplus in the cooperation. Utility and benefit function are formulated in Section 1.3. Section 1.4 illustrates the system performance through simulation. Conclusions are drawn in Section 1.5.



## 1.2 Network Structure and Scenarios

In this Section, a game model will be established for three-layers cellular Het-Nets. Each layer is considered to cooperate with other layers to maximize its allocated bandwidth and subscribers. Several properties of the game will be announced and proved.

The cells in LTE standard are considered as a regular Base Station (BS), which cover a large area up to 62miles (100Km). In some indoor areas where the outdoor signals have a small SNR, Picocells are deployed. The Picocells are also used to increase the network capacity in some public place with dense wireless service request. The femtocell, generally, is defined as a home eNodeB (eNB), which only provides service to few devices. To achieve a larger capacity, in this paper we assume that Femtocells are always working in "Open Access Mode", which means that all users can connect to Femtocells.

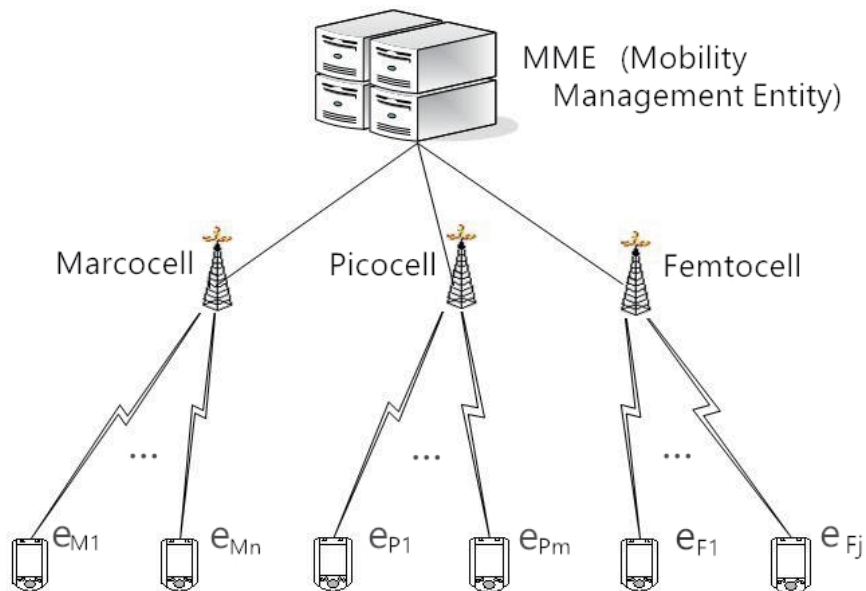


Figure 1.1. Schematic Representation of HetNets.

Figure 1.1 summarizes the structure of HetNets which studied in this paper. Users are located in an indoor area will be and it is covered by macrocell, picocell and femtocell. Three groups of users are attached to macrocell, picocell and femtocell. And to simplify the game model, this paper does not consider the Coordinated Multi-points (CoMP) case but it is possible to deploy in LTE to get higher spectrum efficiency. In the CoMP case, users are allowed to connect with two cells simultaneously. However, in this paper, each user has a choice to connect to only one cell among the three to achieve the maximum utility. The utility here indicates allocated bandwidth or lower power consumption.

In real world, UEs cannot decide its attached cell. All users schedule and release are managed by operator's network such as Radio Access Network (RAN) in LTE. Based on the network capacity and reference signal receiving power (RSRP) reported by UE, eNodeB could require UE to perform multiple commands (handover, cell reselection, etc.). From operator's point of view, more UEs should connect to femtocell or picocell. Because it can release the load of macrocell which may have a huge number of users. Considering the above situation, this paper introduces a concept known as "User Stream". Just like a river, the users flow from upstream to downstream. The upstream here is femtocell and the downstream is macrocell. In game theory, for the river sharing game, there are two doctrines restrict each other. The absolute territorial sovereignty (ATS) theory states that a country has absolute sovereignty over its territory for any river flowing through it. But the theory of unlimited territorial integrity (UTI) forbids a country to alter the natural conditions that may effect neighboring country on its own territory. Similarly, each cell can decide its subscriber set and how to allocate its resources. On the other hand, the cell can only "pick up" users uniformly, but not just left the user who use heavy data service

to downstream cells. One of this article's important target is making a compromise between these two constraints.

Suppose there are totally  $X$  players (Users) in the network. All users have to choose a coalition  $i$  in the coalition set  $I = \{M, P, F\}$ , where "M", "P", "F" indicates macrocell, picocell and femtocell, so that each user could maximize its utility.  $M \in N, P \in N, F \in N$ . As each user has to choose only one cell to attach, therefore  $M \cap P = P \cap F = M \cap F = \emptyset$ . Users and the cell constitute a coalition. Now this problem is divided into two parts:

1. Which cell should the user choose? It is typical coalition formation problem.
2. How the cell allocate the resources among its subscribers? It is a typical utility allocation problem.

### 1.3 Non-Cooperative Game

In this section, a non-cooperative game model for the resource sharing problem will be established. The essential parts for a non-cooperative game are players, strategies and payoffs. Three layers' eNBs are players in this problem. Strategies is the operation set for players with certain information. Payoff means that under some strategies combination, the utility a player will finally get. The goal for a player in the non-cooperative game is choose a strategy to maximize his utility function.

#### 1.3.1 The Game Model

Figure 1.2 shows the architecture of HetNets. Usually, the femtocell's covered area is located in a Picocell. And also a Picocell is in a Macrocell.

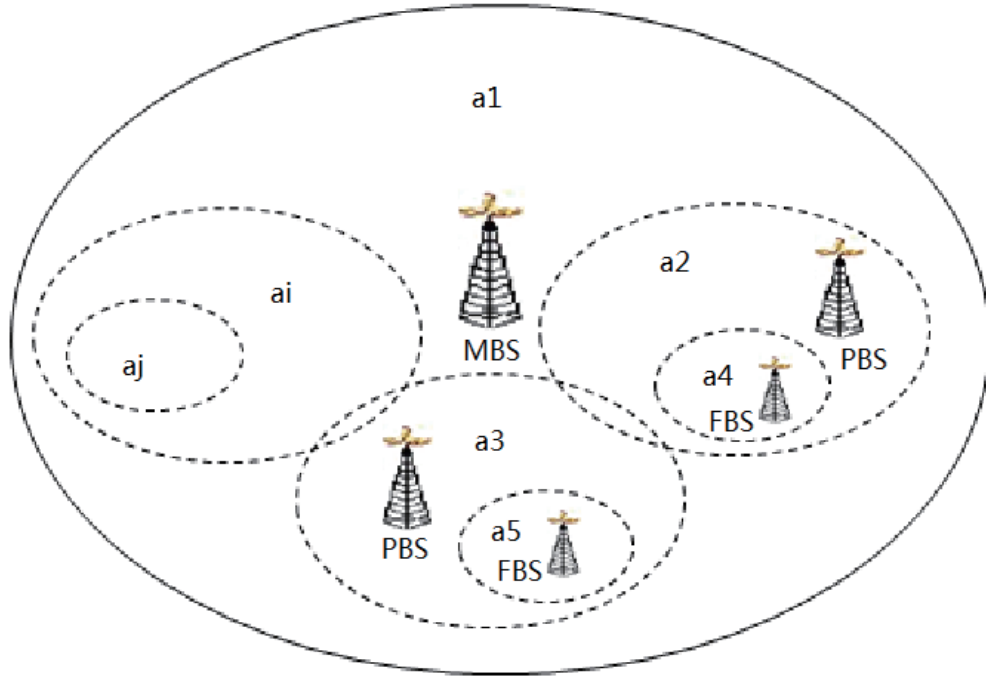


Figure 1.2. Architecture of HetNets.

**Definition 1 (HetNets Unit)**

A HetNets Unit consists with a macrocell. There are  $m$  Picocell located in one macrocell. And  $n$  Femtocell are located within a Picocell covered area. Both  $m$  and  $n$  are greater or equal to 1. And also we suppose all base stations in the model could be represented as a set  $\{BS_m, BS_{p_1}, BS_{p_2}, \dots, BS_{p_m}, BS_{f_1}, \dots, BS_{f_{m*n}}\}$

**Definition 2 (Service Area Set)**

The service area set  $a_m$  represents the area covered by Macrocell except Picocell covered range (i.e.  $a_1$  in Figure 1.2); For the service area set  $\{BS_{p_1}, BS_{p_2}, \dots, BS_{p_m}\}$  denotes the area covered by Picocell but not covered by Femtocell. (i.e.  $a_2$  and  $a_3$  in

Figure 1.2); Similarly,  $\{BS_{f_1}, \dots, BS_{f_{m*n}}\}$  denotes the area covered by Femtocell.

According to definition 2, there is only one kind of signal which is sent by Macrocell within  $\{a_1\}$  area. In the area  $\{a_{p_1}, a_{p_2}, \dots, a_{p_m}\}$ , devices can receive signals from both Macrocell and Picocell.  $\{a_{f_1}, \dots, a_{f_{m*n}}\}$  is covered by all three layers base stations.

Based on the service area defined above, we can find the representation of bandwidth. Let  $\{b_1\}$  denotes the total bandwidth that Macrocell could support,  $\{b_{p_1}, \dots, b_{p_m}\}$  denotes the bandwidth allocated by Picocell and  $\{b_{f_1}, \dots, b_{f_{m*n}}\}$  is the bandwidth occupied by femtocell.

The bandwidth allocated by Macrocell in area  $a_1$  could be represented as:

$$\{b_1^{a_1}\}, b_1^{a_1} = b_1 - \sum_{i=1}^m b_1^{a_i} - \sum_{j=m+1}^{m*n} b_1^{a_j} \quad (1.1)$$

The bandwidth allocated by Picocell in area  $\{a_{p_1}, a_{p_2}, \dots, a_{p_m}\}$  could be represented as:

$$\{b_1^{a_{p_1}} + b_{p_1}^{a_{p_1}}, \dots, b_1^{a_{p_m}} + b_{p_m}^{a_{p_m}}\}, b_{p_1}^{a_{p_1}} = b_{p_m} - \sum_{i=m*(n-1)+1}^{m*n} b_{p_m}^{a_i} \quad (1.2)$$

The bandwidth provided by Femtocell in area  $\{a_{f_1}, \dots, a_{f_{m*n}}\}$  is:

$$\{b_1^{a_{f_1}} + b_{p_1}^{a_{f_1}} + b_{f_1}^{a_{f_1}}, \dots, b_1^{a_{f_{m+n}}} + b_{p_1}^{a_{f_{m+n}}} + b_{f_{m+n}}^{a_{f_{m+n}}}, \dots, b_1^{a_{f_{m*n}}} + b_{p_m}^{a_{f_{m*n}}} + b_{f_{m*n}}^{a_{f_{m*n}}}\} \quad (1.3)$$

### 1.3.2 The Nash Equilibrium

#### 1.3.2.1 The Definition of Nash Equilibrium

The Nash Equilibrium is the set of optimized strategies' from all players in this case. If  $NE^*$  is the Nash Equilibrium, then

$$NE^* = (s_1^*, s_2^*, \dots, s_i^*) \quad (1.4)$$

where  $s_i$  is the optimized strategy of  $i^{th}$  player. It is the strategy which could maximize eNB  $i$ 's utility among lots strategies. Suppose the utility function in this game is a function of combination of strategies from all players. It is noteworthy that  $i^{th}$  eNB optimized strategy usually depends on other players' choice. Let  $s_{\bar{i}} = (s_1, s_2, \dots, s_{i-1}, s_{i+1}, \dots, s_n)$  denotes the strategies combination from all eNB excepte  $i^{th}$  eNB. And  $s_i^*$  is the optimized strategy of  $i^{th}$  eNB with given  $s_{\bar{i}}$ , which means:

$$u_i(s_i^*|s_{\bar{i}}) \geq u_i(s'_i|s_{\bar{i}}), \forall s'_i \neq s_i^* \quad (1.5)$$

In other word, the problem is to find an  $s_i^*$  which could maximize the utility function:

$$\arg \max_{s_i^*} u_i(s_1^*, \dots, s_{i-1}^*, s_i^*, s_{i+1}^*, \dots, s_n^*) \quad (1.6)$$

#### 1.3.2.2 The Utility Function

For the HetNets system, bandwidth is a significant resource, however, when talking to the performance, the capacity is one of the most important indicators. To calculate the capacity, firstly, the receiving power of each user should be found. Suppose  $X = x_1, x_2, \dots, x_t, \dots, x_N$  is the index of users,  $N$  is the total number of users

from all cells.

$$N = n_{a_1} + n_{p_1} + \dots + n_{p_m} + n_{f_1} + \dots + n_{f_{m*n}} \quad (1.7)$$

And in [15], an equation on RSRP has been defined as:

$$RSRP_{i,x_t} = P_{MAX,i} \cdot L_{i,x_t}, \quad (1.8)$$

where  $P_{MAX,i}$  is the maximum transmission power of eNB  $i$  and  $L_{i,x}$  is the large scale channel gain including path loss, shadowing, penetration loss between eNB  $i$  and user  $x_t$ . Based on the RSRP, a function of capacity could be derived:

$$C_i = \sum_{t=1}^n B \cdot \log_2 \left( 1 + \frac{P_{MAX,i} \cdot L_{i,x_t}}{\sigma_N^2 + \sum_{i' \in I, i' \neq i} P_{MAX,i'} \cdot L_{i',x_t}} \right), \quad (1.9)$$

where,  $n$  is the number of users in cell  $i$ ,  $b$  here denotes the sum of bandwidth allocated macro, pico and femto cells. Based on the capacity, the utility function in specific area (area  $a_1$ ) could be defined as:

$$U_{a_1} = \sum_{t=1}^{n_{a_1}} \left( \frac{b_1 - \sum_{i=1}^m b_1^{a_{p_i}} - \sum_{i=1}^{m*n} b_1^{a_{f_i}}}{n_{a_1}} \cdot \log_2 \left( 1 + \frac{P_{MAX,i} \cdot L_{i,x_t}}{\sigma_N^2 + \sum_{i' \in I, i' \neq i} P_{MAX,i'} \cdot L_{i',x_t}} \right) \right) \quad (1.10)$$

### 1.3.2.3 Find A Nash Equilibrium

Now the non-cooperative game becomes more clear depending on earlier definitions and equations.

a) Players: Macrocell base station and Picocell base stations. As femtocells are not allowed to reallocate their bandwidth to each other, to simplify the model, only two players are considered in this game.

b) Strategies:

For Macrocell, the strategies are  $S_m = \{b_1^{a_{p_1}}, \dots, b_1^{a_{p_m}}, \dots, b_1^{a_{f_{m*n}}}\}$ , in other words,

Macrocell could adjust its bandwidth allocation in areas  $a_{p1}, \dots, a_{fm*n}$  to effect other eNB's utility.

For Picocell, similarly, the strategies are  $S_p = \{b_{p1}^{ap1}, \dots, b_{p1}^{afn}, \dots, b_{pm}^{afm*n}\}$ , which means Picocells can assign its bandwidths to maximize its utility.

c) Payoffs(Utilities): The utility of Macrocell in this game is the total capacity that the system get by allocating bandwidth in area  $a_{p1}, \dots, a_{fm*n}$ . And Picocell's utility is the capacity by allocating bandwidth in  $a_{p1}, \dots, a_{fm*n}$ .

Let

$$\Gamma_{i,t} = \log_2\left(1 + \frac{P_{MAX,i} \cdot L_{i,x_t}}{\sigma_N^2 + P_{MAX,i' \in I, i' \neq i} \cdot L_{i',x_t}}\right) \quad (1.11)$$

The utility of Macrocell can be represented as:

$$U_m = \left[ \begin{array}{l} \sum_{t=1}^{n_{a1}} \left( \frac{b_1 - \sum_{i=1}^m b_1^{ap_i} - \sum_{i=1}^{m*n} b_1^{af_i}}{n_{a1}} \cdot \Gamma_{macro,t} \right) \\ + \sum_{t=1}^{n_{p1}} \left( \frac{b_1^{ap1}}{n_{p1}} \cdot \Gamma_{macro,t} \right) + \\ \dots \\ + \sum_{t=1}^{n_{f1}} \left( \frac{b_1^{af1}}{n_{p1}} \cdot \Gamma_{macro,t} \right) + \\ \dots \\ + \sum_{t=1}^{n_{fm*n}} \left( \frac{b_1^{afm*n}}{n_{p1}} \cdot \Gamma_{macro,t} \right) \end{array} \right] \quad (1.12)$$



Where,  $I$  is the set of base stations. Likewise, Picocells' utility function could be derived:

$$U_p = \begin{bmatrix} \sum_{t=1}^{n_{p1}} \left( \frac{b_{p1}^{ap1}}{n_{p1}} \cdot \Gamma_{pico,t} \right) + \\ \dots \\ \sum_{t=1}^{n_{pm}} \left( \frac{b_{pm}^{apm}}{n_{pm}} \cdot \Gamma_{pico,t} \right) + \\ \dots \\ \sum_{t=1}^{n_{f1}} \left( \frac{(b_{p1} - b_{p1}^{ap1}) \div n}{n_{f1}} \cdot \Gamma_{pico,t} \right) + \\ \dots \\ \sum_{t=1}^{n_{fm*n}} \left( \frac{(b_{pm} - b_{pm}^{apm}) \div n}{n_{fm*n}} \cdot \Gamma_{pico,t} \right) \end{bmatrix} \quad (1.13)$$

If the Femtocell also been considered, then total utility function is formed as:

$$U_{all} = \begin{bmatrix} \sum_{t=1}^{n_{a1}} \left( \frac{b_1 - \sum_{i=1}^m b_1^{api} - \sum_{i=1}^{m*n} b_1^{afi}}{n_{a1}} \cdot \Gamma_{macro,t} \right) + \\ \dots \\ \sum_{t=1}^{n_{p1}} \max \left( \left( \frac{b_{p1}^{ap1}}{n_{p1}} \cdot \Gamma_{pico,t} \right), \left( \frac{b_{a1}^{ap1}}{n_{p1}} \cdot \Gamma_{macro,t} \right) \right) + \\ \dots \\ \sum_{t=1}^{n_{pm}} \max \left( \left( \frac{b_{pm}^{apm}}{n_{pm}} \cdot \Gamma_{pico,t} \right), \left( \frac{b_{a1}^{apm}}{n_{pm}} \cdot \Gamma_{macro,t} \right) \right) + \\ \dots \\ \sum_{t=1}^{n_{f1}} \max \left( \left( \frac{b_{f1}^{af1}}{n_{f1}} \cdot \Gamma_{femto,t} \right), \left( \frac{b_{a1}^{af1}}{n_{f1}} \cdot \Gamma_{macro,t} \right), \right. \\ \left. \left( \frac{b_{p1}^{af1}}{n_{f1}} \cdot \Gamma_{pico,t} \right) \right) + \\ \dots \\ \sum_{t=1}^{n_{fm*n}} \max \left( \left( \frac{b_{fm*n}^{afm*n}}{n_{fm*n}} \cdot \Gamma_{femto,t} \right), \left( \frac{b_{a1}^{afm*n}}{n_{fm*n}} \cdot \Gamma_{macro,t} \right), \right. \\ \left. \left( \frac{b_{pm}^{afm*n}}{n_{fm*n}} \cdot \Gamma_{pico,t} \right) \right) \end{bmatrix} \quad (1.14)$$

According to equation 1.6 and 1.14, the corresponding function of maximizing system's utility function is:

$$\arg \max_{s_m^*, s_p^*} U_{all}(S_m, S_p) \quad (1.15)$$

Which means system has to find a strategy pair  $(s_m^*, s_p^*)$ (allocation plan) to maximize its utility function  $U_{all}$ .

## 1.4 Cooperative Game for Bandwidth Sharing

### 1.4.1 The Game Model

Based on [16] [17], the characteristic function form of this game can be easily built.

#### **Definition 3 (Bandwidth Sharing Game)**

Considering a three layers HetNets, a cooperative bandwidth sharing game is defined as:

$$\langle I, S_n, U_n \rangle, \quad (1.16)$$

Where  $I$  is the player set, three cells are sharing the resources so  $I = \{1, 2, 3\}$  and  $n = \{1, \dots, 2^N\}$  is the strategy vector index of player's strategy,  $X$  is the set of users. For example  $S_3$  means the cell take strategy 3 and this vector indices users in that cell should establish connection or not (0 means not).  $S_{n,x} = (S_{1,1}, \dots, S_{n,X}) \in \mathfrak{R}^X$ .  $U$  is the utility set of players.

The utility of eNb  $I \in \{1, 2, 3\}$  is composed by allocating  $w_i$  units of bandwidth to users and surplus from user.

$$U_i(w, e) = \sum_{i,x} [b_i(w_x) + Y(w_x - e_x)], \quad (1.17)$$

where  $b_i$  is the benefit function which denotes the credit by providing service to users,  $i \in 1, 2, 3$ . Lets assume that at every  $w_x > 0$ ,  $b_i$  is strictly concave and strictly increasing. If  $b'_i$  is the derivative of  $b_i$ , then  $b'_i(w_x)$  tends to infinity as  $w_x$  goes to 0. That means each cell consume less wireless resources and provide better service to users getting better benefit or credit.  $w_x \in W$  is the bandwidth allocation plan.  $e_x$  is the bandwidth that user actually used,  $Y$  is the function of surplus bandwidth.

The bandwidth in the paper is considered similar as goods, could be transferred to each other. Bandwidth allocated to each user  $w_x$  can only be used or occupied by subscribers of cell  $i$ . This makes our problem totally different from traditional economy allocation or sharing problem.

And the constraint must be added to the utility function:

$$\sum_{p=1}^n e_{1,p} + \sum_{d=1}^m e_{2,d} + \sum_{r=1}^j e_{3,r} \leq \sum_{x=1}^X W_x, \quad (1.18)$$

$$\sum_{x=1}^X (W_x - e_{i,x}) \geq 0 \quad (1.19)$$

Where  $n + m + j = X$ .

As equation 1.2 has a quasi-linear form, another important definition can be given based on its linear properties:

#### **Definition 4 (Pareto Optimal Allocation)**

Suppose  $(w^*(N), e^*(N))$  is an allocation made by Base Station, if and only if this allocation can maximize the utility function and does not waste any wireless resources (bandwidth), then this allocation is Pareto Optimal.

Note that the Pareto optimal here means that the system cannot improve any user service, and does not affect other users at the same time.  $W'(N)$  can be called as an optimal occupancy plan.

**Definition 5 (Marginal Benefits of The Game)**

If the marginal benefits increase as one user connect to another cell, in another words, if two cells have different marginal benefit, some binding cooperative agreements or constraints must exist:

Suppose there are groups of users  $U_P \in X, P = 1, \dots, p$ , and the corresponding benefits from these users can be presented as a list of positive values  $\beta_{P, P=1, \dots, p}$  if

$$b_i (W_{i,x}^* (U_p)) < b_{i'} (W_{i,x}^* (U_p)) , \tag{1.20}$$

$$\beta_{i,p} \geq \beta_{i',p} \tag{1.21}$$

then

$$b_{i'} (W_{i,x}^* (U_p)) = \beta_{i,p} \tag{1.22}$$

for every  $i \in I, x \in U_p$  and every  $p = 1, \dots, P$ .

And

$$\sum_{x \in U_P} (W_{i,x}^*(U_p) - e_{i,x}) = 0 \quad (1.23)$$

for every  $p = 1, \dots, P$ .

#### 1.4.2 Agreement of Transferable Surplus

It is easy to find that the benefit function we devised before is convex. From the physical layer point of view, each cell has a capacity upper bound. The cell cannot serve too many users due to the system performance or channel limitation. On the other hand, if the marginal benefit of a user is higher for downstream cells, then the upstream cell can get extra credit for passing it to other cells. It is also possible that some of the passed users from Femtocell are connected to Picocell but not Macrocell. Therefore, the utility of a cell (coalition)  $I$  depends on its own and other cells behavior.

Based on the above fact, let's assume Pico and Macro cell form a partition (not coalition) and both of them are trying to maximize their surplus for any amount of unused bandwidth by Femtocell (Picocell). Besides, any amount of unallocated bandwidth can only be transferred to Picocell or Macrocell, and each user that belongs to these coalitions is maximizing its surplus for its peers.

Similar to [17], we can easily describe players' and coalitions' relationship using mathematical language. Let  $P$  denote the partition of  $X$  and all users in that partition  $P$  are able to maximize their surplus of occupied bandwidth. Let  $\bigcup_{K \in P} C(K) = K_1, \dots, K_t$  and  $K_1 < \dots < K_t$ . There is an algorithm called backwards induction (BIA) ([18][19][20]) which can find an optimal allocation plan for each unit of unallocated bandwidth received by the user. And let  $S'$  denote the surplus after allocation,  $w^*(K_t, S')$  is the allocation plan for user  $K$  in algorithm's step  $t$ .

At step (t):

For all  $S' \geq 0$ , let  $w^*(K_t, S')$  be the final optimal allocation plan for  $(K_t, (e_{\min(K_t)} + S', e_{K_t \min K_t}), b_{K_t})$ .

At step (t-1):

For all  $S' \geq 0$ , let  $w^*(K_{t-1}, S')$  be the optimal allocation plan for  $(K_{t-1}, (e_{\min K_{t-1}} + S', e_{K_{t-1} \min K_{t-1}}), b_{K_{t-1}})$ . Note that  $K_t$  and  $K_{t-1}$  have to be two different users in set  $P$ . After choose the plan  $w^*(K_{t-1}, S')$ , the surplus

$$S_t(w^*(K_{t-1}, S')) = S' + \sum_{x \in K_{t-1}} (e_x - W_x^*(K_{t-1}, S')) \quad (1.24)$$

is saved by  $K_{t-1}$  and give it to  $K_t$ . And  $K_t$  chooses the plan  $w^*(K_t, S_t(w^*(K_{t-1}, S')))$ .

·  
·  
·

At step (j):

Let's define  $K_j$  as the bandwidth aggregated from previous users, and also  $S' \geq 0$ ,  $w(K_j, S')$  is an allocation (May Not be Optimal) for  $K_j$  if  $S' + \sum (e_i - w_i(K_j, S')) \geq 0$ . Suppose for all users,  $K_{j'}$  ( $j' \in j + 1, \dots, t$ ). Following the conclusion above, we can get:

$$S_{j+1}(w(K_j, S')) = S' + \sum_{x \in K_j} (e_x - W_x(K_j, S')) \quad (1.25)$$

be the bandwidth saved by  $K_j$  and passing to  $K_{j+1}$ . And also let

$$S_{j+2}(w(K_j, S')) = S_{j+2}(w^*(K_{j+1}, S_{j+1}(w(K_j, S')))) \quad (1.26)$$

be the bandwidth saved by  $K_j$  and  $K_{j+1}$  and passing to  $K_{j+2}$ . By deriving (11), we can easily get:

$$S_{j+k}(w(K_j, S')) = S_{j+k}(w^*(K_{j+k-1}, S_{j+k-1}(w(K_j, S')))) \quad (1.27)$$

which is presenting the bandwidth saved by  $K_j, \dots, K_{j+k-1}$  to  $K_{j+k}$ . Where  $k \in 1, \dots, t - j$

Based on [17], if  $K \in P$  and  $K_j \subseteq K$ , and if surplus  $S' \geq 0$ , then the allocation plan  $w^*(K_j, S')$  solves

$$\begin{aligned} & \max_{x(k_j, S')} \sum_{i \in k_j} b_i(w_i(k_j, S')) + \\ & \sum_{i \in K_{j'}} b_i(w_i^*(k_{j'}, S_{j'}(w(K_j, S')))) \end{aligned} \quad (1.28)$$

According to this equation,  $w(k_j, S')$  maximizes  $K$ 's surplus. Then we can conclude that the result of value of transferable surplus of this game can be calculated by BIA:

$$v = \sum_{i \in X} b_i(w^*(K_i, S_i(w^*(K_1, 0)))). \quad (1.29)$$

We will call  $v$  as the lower bound of coalition  $I$  given partition  $P$ ,  $P \in X$ .

### Definition 6 (Cooperative Lower Bound)

For coalitions  $I$ , let  $v(I) = v(I, \{I, X/I\})$ .

If for any partition  $P \in X$ , the cooperation does not make any positive effect on coalition  $I$ ,

then

$$v(I) = v(I, P) \quad (1.30)$$

If for any partition  $P \in X$ , the cooperation does make some positive effects on coalition  $I$ ,

$$v(I) \leq v(I, P) \quad (1.31)$$

We can further conclude that comparing to non-cooperation case, the cooperation does not decrease the benefit of a coalition which benefits greater than or equal to the lower bound.

Different from real upper bound, we can define an expectation upper bound for this game. This upper bound does not depend on how other coalitions (cells) behave, but is related with coalition  $i$ 's highest benefit and surplus it can achieve. Suppose other cells are absent for this game, coalition  $i$  is asked to choose a allocation plan  $h(I) \in \mathfrak{R}_+^I$  to maximize  $\sum_{i \in X} b_i(h_i(I))$  with following constraints:

$$\sum_{i \in P \cap I} h_i(I) \leq \sum_{i \in P} e_i \quad (1.32)$$

This maximization problem has only one solution due to its concave property. Suppose  $h_i^*(I)$  is the solution, then the expected benefit of coalition  $I$  is:

$$S(I) = \sum_{i \in I} b_i(h_i^*(I)) \quad (1.33)$$



In this paper, three layers HetNets are working in the same bandwidth, so there is strong interference between these cells. We assume the capacity of cell equals to 0 if there is no user subscribed to it. As the number of users goes on increasing (actually is the total bandwidth usage), the capacity goes on increasing. The capacity improvement by allocating bandwidth  $w_x$  to user  $x \in X$  can be formulated as [21]:

$$C_{i,x} = w_x \cdot \log_2 \left( 1 + \frac{P_{MAX,i} \cdot L_{i,x}}{\sigma_N^2 + P_{MAX,i' \in I, i \neq i'} \cdot L_{i',x}} \right), \quad (1.34)$$

### 1.4.3 The Benefit Function

A utility function of bandwidth sharing game was mentioned in the last Section. Let's supplement more details to make it more straightforward in wireless communication problems. To make it simple, the utility function can be defined related to channel capacity. The first part of equation 1.2 which is benefit function denotes the capacity improvement by allocating bandwidth to users who subscribe to it; and the second part, which is quite important in cooperative game, shows its contribution to other players (cells). The surplus bandwidth from user can be used by other cell's subscribers.

However, the utility function cannot simply be used to denote the capacity improvement. Because we built a cooperative model in last section. In other words, the cell should consider the bandwidth surplus after allocation. Let's assume users not only report their RSRP to the cell but also predict QoS. This paper will not dig more details in QoS issues. According to equations 1.13 and 1.14, allocation plan  $w(k_j, S')$  which considered surplus  $S'$  could maximize coalition surplus. A surplus factor  $S_f$  could be introduced to calculate the benefit function.

$$S_{f,x} = \max(C_{i,x}(\Delta L_{i,x}), \frac{q'}{q}) \quad (1.35)$$

Obviously,  $S_{f,x} \in [0, 1]$  If  $S_f = 0$ , then user must have lost the connection like power off the device. If  $S_f = 1$ , no change for the bandwidth usage. Based on this, we can derive our surplus function:

$$Y_i = \sum_x C_{i,x} \cdot \frac{1}{S_{f,x}}, \quad (1.36)$$

Then the utility function becomes:

$$U_i = \max(b_{i,x}(w_{i,x})) + \sum_x C_{i,x} \cdot \frac{1}{S_{f,x}}, \quad (1.37)$$

## 1.5 Performance Analysis

In the last section, we formulated the utility function and the surplus function. Consider the HetNets scenario in next generation cellular networks, we assume that macrocell cover a range of 600m which is smaller than the cell in LTE standard. And the picocell's transmission range equals to 150m. Femtocell is an indoor BS that only covers a  $25m \times 25m$  room. Suppose the system bandwidth is 20 MHz. The maximum transmission power for macrocell is 33 dBm, 20 dBm for picocell and 10 dBm for femtocell. Consider femtocell is available only in indoor environment, the number of users should not be large, so we assume there are up to 60 users in the system. When speaking of indoor environment, the wall penetration loss has to be considered which we have set as 20 dB.

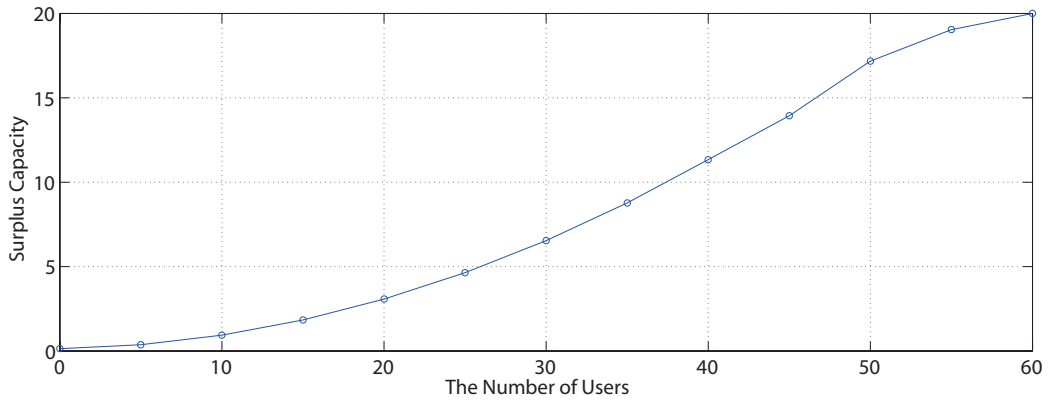


Figure 1.3. Surplus Capacity versus number of users.

Figure 1.3 shows the sum of surplus as a function of the number of user. According to equation 1.13 in Section 1.2, by applying backwards induction algorithm, the surplus is increasing as of users increasing. But it is a quite random value of each user's surplus because the behavior of user is uncertain. The result proves that the surplus function is monotonically increasing.

In our system, cells are sharing the bandwidth, as a consequence, interference may be a big issue for the sharing game. Consider this problem, we design a simulation related with interference. Suppose the distance between femtocell and picocell equal to 100m.

Figure 1.4 shows average capacity of users versus the distance between femtocell and macrocell. It can be seen that the average capacity improve as distance increase. The main reason is that macro base station is transmitting with a high power. This signal is treated as noise at femtocell (as well as picocell). Moreover, due to the cooperation between cells, if the channel condition is not good for a user, then its benefit and surplus value will be small. This directly leads the user to connect to a downstream cell to maximize its surplus. That's why the system is more efficient than the traditional access schemes which majorly depends on RSRP. A random access

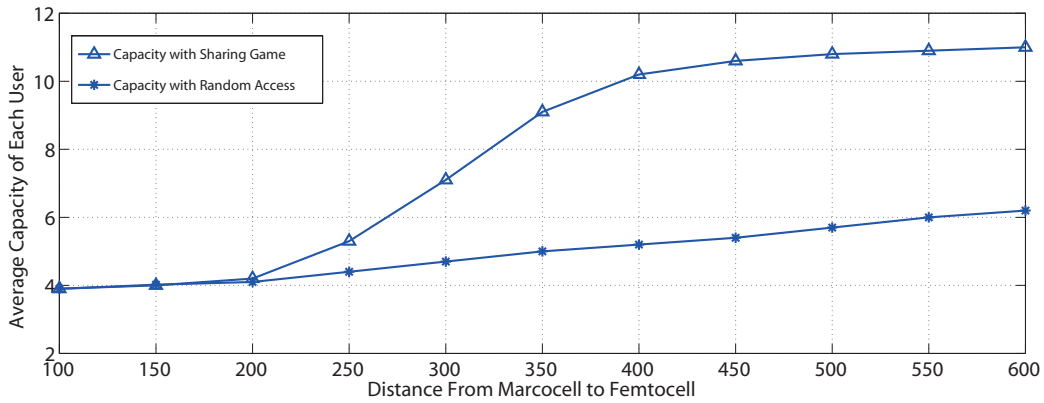


Figure 1.4. Average capacity of each user as the distance between macrocell and femtocell increases.

performance is shown in figure 1.4 to make a comparison to game theoretic method. The results turn out that there is a big plus on capacity by applying cooperative bandwidth sharing method.

## 1.6 Conclusion

In this article, a bandwidth sharing game has been proposed for 5G HetNets to optimize the wireless resources allocation by cooperation among cells. According to the model, cells are trying to maximize their surplus of allocation, while surplus could be reused by other users. With the assumption of upstream base station, users are encouraged to connected to femtocell, which meets the operator's expectation. The utility function of this game was formulated with two parts: benefit function and surplus function. Both of them are based on information theory and indicates the capacity improvement of the system. Numerical results from simulation can be summarized as follows:

- Cooperative allocation get better performance with more subscribers.
- Spectrum efficiency is higher in a three layers HetNets compare to two layers only.
- The cooperative approach get better or equal performance than the non-cooperative in bandwidth sharing.

Some future works are possible based on this paper. If subscribers are allowed to connect with two cells, the problem will become a CoMP resources sharing problem. To derive the conclusion of this paper to CoMP, it is possible to get performance improvement. On the other hand, the bandwidth allocation could be linked to carrier aggregation technology. With the cooperative game, spectrum efficiency may also improve in carrier aggregation problem.

## CHAPTER 2

### Game Theoretical Method for Sum-Rate Maximization in Full-Duplex Massive MIMO Heterogeneous Networks

#### 2.1 Introduction

4G LTE standard has been released several years ago, however, high speed data demand is still increasing. Although 4G network is not yet universal on a global scale, engineers start studying 5G technologies. 5G does not have a unique definition yet [1][22]. Generally, 5G network is considered working in high frequency band from 20GHz to even 50GHz [23], and it has a higher spectrum efficiency and also higher power efficiency [24]. Pekka Pirinen summarized recent years' research on 5G and suggested a possible technical requirements over currently existing technologies (4G) [25]:

- 1000 times higher mobile data volume per area,
- 10 to 100 times higher typical user data rate,
- 10 to 100 times higher number of connected devices,
- 10 times longer battery life for low power devices,
- 5 times reduced end-to-end latency.

However people proposed many techniques to achieve these requirements, i.e. Full-Duplex Radios for Local Access [26] and Massive MIMO technology [27][28] [29]. The half-duplex wireless communication system, usually are called FDD and TDD in 4G standard, use two different channels for uplink and downlink. Full-duplex wireless communication, compared to half-duplex, allows devices transmit and receive data simultaneously [30]. It has been considered as a promising technique to next gen-

eration wireless communication systems because it's possible to double the capacity theoretically [31][32][33][34]. However, the full-duplex wireless system has an interference problem which cannot be ignored. [35][36][37] proposed some approach to solve interference problem. [38] presented an interference alignment method for K-user interference channel and [39] discussed the feasibility of this method over measured MIMO-OFDM channels.

Heterogeneous Networks (HetNets) were proposed several years ago and became a part of 4G-LTE standard. Although it is not been widely deployed, some wireless operators have deployed it in the market. It is foreseeable that the HetNets will become a more popular technique in next generation wireless communication system. If all Base Stations (BS) are equipped large number of transmission and reception antennas, the technical realization and even the system modeling will be very complicated. HetNets modeling and potential gains with Massive MIMO were analyzed in [40]. [41] studied a density HetNets over a Massive MIMO channel.

In a cellular HetNets, if a user locates in a small cell, then it has more than one access strategies. Assumed that inside the macro cell, there are multiple pico cells in this area. The user can either connect to macro cell BS or communicate with pico cell BS. It is really hard to find a universal strategy in this situation, because it depends on the number users in this small cell and also the system has to know all users' QoS. Moreover, for each user, the interference from other users and other cells should be taken into account. Game theory is a good choice for this kind of problem. The Nash Equilibrium, as the optimized solution of a non-cooperative game, indicates that for any user, it cannot get more utility by changing its strategy. Past research on HetNet using Game Theory covered many aspects. [42] analyzed cooperation and

competition games in MIMO HetNets. [43] studied the information rate for a MIMO system using Game theory. However, very few papers focus on Massive MIMO in HetNets.

In this chapter, we consider a scenario that one macro cell and several small cells deploy in HetNets, and massive MIMO are equipped on all BSs and users. Each link between BS antennas and user antennas working in full-duplex mode which allow nodes to exchange information simultaneously. Due to the full-duplex, each pair of nodes is suffered from self-interference, and the inter-user interference is considered in our model. The game theoretical approach is applied in this problem to find an optimal access strategy. For each user device and all BS, power constraint is considered, and the system total power consumption is limited.

The rest of this chapter is organized as follows. Section 2.2 introduces the system scenarios, and a system model is built. In Section 2.3, a cooperative game is introduced to achieve the maximum sum-rate with an optimal user access strategy. Some numerical results as well as essential analysis are provided in Section 2.4. Finally, conclusions on this research are made in the last section of this chapter.

## 2.2 System Model

In this section, a HetNet with Massive MIMO will be modeled. It is a cellular system in which both macro cell and small cells communicate with users in full-duplex mode. Thus BS can transmit(receive) data to(from) multiple users simultaneously. It is assumed that users are communicating with BS in half-duplex mode. In this area as shown in Figure 2.1, there are two types of users. Some users have to connect to macro cell as they are not covered by pico cell signals. Another situation is that



users have to connect to macro cell because the small cell has too many users to serve and it reaches the capacity limit defined by the system. The other type of users is to connect to small cells.

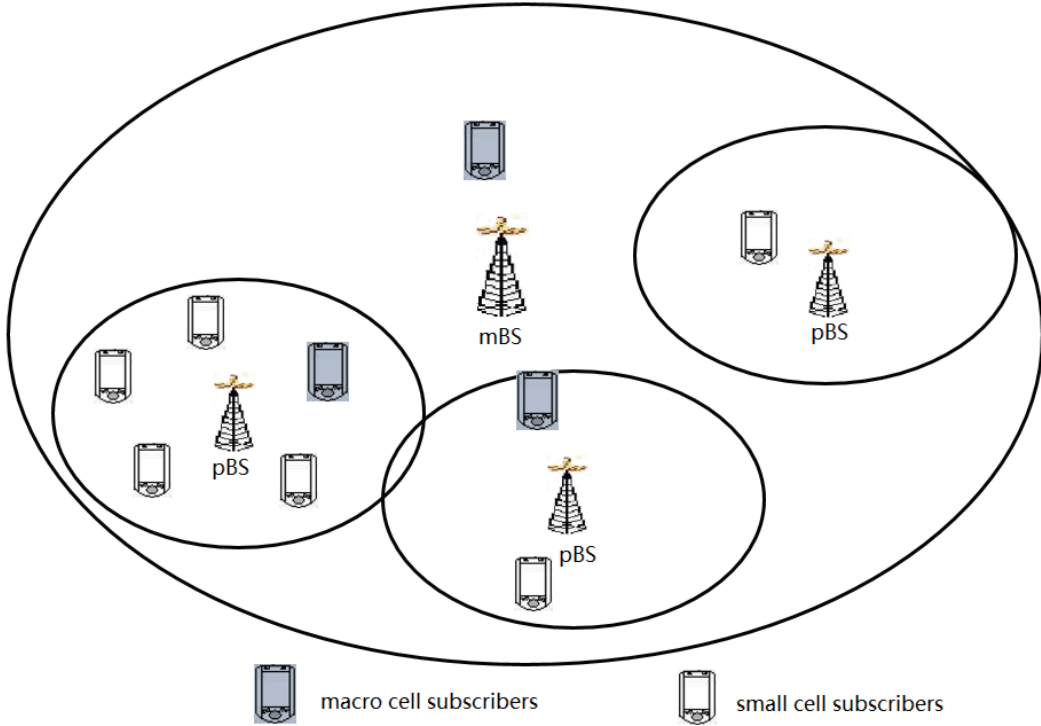


Figure 2.1. HetNets scenario.

Assume there are  $K$  uplink (UL) users and  $J$  downlink (DL) users in this area and they will be served by macro and pico cells. There are  $M_0$  transmission and  $N_0$  receiving antennas equipped by macro cell BS. And for each small cell BS, it has  $M_s$  antennas for DL transmission and  $N_s$  antennas for receiving data from its subscribers.  $M_k$  denotes  $k$ -th UL user's antenna number and  $N_j$  is the  $j$ -th DL user's antenna number respectively,  $k = 1, \dots, K$  and  $j = 1, \dots, J$ . And  $d_k^{UL}$  represents the number of data steams transmitted from  $k$ -th UL user. Similarly,  $d_j^{DL}$  is the number

of data streams transmitted to j-th DL user.

For the UL channel, if the user communicates with p-th small cell BS, we have  $H_{k,SC_p}^{UL} \in C^{N_s * M_k}$  to represent the k-th UL user's channel. And if k-th user transmits data to mBS, then the channel is  $H_{k,mBS}^{UL} \in C^{N_0 * M_k}$ .

For the DL channel, if the user communicates with p-th small cell BS, we have  $H_{j,SC_p}^{DL} \in C^{N_j * M_s}$  to represent the j-th DL user's channel. And if j-th user receives data from mBS, then the channel is  $H_{j,mBS}^{DL} \in C^{N_j * M_0}$ .

Several types of interference are considered in this model.  $H_p^{mS} \in C^{N_s * M_0}$  denotes the CCI channel from DL of mBS to reception antenna of p-th small cell BS.  $H_p^{Sm} \in C^{N_0 * M_s}$  is the CCI channel from DL of small cell BS to reception antenna of mBS. And  $H_{jk}^{DU} \in C^{N_j * M_k}$  represents CCI channel from k-th UL user to j-th DL user.  $H_{mBS} \in C^{N_0 * M_0}$  denotes the self-interference channel from transmission antennas to reception antennas of mBS. Respectively,  $H_{SC_p} \in C^{N_s * M_s}$  denotes the self-interference channel from transmission antennas to reception antennas of p-th small cell BSs.

Figure 2.2 illustrates all channels considered in this model. User's device is working in half-duplex mode. So when it's transmitting data, it cannot receive at the same time. So it does not have the self-interference.

The original symbols need precoding process before transmitting. For the UL process,  $V_k^{UL,mBS} = [V_{k,1}^{UL,mBS}, \dots, V_{k,d_k^{UL}}^{UL,mBS}] \in C^{M_k * d_k^{UL}}$  denotes the precoders for transmission data stream from k-th UL user if the user connect to mBS. And if the user is a p-th small cell's subscriber, the precoders of data stream should

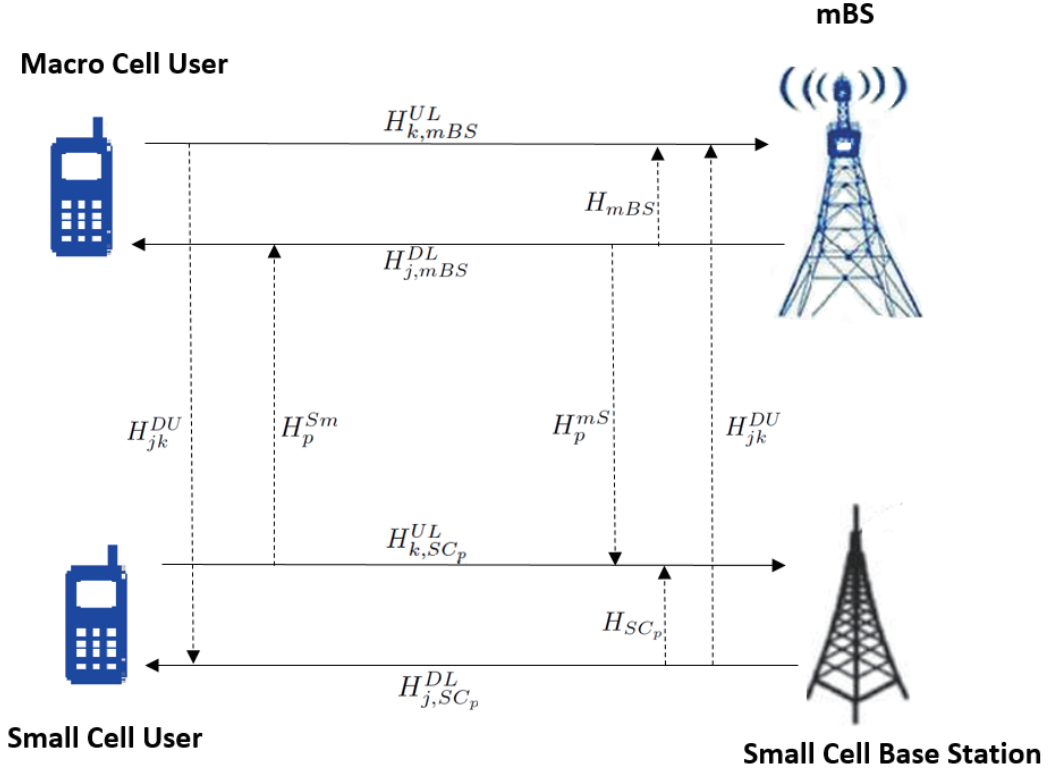


Figure 2.2. Full-duplex Massive MIMO Channels.

be  $V_k^{UL,SC_p} = [V_{k,1}^{UL,SC_p}, \dots, V_{k,d_k^{UL}}^{UL,SC_p}] \in C^{M_k * d_k^{UL}}$ . Respectively, for the DL process,  $V_j^{DL,mBS} = [V_{j,1}^{DL,mBS}, \dots, V_{j,d_j^{DL}}^{DL,mBS}] \in C^{M_0 * d_j^{DL}}$  denotes the precoders for j-th user's DL data stream if user connect to mBS. Similarly,  $V_j^{DL,SC_p} = [V_{j,1}^{DL,SC_p}, \dots, V_{j,d_j^{DL}}^{DL,SC_p}] \in C^{M_k * d_j^{DL}}$  represents the precoders for j-th user's DL data stream if the user receives signals from p-th small cell BS.

The k-th UL user's transmission source symbols is represented as  $S_k^{UL} = [S_{k,1}^{UL}, \dots, S_{k,d_k^{UL}}^{UL}]^T$ . Similarly,  $S_j^{DL} = [S_{j,1}^{DL}, \dots, S_{j,d_j^{DL}}^{DL}]^T$  denotes the transmitted source symbols to j-th DL user. As in [44], we assumed that the symbols are i.i.d. with unit power ( $E[S_k^{UL}(S_k^{ULH})] = I_{d_k^{UL}}, E[S_j^{DL}(S_j^{DLH})] = I_{d_j^{DL}}$ ). Then we can define the transmitted

signal of k-th UL user as follows:

$$X_k^{UL,mBS} = V_k^{UL,mBS} \cdot S_k^{UL} \quad (2.1)$$

$X_k^{UL,mBS}$  denotes the k-th user sending its signal to mBS, and if user upload data to p-th small cell BS, the signal should be written as:

$$X_k^{UL,SC_p} = V_k^{UL,SC_p} \cdot S_k^{UL} \quad (2.2)$$

Likewise, for the DL, we can define the signal transmitted from mBS and p-th small cell BS as:

$$X_{mBS} = \sum_{j=1, j \in J^{mBS}}^J V_j^{DL,mBS} \cdot S_j^{DL} \quad (2.3)$$

$$X_{SC_p} = \sum_{j=1, j \in J^{SC_p}}^J V_j^{DL,SC_p} \cdot S_j^{DL} \quad (2.4)$$

Where  $J^{mBS} \in J$  is a user set denotes the user who receives DL data from mBS. And p-th small cell BS provides DL service to the user in user set  $J^{SC_p}$ ,  $J^{SC_p} \in J$ .  $J^{mBS} \cup J^{SC_1} \dots \cup J^{SC_p} \dots \cup J^{SC_P} = J$ .

As CCI and self-interference are considered in this Full-duplex massive MIMO HetNet system, the received signal transmitted by k-th user at mBS could be written as:

$$\begin{aligned}
y_{mBS} = & \sum_{k=1, k \in K^{mBS}}^K H_{k,mBS}^{UL} (X_k^{UL,mBS} + c_k^{UL,mBS}) + \sum_{p=1}^P H_p^{Sm} (X_{SC_p} + c_{SC_p}) \\
& + H_{mBS} (X_{mBS} + c_{mBS}) + e_{mBS} + n_{mBS}
\end{aligned} \tag{2.5}$$

Where  $c_k^{UL,mBS}$  is the transmitter distortion at k-th UL user,  $c_{SC_p}(c_{mBS})$  denotes the transmitter distortion at p-th small cell BS(mBS).  $e_{mBS}$  is the receiver distortion at mBS and  $n_{mBS}$  is the AWGN with zero mean unit covariance matrix at mBS.

If k-th user transmit data to p-th small cell BS, the received signal by the BS should be:

$$\begin{aligned}
y_{SC_p} = & \sum_{k=1, k \in K^{SC_p}}^K H_{k,SC_p}^{UL} (X_k^{UL,SC_p} + c_k^{UL,SC_p}) + H_p^{mS} (X_{mBS} + c_{mBS}) \\
& + H_{SC_p} (X_{SC_p} + c_{SC_p}) + e_{SC_p} + n_{SC_p}
\end{aligned} \tag{2.6}$$

Similar as before,  $c_k^{UL,SC_p}$  represents the transmitter distortion at k-th UL user in p-th small cell.  $e_{SC_p}$  is the receiver distortion at p-th small cell BS and  $n_{SC_p}$  is the AWGN with zero mean unit covariance matrix at small cell BS.

For j-th DL user, if the service provider is macro cell, then received signal can be written as:

$$\begin{aligned}
y_{j,mBS}^{DL} = & \sum_{j=1, j \in J^{mBS}}^J H_{j,mBS}^{DL} (X_{mBS} + c_{mBS}) \\
& + \sum_{k=1, j=1, k \in K^{mBS}, j \in J^{mBS}}^{K,J} H_{jk}^{DU} (X_k^{UL,mBS} + c_k^{UL,mBS}) \\
& + \sum_{p=1}^P \sum_{k=1, j=1, k \in K^{SC_p}, j \in J^{mBS}}^{K,J} H_{jk}^{DU} (X_k^{UL,SC_p} + c_k^{UL,SC_p}) \\
& + \sum_{p=1}^P \sum_{j=1, j \in J^{SC_p}}^J H_{j,SC_p}^{DL} (X_{SC_p} + c_{SC_p}) + e_j^{DL,mBS} + n_j^{DL,mBS}
\end{aligned} \tag{2.7}$$

The DL signal from mBS to j-th user  $y_{j,mBS}^{DL}$  contains several interference terms: CCI from UL signal of users in mBS to j-th user in mBS; CCI from UL signal of users in all small cells to j-th user in mBS; interference from all small cell BS DL signals. The other case is the user receives the data from p-th small cell BS and the signal can be represented as:

$$\begin{aligned}
y_{j,SC_p}^{DL} = & \sum_{j=1, j \in J^{SC_p}}^J H_{j,SC_p}^{DL} (X_{SC_p} + c_{SC_p}) \\
& + \sum_{k=1, j=1, k \in K^{mBS}, j \in J^{SC_p}}^{K, J} H_{jk}^{DU} (X_k^{UL, mBS} + c_k^{UL, mBS}) \\
& + \sum_{p=1}^P \sum_{k=1, j=1, k \in K^{SC_p}, j \in J^{SC_p}}^{K, J} H_{jk}^{DU} (X_k^{UL, SC_p} + c_k^{UL, SC_p}) \quad (2.8) \\
& + \sum_{i=1, i \neq p}^P \sum_{j=1, j \in J^{SC_i}}^J H_{j,SC_i}^{DL} (X_{SC_i} + c_{SC_i}) \\
& + H_{mBS} (X_{mBS} + c_{mBS}) + e_j^{DL, SC_p} + n_j^{DL, SC_p}
\end{aligned}$$

Where  $y_{j,SC_p}^{DL}$  contains following interference terms: CCI from UL signal of users in mBS to j-th user in small cell; CCI from UL signal of users in all small cells to j-th user in small cell; interference from all except p-th small cell BS DL signals.

[44] has provided an approach to model the transmitter and receiver distortion *c.e.* Transmitter distortion  $\mathbf{c} \in C^N$  includes phase noise, non-linearity in the DAC and effects of additive power amplifier noise. Its covariance is given as  $\gamma$  times energy of the signal that intends to be transmitted at each antenna ( $\gamma \ll 1$ ):

$$\mathbf{c} \sim \mathcal{CN}(\mathbf{0}, \gamma \text{diag}(\mathbf{V}\mathbf{V}^H)) \quad (2.9)$$

$\mathbf{c}$  and transmitted signal  $\mathbf{X}$  are statistical independent:  $\mathbf{c} \perp \mathbf{X}$

The distortion of receiver  $\mathbf{e} \in C^M$  contains phase noise, non-linearity in the ADC and combined effects of additive gain control noise. It can be modeled as:

$$\mathbf{e} \sim \mathcal{CN}(\mathbf{0}, \eta \text{diag}(\Phi)) \quad (2.10)$$

$\Phi = \text{Cov}(\mathbf{r})$  and  $\mathbf{r}$  is the undistorted signal ( $\mathbf{r} = \mathbf{y} - \mathbf{e}$ ).  $\mathbf{e}$  and  $\mathbf{r}$  are statistical independent:  $\mathbf{e} \perp \mathbf{r}, \eta \ll 1$

We can extract the interference and noise terms of UL and DL users, based on 2.52.62.72.8.

$$\begin{aligned} m_k^{UL,mBS} &= \sum_{t=1, t \neq k}^K H_{t,mBS}^{UL} X_t^{UL,mBS} + \sum_{t=1}^K H_{t,mBS}^{UL} c_t^{UL,mBS} \\ &\quad + \sum_{p=1}^P H_p^{Sm}(X_{SC_p} + c_{SC_p}) + H_{mBS}(X_{mBS} + c_{mBS}) + e_{mBS} + n_{mBS} \end{aligned} \quad (2.11)$$

$$\begin{aligned} m_k^{UL,SC_p} &= \sum_{t=1, t \neq k}^K H_{t,SC_p}^{UL} X_t^{UL,SC_p} + \sum_{t=1}^K H_{t,SC_p}^{UL} c_t^{UL,SC_p} + H_p^{mS}(X_{mBS} + c_{mBS}) \\ &\quad + \sum_{r=1, r \neq p}^P H_{SC_r}(X_{SC_r} + c_{SC_r}) + e_{SC_p} + n_{SC_p} \end{aligned} \quad (2.12)$$

$$\begin{aligned}
m_j^{DL,mBS} &= H_{j,mBS}^{DL} \sum_{i=1, i \neq j}^J V_i^{DL,mBS} S_i^{DL} + H_{j,mBS}^{DL} c_{mBS} \\
&+ \sum_{k=1, t=1, k \in K^{mBS}, t \in J^{mBS}}^{K, J} H_{tk}^{DU} (X_k^{UL,mBS} + c_k^{UL,mBS}) \\
&+ \sum_{p=1}^P \sum_{k=1, k \in K^{SC_p}}^K H_{jk}^{DU} (X_k^{UL,SC_p} + c_k^{UL,SC_p}) \\
&+ \sum_{p=1}^P \sum_{t=1, t \in J^{SC_p}}^J H_{t,SC_p}^{DL} (X_{SC_p} + c_{SC_p}) \\
&+ e_j^{DL,mBS} + n_j^{DL,mBS}
\end{aligned} \tag{2.13}$$

$$\begin{aligned}
m_j^{DL,SC_p} &= H_{j,SC_p}^{DL} \sum_{i=1, i \neq j}^J V_i^{DL,SC_p} S_i^{DL} + H_{j,SC_p}^{DL} c_{SC_p} \\
&+ \sum_{k=1, k \in K^{mBS}}^K H_{jk}^{DU} (X_k^{UL,mBS} + c_k^{UL,mBS}) \\
&+ \sum_{p=1}^P \sum_{k=1, k \in K^{SC_p}}^{K, J} H_{jk}^{DU} (X_k^{UL,SC_p} + c_k^{UL,SC_p}) \\
&+ \sum_{i=1, i \neq p}^P \sum_{t=1, t \in J^{SC_i}}^J H_{t,SC_i}^{DL} (X_{SC_i} + c_{SC_i}) \\
&+ H_{mBS} (X_{mBS} + c_{mBS}) + e_j^{DL,SC_p} + n_j^{DL,SC_p}
\end{aligned} \tag{2.14}$$

The covariance matrix of  $m_k^{UL,mBS}$  is denoted as  $\Sigma_k^{UL,mBS}$ , similarly,  $Cov(m_k^{UL,SC_p}) = \Sigma_k^{UL,SC_p}$ ,  $Cov(m_j^{DL,mBS}) = \Sigma_j^{DL,mBS}$  and  $Cov(m_j^{DL,SC_p}) = \Sigma_j^{DL,SC_p}$ .

According to equation 2.92.10 and under  $\gamma \ll 1, \eta \ll 1$  we can approximately calculate the covariance matrix. For example,  $\Sigma_k^{UL,mBS}$  and  $\Sigma_j^{DL,mBS}$  are derived in equations 2.15 and 2.16. Similarly,  $\Sigma_k^{UL,SC_p}$  and  $\Sigma_j^{DL,SC_p}$  can be defined.

We have derived the received signal as well as the interference terms. To calculate the rate, a decoding process has to be apply to the received signals. Receivers



$$\begin{aligned}
\Sigma_k^{UL,mBS} &= \sum_{t=1, t \neq k}^K H_{t,mBS}^{UL} V_t^{UL,mBS} (V_t^{UL,mBS})^H (H_{t,mBS}^{UL})^H \\
&+ \gamma \sum_{t=1}^K H_{t,mBS}^{UL} \text{diag}(V_t^{UL,mBS} (V_t^{UL,mBS})^H) (H_{t,mBS}^{UL})^H \\
&+ \sum_{p=1}^P \sum_{t=1, t \in J^{SC_p}}^J H_p^{Sm} (V_t^{DL,SC_p} (V_t^{DL,SC_p})^H + \gamma \text{diag}(V_t^{DL,SC_p} (V_t^{DL,SC_p})^H)) (H_p^{Sm})^H \\
&+ \sum_{t=1}^J H_{mBS} (V_t^{DL,mBS} (V_t^{DL,mBS})^H + \gamma \text{diag}(V_t^{DL,mBS} (V_t^{DL,mBS})^H)) (H_{mBS})^H \\
&+ \eta \sum_{t=1}^K \text{diag}(H_{t,mBS}^{UL} V_t^{UL,mBS} (V_t^{UL,mBS})^H (H_{t,mBS}^{UL})^H) \\
&+ \eta \sum_{t=1}^J \text{diag}(H_{mBS} V_t^{DL,mBS} (V_t^{DL,mBS})^H (H_{mBS})^H + I_{N_{UL,mBS}})
\end{aligned} \tag{2.15}$$

need a decoding vector to get the decoded data stream based on received signal, which can be written as  $\mathbf{U}_{k,k \in K^{mBS}}^{UL,mBS} = [\mathbf{u}_{k,1}^{UL,mBS}, \dots, \mathbf{u}_{k,d_k^{UL}}^{UL,mBS}]$  for k-th UL user's decoder at mBS. And  $\mathbf{U}_{k,k \in K^{SC_p}}^{UL,SC_p} = [\mathbf{u}_{k,1}^{UL,SC_p}, \dots, \mathbf{u}_{k,d_k^{UL}}^{UL,SC_p}]$  is the decoder at p-th small cell BS. Similarly, the decoder at j-th DL user can be written as  $\mathbf{U}_j^{DL,SC_p} = [\mathbf{u}_{j,1}^{DL,SC_p}, \dots, \mathbf{u}_{j,d_k^{DL,SC_p}}^{DL,SC_p}]$  or  $\mathbf{U}_j^{DL,mBS} = [\mathbf{u}_{j,1}^{DL,mBS}, \dots, \mathbf{u}_{j,d_k^{DL,mBS}}^{DL,mBS}]$ .

Based on the interference equation and decoding vectors, the signal to interference plus noise ratio can be derived. For k-th UL user in mBS, the h-th data stream's SINR can be written as:

$$\begin{aligned}
\Sigma_j^{DL,mBS} = & \sum_{i=1, i \neq j}^J H_{j,mBS}^{DL} V_i^{DL,mBS} (V_i^{DL,mBS})^H (H_{j,mBS}^{DL})^H \\
& + \gamma H_{j,mBS}^{DL} \text{diag}(V_j^{DL,mBS} (V_j^{DL,mBS})^H) (H_{j,mBS}^{DL})^H \\
& + \sum_{k=1, t=1, k \in K^{mBS}, t \in J^{mBS}}^{K, J} H_{tk}^{DU} (V_k^{UL,mBS} (V_k^{UL,mBS})^H) \\
& + \gamma \text{diag}(V_k^{UL,mBS} (V_k^{UL,mBS})^H) (H_{tk}^{DU})^H \\
& + \sum_{p=1}^P \sum_{k=1, k \in K^{SCp}}^K H_{tk}^{DU} (V_k^{UL,SCp} (V_k^{UL,SCp})^H) + \gamma \text{diag}(V_k^{UL,SCp} (V_k^{UL,SCp})^H) (H_{tk}^{DU})^H \\
& + \sum_{p=1}^P \sum_{t=1, t \in J^{SCp}}^J H_{t,SCp}^{DL} (V_t^{DL,SCp} (V_t^{DL,SCp})^H) + \gamma \text{diag}(V_t^{DL,SCp} (V_t^{DL,SCp})^H) (H_{t,SCp}^{DL})^H \\
& + \eta \sum_{i=1}^J \text{diag}(H_{i,mBS}^{DL} V_i^{DL,mBS} (V_i^{DL,mBS})^H (H_{i,mBS}^{DL})^H) \\
& + \eta \sum_{k=1, t=1}^{K, J} \text{diag}(H_{tk}^{DU} V_k^{UL,mBS} (V_k^{UL,mBS})^H (H_{tk}^{DU})^H) + I_{N_{DL,mBS}}
\end{aligned} \tag{2.16}$$


---

$$\begin{aligned}
\rho_{k,h}^{UL,mBS} = & \frac{\left| (\mathbf{u}_{k,h}^{UL,mBS})^H H_{k,mBS}^{UL} V_{k,h}^{UL,mBS} \right|^2}{(\mathbf{u}_{k,h}^{UL,mBS})^H \Sigma_k^{UL,mBS} \mathbf{u}_{k,h}^{UL,mBS} + \sum_{g \neq h}^{d_k^{UL}} \left| (\mathbf{u}_{k,h}^{UL,mBS})^H H_{k,mBS}^{UL} V_{k,h}^{UL,mBS} \right|^2}
\end{aligned} \tag{2.17}$$

If the user is connecting to p-th small cell,

$$\rho_{k,h}^{UL,SC_p} = \frac{\left| (\mathbf{u}_{k,h}^{UL,SC_p})^H H_{k,SC_p}^{UL} V_{k,h}^{UL,SC_p} \right|^2}{(\mathbf{u}_{k,h}^{UL,SC_p})^H \sum_k^{UL,SC_p} \mathbf{u}_{k,h}^{UL,SC_p} + \sum_{g \neq h}^{d_k^{UL}} \left| (\mathbf{u}_{k,h}^{UL,SC_p})^H H_{k,SC_p}^{UL} V_{k,h}^{UL,SC_p} \right|^2} \quad (2.18)$$

Likewise, DL SINR for j-th user can be formulated as:

$$\rho_{j,h}^{DL,mBS} = \frac{\left| (\mathbf{u}_{j,h}^{DL,mBS})^H H_{j,mBS}^{DL} V_{j,h}^{DL,mBS} \right|^2}{(\mathbf{u}_{j,h}^{DL,mBS})^H \sum_j^{DL,mBS} \mathbf{u}_{j,h}^{DL,mBS} + \sum_{g \neq h}^{d_j^{DL}} \left| (\mathbf{u}_{j,h}^{DL,mBS})^H H_{j,mBS}^{DL} V_{j,h}^{DL,mBS} \right|^2} \quad (2.19)$$

$$\rho_{j,h}^{DL,SC_p} = \frac{\left| (\mathbf{u}_{j,h}^{DL,SC_p})^H H_{j,SC_p}^{DL} V_{j,h}^{DL,SC_p} \right|^2}{(\mathbf{u}_{j,h}^{DL,SC_p})^H \sum_j^{DL,SC_p} \mathbf{u}_{j,h}^{DL,SC_p} + \sum_{g \neq h}^{d_j^{DL}} \left| (\mathbf{u}_{j,h}^{DL,SC_p})^H H_{j,SC_p}^{DL} V_{j,h}^{DL,SC_p} \right|^2} \quad (2.20)$$

### 2.3 Resource Allocation Game

In this Section, a game model will be established for the system to achieve maximum sum-rate. Transmit power constraint is considered in this game. An example

is shown to explain how this algorithm works.

The game theory is a useful tool in complex decision problem, especially in resource allocation problem. General speaking, there are two types of games, non-cooperative game and cooperative game [45]. The major different thing is cooperative game allows players(agents) act as a group and finally get a everyone acceptable utility allocation [10]. Besides, there is a special game although it belongs to cooperative game, it has to use a non-cooperative method to find out the solution. It allows some limited cooperation. In [46]'s research, three game theoretical resource allocation mechanisms are considered, analyzed and compared, the cooperative game has high computational complexity. But there are several advantages on performance compare to non-cooperative game. Non-cooperative games may have multiple Nash Equilibrium (NE) points. Sometimes the optimal solution may not be found among those NE points. For instance, in the famous problem of Prisoner's Dilemma, the best choice is not the NE point [47]. It is noteworthy that cellular communication system is not a delay-tolerant system because of some new technologis applied i.e. VoLTE [48].

For a game, there are three essential elements: players, strategies and the utility(payoff). In this paper, users which covered by small cell can be treated as players. Players include UL and DL users in all small cells and it can be wrote as  $\{K^{SC_p}, J^{SC_p}\}$ .  $\{A_{SC_p}^{UL}, A_{SC_p}^{DL}\}$  denotes the actions or strategies which can be took by players. Let  $\Psi$  be the utility which the system can get. Then this game can be defined as:

$$G = \langle \{K^{SC_p}, J^{SC_p}\}, \{A_{SC_p}^{UL}, A_{SC_p}^{DL}\}, \Psi \rangle \quad (2.21)$$

### 2.3.1 The Game model

As shown in Fig.1, there are two types of users. For some users, they are not covered by pico cell signals and they have to connect to macro cell. However, some users are located in a small cell covered area, that means they can choose either mBS or small cell BS to get better service. In other words, users in user set  $K^{mBS}$  and  $J^{mBS}$  have no choice but to communicate with mBS. To simplify the optimization problem, we only consider the strategies of users in small cell. For users in user set  $K^{SC_p}$  and  $J^{SC_p}$ , the strategy set can be written as:

$$\begin{aligned} A_{SC_p}^{UL} &= \{a_{1^{SC_p}}^{UL}, a_{2^{SC_p}}^{UL}, \dots, a_{k^{SC_p}}^{UL}\}, \\ A_{SC_p}^{DL} &= \{a_{1^{SC_p}}^{DL}, a_{2^{SC_p}}^{DL}, \dots, a_{j^{SC_p}}^{DL}\} \end{aligned} \quad (2.22)$$

Where,

$$\begin{aligned} a_{k^{SC_p}}^{UL} &= \{mBS\} \text{ or } \{SC_p\}, \\ a_{j^{SC_p}}^{DL} &= \{mBS\} \text{ or } \{SC_p\} \end{aligned} \quad (2.23)$$

The utility function of p-th small cell can be defined as:

$$\arg \max_{A_{SC_p}^{UL*}, A_{SC_p}^{DL*}} \Psi_p(a_{1^{SC_p}}^{UL*}, \dots, a_{k^{SC_p}}^{UL*}, a_{1^{SC_p}}^{DL*}, \dots, a_{j^{SC_p}}^{DL*}) \quad (2.24)$$

The optimal solution can be written as:

$$\Psi^* = \Psi(\{A_{SC_p}^{UL*}, A_{SC_p}^{DL*}\}) \quad (2.25)$$

The utility function can be consider as the sum-rate of system, which means to maximize the utility, system allows users to choose strategies. The utility function based on previous system model can be represented as:

$$\begin{aligned}
\Psi = & \max_{A_{SC_P}^{UL}, A_{SC_P}^{DL}} \sum_{k=1, k \in K^{mBS}}^K \sum_{h=1}^{d_k^{UL, mBS}} \log_2(1 + \rho_{k,h}^{UL, mBS}) \\
& + \sum_{p=1}^P \sum_{k=1, k \in K^{SC_P}}^K \sum_{h=1}^{d_k^{UL, SC_P}} \log_2(1 + \rho_{k,h}^{UL, SC_P}) \\
& + \sum_{j=1, j \in J^{mBS}}^J \sum_{h=1}^{d_j^{DL, mBS}} \log_2(1 + \rho_{j,h}^{DL, mBS}) \\
& + \sum_{p=1}^P \sum_{j=1, j \in J^{SC_P}}^J \sum_{h=1}^{d_j^{DL, SC_P}} \log_2(1 + \rho_{j,h}^{DL, SC_P})
\end{aligned} \tag{2.26}$$

The power constraints should be considered, for BS and k-th user we have:

$$\sum_{h=1}^{d_k^{UL, mBS}} (V_{k,h}^{UL, mBS})^H V_{k,h}^{UL, mBS} \leq P_{user} \tag{2.27}$$

$$\sum_{h=1}^{d_k^{UL, SC_P}} (V_{k,h}^{UL, SC_P})^H V_{k,h}^{UL, SC_P} \leq P_{user} \tag{2.28}$$

If UL power can be considered as the individual power consumption, then the DL power at base station is the sum of DL transmissions to all users and it can be denoted as:

$$\sum_{j=1, j \in J^{mBS}}^J \sum_{h=1}^{d_j^{DL, mBS}} (V_{j,h}^{DL, mBS})^H V_{j,h}^{DL, mBS} \leq P_{mBS} \tag{2.29}$$

$$\sum_{j=1, j \in J^{SC_P}}^J \sum_{h=1}^{d_j^{DL, SC_P}} (V_{j,h}^{DL, SC_P})^H V_{j,h}^{DL, SC_P} \leq P_{SC_P} \tag{2.30}$$

### 2.3.2 An Example

Following is an example to show you how this game works. Suppose there is one device located in a small cell and of course it is also been covered by macro cell. This small cell's id is 5 in whole system which means  $p = 5$ .  $H_{3,SC_5}^{UL}$  represents the UL channel if this device connects to small cell and it is the 3rd UL user in 5-th small cell.  $H_{4,SC_5}^{DL}$  is the DL channel and this device is the 4th DL user in 5th small cell. The index  $k = 3 \neq j = 4$  is because some devices in this small cell may only downloading data from network because they are working in half-duplex mode as we mentioned at the beginning. Similarly, if this device connect to mBS,  $H_{20,mBS}^{UL}$  and  $H_{36,mBS}^{DL}$  denote the UL and DL channel. The index  $k = 20$  and  $j = 36$ , as an example, means this device is the 20-th UL user and 36-th DL user in mBS.

Simply put, each device covered by both cells has two choices, small cell and macro cell. Before the connection setting up, all channels must be tested. In this example,  $H_{3,SC_5}^{UL}$ ,  $H_{4,SC_5}^{DL}$ ,  $H_{20,mBS}^{UL}$  and  $H_{36,mBS}^{DL}$  are known by the system. If the device is connected to small cell,  $H_{3,SC_5}^{UL}$  and  $H_{4,SC_5}^{DL}$  are activated and  $H_{20,mBS}^{UL}$  and  $H_{36,mBS}^{DL}$  are known but not been used. Like this device, all users covered by small cells have two choices and each of them has four channels must be tested before data transmitting.

DL	User1	User2	User3	User4
mBS	$H_{36,mBS}^{DL}$	$H_{37,mBS}^{DL}$	$H_{38,mBS}^{DL}$	$H_{39,mBS}^{DL}$
5th small cell	$H_{1,SC_5}^{DL}$	$H_{2,SC_5}^{DL}$	$H_{3,SC_5}^{DL}$	$H_{4,SC_5}^{DL}$

Table 2.1. DL users in 5th small cell

Table 2.1 illustrates an example of possible channel parameters of DL users in 5th small cell. As each user has two choices, for these 4 users, there are totally  $2^4 = 16$  possible cases. The strategy set  $S_{SC_5}^{DL}$  has 16 elements in this example.

Likewise, we can assume there are 3 users in 5th small cell are planning to do UL transmission. Their transmission channel to small cell base station and mBS can be find in following table:

UL	User1	User2	User3
mBS	$H_{20,mBS}^{UL}$	$H_{21,mBS}^{UL}$	$H_{22,mBS}^{UL}$
5th small cell	$H_{1,SC_5}^{UL}$	$H_{2,SC_5}^{UL}$	$H_{3,SC_5}^{UL}$

Table 2.2. UL users in 5th small cell

As each user has two choices, for these 3 UL users, there are totally  $2^3 = 8$  possible cases. The strategy set  $S_{SC_5}^{UL}$  has 8 elements in this example.

If we use this cooperative game to find out the optimal allocation plan among 5-th small cell, the algorithm will calculate the utility function with all possible strategies. In this case, system has to repeat  $16 \cdot 8 = 128$  times on utility function calculation, and then search and find the largest value. This value is the optimal solution of this problem, and this strategy could be called optimal solution.



## 2.4 Performance Analysis

In this section, we evaluate the performance of game theoretical method in sum-rate maximization problem. In order to simplify the experiment, 1 mBS and 2 small cells inside the macro cell are deployed.

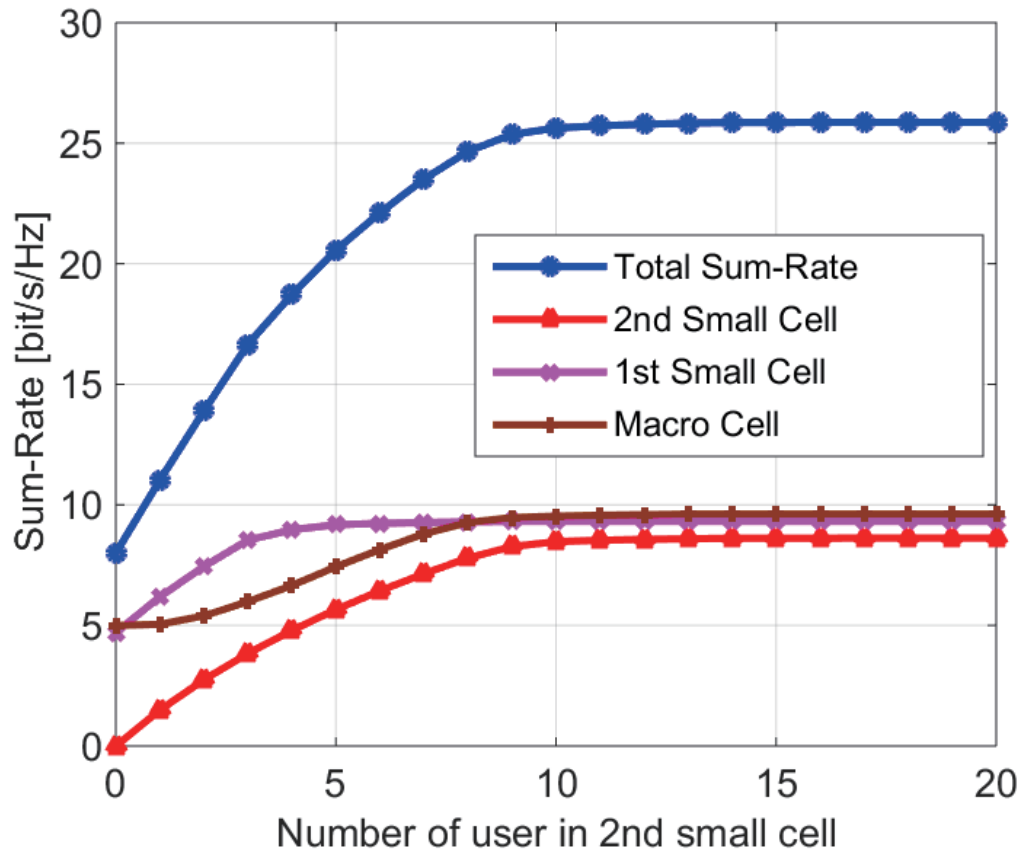


Figure 2.3. Access scheduling by applying game theoretical method.

Figure 2.3 illustrates the achievable sum-rate of system and cells, as user number changing in specific area. Assumed that in macro cell there are 5 users and 10 users are staying in 1st small cell. The number of user in 2nd small cell is increasing from 0 to 15,  $SNR = 10dB$ . It shows that the total sum-rate (system sum-rate) is

increasing as more connections established, and finally, it converges due to the total power constraint. Sum-rate of 1st small cell increases because previously, some users in small cell 1 are served by macro cell. When total user number in this area increased, macro cell has to allocate some resource to support. That's why small cell 1 is affected by other small cell. It shows the advantages of game theoretical method in resource allocation and access scheduling.

The comparison of sum-rate with game theoretical method and non-optimization are shown in Figure 3.9. In this case, we fixed the interference to noise ratio to 20 dB. As the SNR increasing, the sum-rate of system increases, for both non-optimized model and game theory applied model. Apparently, after game theory applied, the system can achieve higher sum-rate.

Consider this system is working under full-duplex mode, self interference is a very important parameter. In Figure 2.5, the effect of self interference is examined.

Compared to baseline method, the game theoretical method has better sum rate performance for the same self interference. As the self interference increasing, sum rate drop quickly, especially after 40 dB in this experiment. It must be a very significant aspect that to keep the self interference in a low level in Full-duplex communication.

Figure 2.6 shows the sum-rate calculation with different power constraints applied. It turns out that the power constraint of base station is more relax than users' power constraints. The sum-rate after game theoretical method applied is higher than baseline method. As it's required, the system can allocate more power to the base station for DL transmission. The main obstacle to improve system sum-rate is still

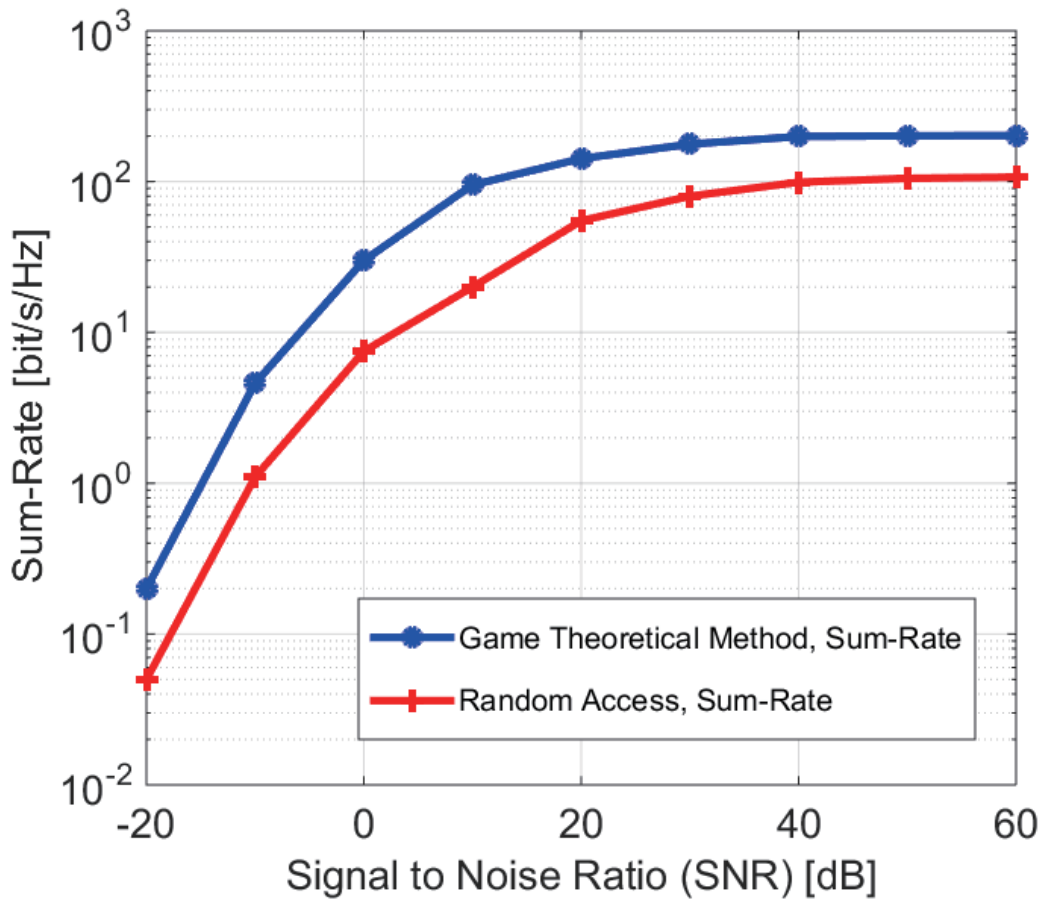


Figure 2.4. Sum-Rate comparison versus signal to noise ratio.

the user side power constraint. Due to the physical limitation, user's device cannot allocate too much power on transmitting and receiving data.

## 2.5 Conclusion

In this paper, we modeled a two-layer HetNets with Massive MIMO applied. The system works in Full-duplex mode. Even Full-duplex leads a huge interference, it is a more efficient system. The Game theoretical method is chosen to decline the effect of interference. And also it is a good tool to optimize the resource allocation

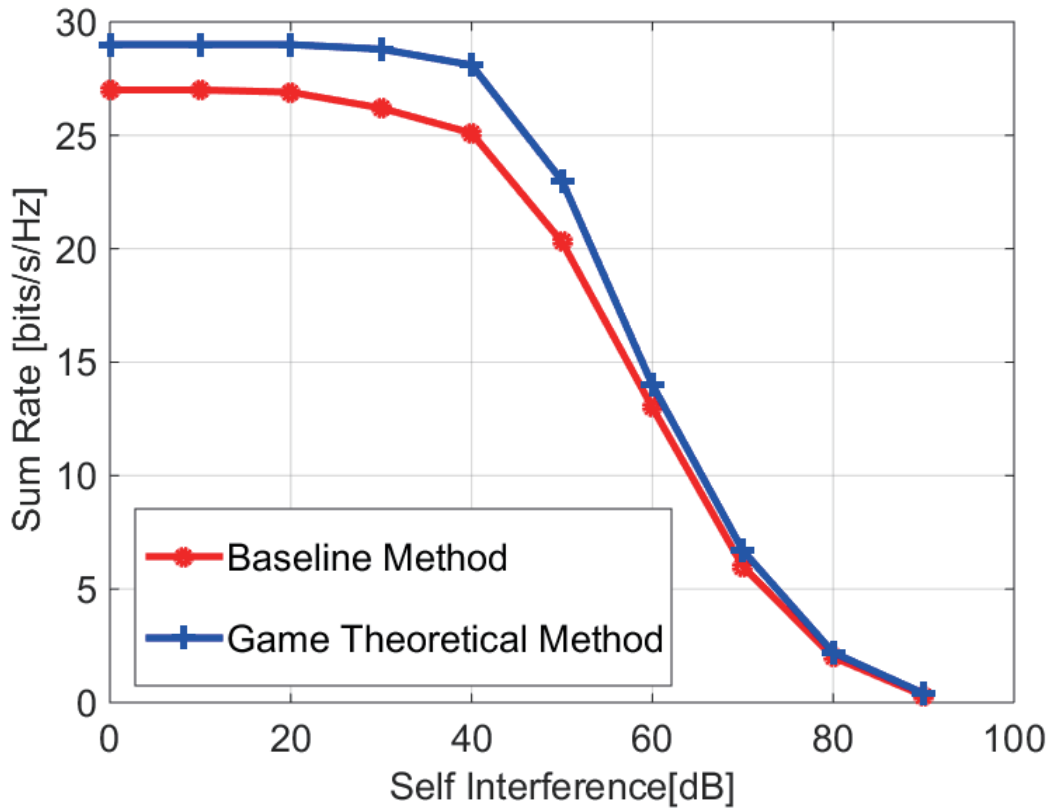


Figure 2.5. Sum-Rate versus Self Interference.

inside the system. By applying the Game theoretical method, the maximum system sum rate is reached. In the experiment Game theoretical method indeed perform better (higher sum rate) than base line method. For the power constraints, users' power constraint (UL transmission and DL receiving constraints) is the major factor which limits system's performance. It performed a better access scheduling in a dynamic system. And compared to non-optimized model, game theoretical method has a better anti-interference ability.

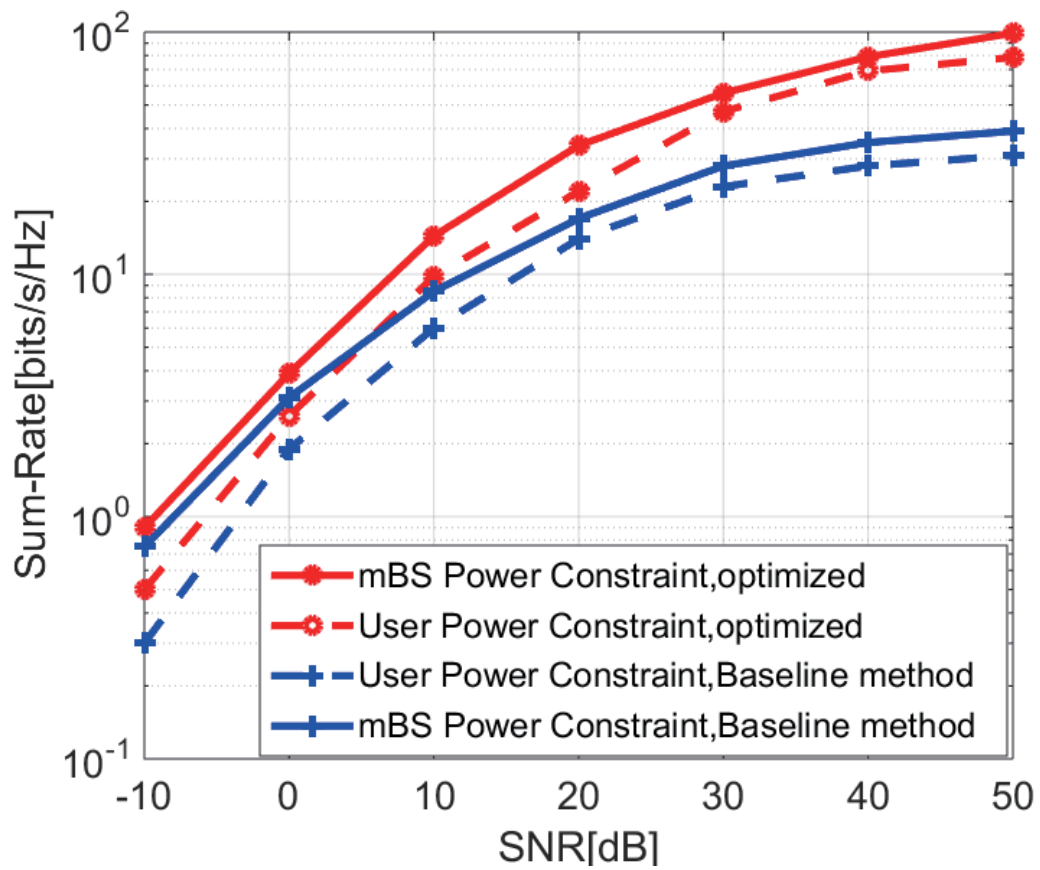


Figure 2.6. Sum-Rate with different power constraints versus SNR.

## CHAPTER 3

### Massive MIMO with Much Less Antennas Using Nested Placement

#### 3.1 Introduction

Along with development of the Internet technology, demand for data throughput will keep increasing. Recent years, smart devices become more popular as the breakthrough of hardware. At the same time, wireless communication becomes the most important way for people to get information from outside world. These mobile and massive number of user terminals which have a huge data demanded, bring a big challenge to our current communication and data networks. It could be as large as 100MB per user per second [49]. That means we may serious lack of wireless resources in densely populated area in the near future.

To solve the problem above, people proposed many solutions and all of them fall into one of three following categories:

1. Utilization of spectrum which is unused in cellular communication.
2. Deploy smaller cells which could improve the spectrum reuse rate.
3. Taking advantage of multiple antennas technology.

The first solution is depended on millimeter wave technology and the second one is trying to adequately use spectrum physically. The third one is known as Multiple Input Multiple Output(MIMO), which is always a hot topic in wireless communication as it been invented. Lots of research works on MIMO has been done on MIMO in past few years, this chapter will focus on Massive MIMO.

Massive MIMO is considered as a key technology in next generation wireless com-

munication system. Currently, up to 8 antennas is used in 4G LTE(release 12)[50]. There is no precise definition for massive MIMO technology, generally the number of antennas could scaling up to more than 100 [51]. [29] proposed a method which could achieve spectral efficiencies comparable with Massive MIMO, with fewer antennas. Massive MIMO could also be grouped to achieve a reduction in the CSI feedback overhead[52]. In [53], advantages of the huge degrees-of-freedom offered by massive MIMO was explored. A beam design approach for massive MIMO was proposed in [54].

However, on the other hand, there are still several intrinsic problems for Massive MIMO system. First, the electrical circuits complexity and the power consumption of this large scale system limit the system performance and the feasibility implementation [55] [56]. Besides, if massive MIMO antennas are considered as a cooperative network, the interference would discourage further improvement as increasing transmission power[57] and antenna number.

In this chapter, a novel Massive MIMO antenna network is proposed to facilitate the study on antenna placement and cooperation. The most attractive point of nested ditributed MIMO is it could achieve the same sum-rate capacity with less antennas. And also, this is the first literature on modeling and analyzing the cellular system with nested deployed MIMO antennas. Initially, nested array was proposed as a novel approach to enhance the degrees of freedom of an array[58]. Following that, [59][59] exhaustive discussed and studied the sensors' placement and degree of freedom analysis with nested-array configuration.

The rest of this chapter is organized as follows. Section 3.2 briefly introduces the theoretical background of two dimensional nested array. In Section 3.3, virtual channels of uplink and downlink of nested-distributed Massive MIMO antenna system

is modeled. Section 3.4 introduced the modeling of nested deployed antenna system. It also illustrates how to calculate sum rate capacity as well as the spectral efficiency based on zero forcing detector. After that, in Section 3.5 some numerical results are provided to verify the feasibility of our proposed scheme. Finally, we summarize our work on 2D Nested distributed Massive MIMO and make a conclusion in Section 3.6.

### 3.2 Preliminary Work

Firstly, let us review several important concepts related to multi-dimensional lattice and nested array, which are necessary for deriving our Massive MIMO placement method.

**Definition 1:** (Fundamental parallelepiped(FPD) [59]) *The FPD is defined as the set of all vectors of the following form:*

$$FPD(\mathbf{V}) = \{\mathbf{V}\mathbf{x}, \mathbf{x} \in [0, 1)^D\}$$

Where  $\mathbf{V} \in \mathbb{C}^{D \times D}$ . Apparently, the  $FPD(\mathbf{V})$  contains all points inside the parallelepiped and its two sides are actually given by two columns vectors of  $\mathbf{V}$ . The volume of  $FPD(\mathbf{V})$  is given by  $\|\det(\mathbf{V})\|$ , it represents the area in 2-D cases. And  $1/\|\det(\mathbf{V})\|$  is the density of arrays(antennas) correspondingly.

**Definition 2:** (Shift (SFPD)) *Consider  $k_1, k_2$  as two integers, the  $FPD(N^{(s)})$  shifted by  $[k_1, k_2]^T$  could obtain  $SFPD(N^{(s)})$ , mathematically could be defined as:*

$$SFPD(N^{(s)}, k_1, k_2) \equiv \{N^{(s)}([k_1, k_2]^T - x), x \in [0, 1)^2\}.$$

**Definition 3:** (Cross Difference Co-array) *let us consider an array of  $N$  antennas, with  $\vec{v}_n$  denoting the position of  $n$ -th sensor(antenna). Then the difference co-array could be written as:*

$$\{\vec{v}_n - \vec{v}_m\}, \forall m, n = 1, 2, \dots, N.$$



Based on difference co-array, the cross difference co-array could be considered as: given two arrays, one with  $N_1$  sensors with locations  $\{\vec{v}_{1i}, 1 \leq i \leq N_1\}$  and the other with  $N_2$  sensors with locations  $\{\vec{v}_{2i}, 1 \leq i \leq N_2\}$ , their cross difference co-array is defined as the set:

$$\pm\{\vec{v}_{1i} - \vec{v}_{2i}, 1 \leq i \leq N_1, 1 \leq i \leq N_2\}$$

**Definition 4:** (Two Dimensional Nested Array) A  $2 \times 2$  non-singular matrix  $\mathbf{N}^{(d)}$ , an integer matrix  $\mathbf{P}$  and integers  $N^{(s)}$  can be used to describe a two dimensional nested array.

1. A dense array generated by  $\mathbf{N}^{(d)}$  with  $N^{(d)} = \det[\mathbf{P}]$  elements on this dense lattice. And the sensors' locations given by  $\{\mathbf{N}^{(d)}\mathbf{n}^{(d)}, \mathbf{n}^{(d)} \in FPD(P)\}$ .
2. A sparse array generated by  $\mathbf{N}^{(s)} = \mathbf{N}^{(d)}\mathbf{P}$  with antennas' location given by:  $\{\mathbf{N}^{(s)}[k_1, k_2]^T, 0 \leq k_1 \leq N_1^{(s)} - 1, 0 \leq k_2 \leq N_2^{(s)} - 1\}$ .

**Theorem 1:** Consider two non-singular  $2 \times 2$  matrices  $\mathbf{N}^{(s)}$  and  $\mathbf{N}^{(d)}$  related by integer  $\mathbf{P}$  as  $\mathbf{N}^{(s)} = \mathbf{N}^{(d)}\mathbf{P}$ .

1. Any point on dense lattice  $\mathbf{N}^{(d)}$  has a location vector denoted as  $\mathbf{N}^{(d)}\mathbf{n}$ .  $\mathbf{N}^{(d)}\mathbf{n} = \mathbf{N}^{(s)}\mathbf{n}^{(s)} - \mathbf{N}^{(d)}\mathbf{n}^{(d)}$ , where  $\mathbf{n}^{(s)}$  is an integer vector and  $\mathbf{n}^{(d)} \in FPD(\mathbf{P})$ .
2. All points within  $SFPD(\mathbf{N}^{(s)}, k_1, k_2)$  can be generated by the differences:  $\{\mathbf{N}^{(s)}[k_1, k_2]^T - \mathbf{N}^{(d)}\mathbf{n}^{(d)}, \mathbf{n}^{(d)} \in FPD(\mathbf{P})\}$ .

### 3.3 Virtual Channel And System Model

#### 3.3.1 Virtual Channel

The definition of a virtual channel can be extended by the definition of cross co-array. We can divide the massive MIMO antennas at base station into two groups. One is the dense deployed antennas, the other is the sparse deployed correspondingly. We are interested in the following question regarding the nested placement of massive MIMO antennas: given dense and sparse, two groups of antennas, and assume their physical channels are easy to obtain, how to establish the virtual channels for improving system performance?

##### 3.3.1.1 Uplink Channels

Consider a nested antenna array with  $M = (2N_1^{(s)} + 1)N_2^{(s)} - 1$  antennas on the sparse lattice generated by  $\mathbf{N}^{(s)}$ . And  $N = \det(\mathbf{P})$  antennas on dense lattice generated by  $\mathbf{N}^{(d)}$ . Following definitions in last section, we can denoting the locations of antennas with  $\mathbf{N}^{(s)}\mathbf{n}^{(s)}$  for sparse antennas array,  $\mathbf{N}^{(d)}\mathbf{n}^{(d)}$  for dense antennas. Where  $\mathbf{n}^{(s)}$  and  $\mathbf{n}^{(d)}$  are integer vectors. Then the signal received at one of sparse array antennas  $m$  form user  $k$  is:

$$y_m^{UL}[k] = h_{k,m}^{UL} e^{j\omega_k^m v_m^{\vec{v}}} x^{UL}[k] + \eta_0 \quad (3.1)$$

Where,  $\omega_k^m = \frac{2\pi}{\lambda} [\cos\theta_k \sin\theta_k]$ ,  $\lambda$  is the signal wave length.  
 $v_m^{\vec{v}} = \mathbf{N}^{(s)}\mathbf{n}_m^{(s)} \cdot \mathbf{n}_m^{(s)}$  is an integer vector.

Similarly, the signal received at any dense array antennas  $n$  from user  $k$  can be written as:

$$y_n^{UL}[k] = h_{k,n}^{UL} e^{j\omega_k^n v_n} x^{UL}[k] + \eta_0 \quad (3.2)$$

The same,  $\omega_k^n = \frac{2\pi}{\lambda} [\cos\theta_k \sin\theta_k]$ , and  $v_n = \mathbf{N}^{(d)} \mathbf{n}_n^{(d)}$ .

Then it is ready to derive the cross correlation between the signal received at  $m$ -th and  $n$ -th antenna from same source user  $k$ :

$$\begin{aligned} E[y_n^{UL}[k](y_m^{UL}[k])^H] &= h_{k,n}^{UL} e^{j(\omega_k^n - \omega_k^m)(v_n - v_m)} x^{UL}[k] (x^{UL}[k])^H (h_{k,m}^{UL})^H \\ &+ \sigma^4 \mathbf{e}_{m,n} \mathbf{e}_{m,n}^H + \sigma^2 h_{k,n}^{UL} e^{j\omega_k^n v_n} x^{UL}[k] \mathbf{e}_{m,n}^H \\ &+ \sigma^2 \mathbf{e}_{m,n} (h_{k,m}^{UL})^H e^{j\omega_k^m v_m} (x^{UL}[k])^H \end{aligned} \quad (3.3)$$

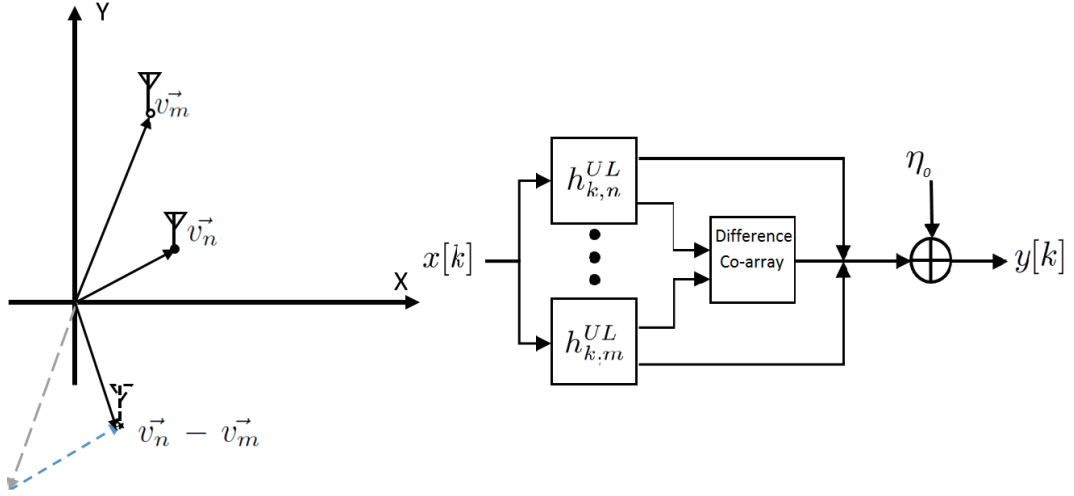


Figure 3.1. A Virtual Antenna Generated By A Pair of Difference Co-array In Uplink.

The first term of above equation has  $v_n - v_m$  element appeared, which is the difference co-array defined in last section. And this behave exactly like those signals received at virtual antennas. Besides, in the equation above, antennas pair which are

chosen to generate the virtual antenna are respectively from dense and sparse array. Actually, any pair of antennas(no matter from sparse or dense array) could be used for obtaining a unique virtual antenna.

### 3.3.1.2 Downlink Channel

An important characteristic of downlink channel is signals and interference have experienced the same channel distortion[60]. However, for different users, the signals arriving at their receivers experienced different channel distortion. Following the idea of uplink channel, analogously, we can easily written the signal transmit from m-th sparse array antenna to k-th user as:

$$y_m^{DL}[k] = h_{k,m}^{DL} e^{j\omega_k^m v_m} x^{DL}[k] + \eta_m[k] \quad (3.4)$$

Homologous, the signal transmit from n-th dense array antenna to k-th user is:

$$y_n^{DL}[k] = h_{k,n}^{DL} e^{j\omega_k^n v_n} x^{DL}[k] + \eta_n[k] \quad (3.5)$$

Repeat the approach in uplink, we can derive the cross correlation between the signal transmitted from m-th and n-th antenna received by user k:

$$\begin{aligned} E[y_n^{DL}[k](y_m^{DL}[k])^H] &= h_{k,n}^{DL} e^{j(\omega_k^n - \omega_k^m)(v_n - v_m)} (x[k] x^{DL}[k])^H (h_{k,m}^{DL})^H \\ &\quad + \sigma_n^2 \sigma_m^2 \mathbf{e}_{m,n} \mathbf{e}_{m,n}^H + \sigma_m^2 h_{k,n}^{DL} e^{j\omega_k^n v_n} x^{DL}[k] \mathbf{e}_{m,n}^H \\ &\quad + \sigma_n^2 \mathbf{e}_{m,n} (h_{k,m}^{DL})^H e^{j\omega_k^m v_m} (x^{DL}[k])^H \end{aligned} \quad (3.6)$$

The down-link received signal at user has a similar form to uplink but different. Figure 3.2 illustrates the block diagram of a pair of difference co-array in downlink

communication.

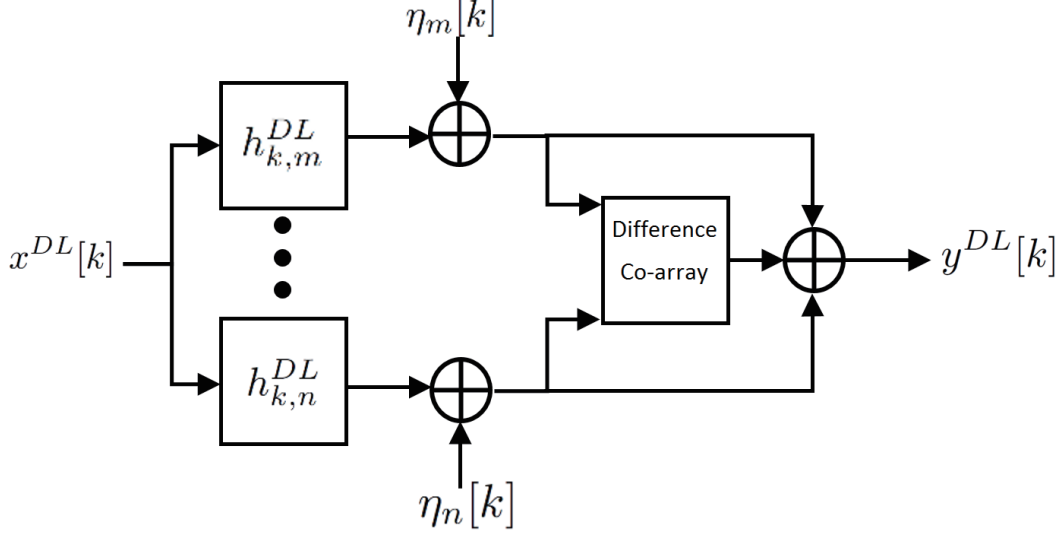


Figure 3.2. A Block Diagram for Downlink.

### 3.3.1.3 An Example of Nested-deployed MIMO Antenna Array

If all possible pair of antennas cooperate for communication, then a nested-distributed antenna network formed. In figure 3.3, an example is provided to show how to deploy antennas in the method that we introduced above. It is easy to generate this array if we use simple parameters and put them in a coordinate.

Its difference co-array for this case is  $\mathbf{N}^{(d)} = \begin{pmatrix} 1 & 0 \\ 0 & 1 \end{pmatrix}$ ,  $\mathbf{P} = \begin{pmatrix} 3 & 0 \\ 0 & 3 \end{pmatrix}$ ,  $N_1^{(s)} = 3$ ,  $N_2^{(s)} = 3$ . According figure 3, apparently, we densely placed 9 antennas and the number of sparse antenna array has 16 antennas as well. Finally, it generates an large array with more than 100 antennas.

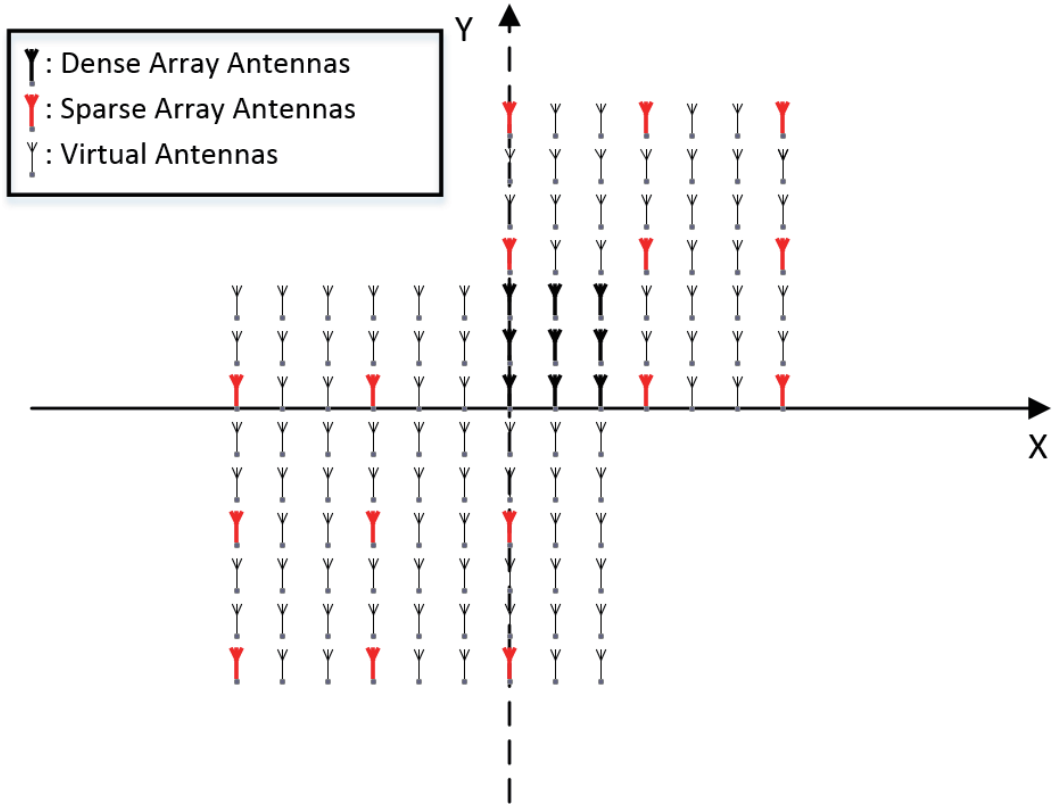


Figure 3.3. An Example of Nested-deployed MIMO Antenna Array.

### 3.4 Sum-Rate Capacity and Spectral Efficiency of Nested Distributed Massive MIMO

#### 3.4.1 Model of Nested Distributed Massive MIMO

In last section, difference co-array is used to model a virtual channel between any pair of antennas. But for the whole system, a Multi-User MIMO(MU-MIMO) model should be established. Assume there are totally  $K$  users in such cell with nested-deployed antennas. The antenna's location in the lattice could be generated by  $\mathbf{N}^{(d)}\mathbf{n}^{(d)}$  and  $\mathbf{N}^{(s)}\mathbf{n}^{(s)}$ . The signal received at the output of these antennas is denoted as:

$$\mathbf{Y}[k] = \begin{pmatrix} \mathbf{H}_s \\ \mathbf{H}_d \end{pmatrix} \mathbf{X}[k] + \eta[k] \quad (3.7)$$

Where  $\mathbf{H}_d$  is a  $\det(\mathbf{P}) \times K$  matrix for dense array and  $\mathbf{H}_s$  is a  $((2N_1^{(s)} + 1)N_2^{(s)} - 1) \times K$  matrix for sparse array.  $\mathbf{X}[k]$  is the source signal vector and the AWGN with power  $\sigma^2$  is represented as  $\eta[k]$ .

For  $\mathbf{H}_d$ , its elements are:

$$[\mathbf{H}_d]_{t,k} = h_{t,k} e^{j \frac{2\pi}{\lambda} [\cos\theta_k \ \sin\theta_k]^T \mathbf{N}^{(d)} \mathbf{n}_t^{(d)}} \quad (3.8)$$

Where  $k = 1, 2, \dots, K$  and  $t = 1, 2, \dots, \det(\mathbf{P})$ .

Similarly, the elements of  $\mathbf{H}_s$  are:

$$[\mathbf{H}_s]_{t,k} = h_{t,k} e^{j \frac{2\pi}{\lambda} [\cos\theta_k \ \sin\theta_k]^T \mathbf{N}^{(s)} \mathbf{n}_t^{(s)}} \quad (3.9)$$

Where  $k = 1, 2, \dots, K$  and  $t = 1, 2, \dots, (2N_1^{(s)} + 1)N_2^{(s)} - 1$ .

Then it is ready to derive to auto correlation of the received signal matrix as:

$$\mathbf{R}_{YY} = E[\mathbf{Y}\mathbf{Y}^H] = \begin{pmatrix} \mathbf{H}_s \\ \mathbf{H}_d \end{pmatrix} \mathbf{R}_{XX} \begin{pmatrix} \mathbf{H}_s \\ \mathbf{H}_d \end{pmatrix}^H + \sigma_n^2 \mathbf{I} \quad (3.10)$$

Next step is to vectorize  $\mathbf{R}_{YY}$ . According to the matrix theory, vectorization is a linear operation that means:

$$\text{Vec}(k_1 \mathbf{A} + k_2 \mathbf{B}) = k_1 \text{Vec}(\mathbf{A}) + k_2 \text{Vec}(\mathbf{B})$$

Where  $k_1$  and  $k_2$  are parameters. And also vectorization has a following important property:

$$\text{Vec}(\mathbf{ABC}) = (\mathbf{C}^T \otimes \mathbf{A}) \text{Vec}(\mathbf{B})$$

Where  $\otimes$  denotes the Kronecker product (also called direct product or tensor product) which is defined as:

$$\mathbf{A} \otimes \mathbf{B} = \begin{bmatrix} A_{11}\mathbf{B} & \cdots & A_{1n}\mathbf{B} \\ \cdot & \cdot & \cdot \\ \cdot & \cdot & \cdot \\ \cdot & \cdot & \cdot \\ A_{m1}\mathbf{B} & \cdots & A_{mn}\mathbf{B} \end{bmatrix}$$

Now we are ready to write the vectorized  $\mathbf{R}_{YY}$  as:

$$\text{Vec}(\mathbf{R}_{YY}) = \begin{pmatrix} \mathbf{H}_s \\ \mathbf{H}_d \end{pmatrix}^* \otimes \begin{pmatrix} \mathbf{H}_s \\ \mathbf{H}_d \end{pmatrix} \tilde{\mathbf{x}} + \sigma_n^2 \tilde{\mathbf{I}} \quad (3.11)$$

Here,  $\tilde{\mathbf{x}}$  is a  $K \times 1$  column vector as  $\tilde{\mathbf{x}} = [\sigma_1^2, \dots, \sigma_K^2]$ .  $\tilde{\mathbf{I}}$  is still a diagonal matrix with all 1, but its size becomes larger to  $((2N_1^{(s)} + 1)N_2^{(s)} + \det(\mathbf{P}) - 1)^2$ . Let

$$\mathbf{H}_{co-array} = \begin{pmatrix} \mathbf{H}_s \\ \mathbf{H}_d \end{pmatrix}^* \otimes \begin{pmatrix} \mathbf{H}_s \\ \mathbf{H}_d \end{pmatrix} \quad (3.12)$$

$\mathbf{H}_{co-array}$  has  $K$  columns. It contains all rows  $h_{t,l}$  and  $h_{t,l}^*$  where

$$\vec{h}_{t,l} = [h_{t,l} e^{j\frac{2\pi}{\lambda} [\cos\theta_1 \ \sin\theta_1]^T (\mathbf{N}^{(s)} \mathbf{n}_t^{(s)} - \mathbf{N}^{(d)} \mathbf{n}_l^{(d)})} \dots h_{t,l} e^{j\frac{2\pi}{\lambda} [\cos\theta_K \ \sin\theta_K]^T (\mathbf{N}^{(s)} \mathbf{n}_t^{(s)} - \mathbf{N}^{(d)} \mathbf{n}_l^{(d)})}]$$

$$t = 1, \dots, (2N_1^{(s)} + 1)N_2^{(s)} - 1, l = 1, \dots, \det(\mathbf{P})$$

Those rows are actually generated by a pair of antennas which one from dense array, the other one from sparse array. And also rows  $h_{t,l}^{(s)}$ ,  $h_{t,l}^{*(s)}$ ,  $h_{t,l}^{(d)}$  and  $h_{t,l}^{*(d)}$  where

$$\vec{h}_{t,l}^{(s)} = [h_{t,l} e^{j\frac{2\pi}{\lambda} [\cos\theta_1 \ \sin\theta_1]^T (\mathbf{N}^{(s)} \mathbf{n}_t^{(s)} - \mathbf{N}^{(s)} \mathbf{n}_l^{(s)})} \dots h_{t,l} e^{j\frac{2\pi}{\lambda} [\cos\theta_K \ \sin\theta_K]^T (\mathbf{N}^{(s)} \mathbf{n}_t^{(s)} - \mathbf{N}^{(s)} \mathbf{n}_l^{(s)})}]$$

$$t, l = 1, \dots, (2N_1^{(s)} + 1)N_2^{(s)} - 1$$



The rows above are generated by two antennas from sparse array.

$$\vec{h}_{t,l}^{(s)} = [h_{t,l} e^{j\frac{2\pi}{\lambda} [\cos\theta_1 \sin\theta_1]^T (\mathbf{N}^{(d)} \mathbf{n}_t^{(d)} - \mathbf{N}^{(d)} \mathbf{n}_l^{(d)})} \dots h_{t,l} e^{j\frac{2\pi}{\lambda} [\cos\theta_K \sin\theta_K]^T (\mathbf{N}^{(d)} \mathbf{n}_t^{(d)} - \mathbf{N}^{(d)} \mathbf{n}_l^{(d)})}]$$

$$t, l = 1, \dots, \det(\mathbf{P})$$

The rows above are generated by two antennas from dense array. These rows and their conjugates together in the matrix  $\mathbf{H}_{co-array}$  behave exactly like the Massive MIMO channel based on a large 2-D nested antenna array generated by their difference co-array. Then we can write the system model as:

$$\mathbf{Y} = \mathbf{H}_{co-array} \tilde{\mathbf{x}} + \sigma_n^2 \tilde{\mathbf{I}} \quad (3.13)$$

### 3.4.2 Sum-Rate Capacity

MIMO technology has an attractive multiplexing gain under a favorable propagation environment as well as a good signal to noise ratio(SNR). So that the LOS channel or the user located at the edge of the cell would lead to a disappoint performance. We will assume this is a time division duplex(TDD) system, so the propagation matrix of uplink is merely the transpose of downlink propagation matrix. The channel coefficient matrix  $\mathbf{H}$  we derived and used before could be treated as the propagation matrix  $\mathbf{G}$  for deriving the sum-rate capacity. In the non-fading case, all channel coefficients are equal to 1.

The Shannon sum-rate capacity for uplink Massive MIMO is[49]:

$$C_{sum \ UL} = \log_2 \left| \mathbf{I}_K + \frac{\rho_u}{K} \mathbf{G}_u^H \mathbf{G}_u \right| \quad (3.14)$$

Where  $\rho_u$  is expected SNR at any antennas of base station. And the formula for downlink Shannon sum-rate capacity requires the solution of a convex optimization

problem, that is:

$$C_{sum\ DL} = \sup_{\mathbf{a}} \{ \log_2 |\mathbf{I}_L + \rho_d \mathbf{G}_d \mathbf{D}_a \mathbf{G}_d^H| \}, \quad (3.15)$$

$$\mathbf{a} \geq \mathbf{0}, \mathbf{1}^T \mathbf{a} = 1,$$

Where  $\mathbf{D}_a$  is a diagonal matrix with the diagonal elements  $\mathbf{a}$ .  $\mathbf{a}$  is a  $L \times 1$  vector and  $\mathbf{1}$  is a  $M \times 1$  vector.

### 3.4.3 Spectral Efficiency Analysis

It has been proved that linear detectors perform well in the Massive MIMO system [61]. These linearly detectors Maximum-Ration Combining(MRC), Zero-Forcing(ZF) and Minimum Mean Squared Error(MMSE) receivers. Also in [62], authors investigated the energy efficiency of a large antenna array with these receivers. With the same number of antennas, MRC could support more users and offer a better performance on throughput. So in this paper, we will analyze the spectral efficiency of our nested-distributed Massive MIMO system which been assumed applying the MRC receiver.

Based on equation 3.13, we can write the output of receiver as:

$$\mathbf{Y}_{out} = \mathbf{A}^H \mathbf{Y} \quad (3.16)$$

Where  $\mathbf{A}$  is the conventional linear detector MRC which

$$\mathbf{A} = \mathbf{G} \quad (3.17)$$

Then the received vector after applying the MRC is given by:

$$\mathbf{Y}_{out} = \sqrt{p_u} \mathbf{G}^H \mathbf{G} \tilde{\mathbf{X}} + \sigma_n^2 \mathbf{G}^H \tilde{\mathbf{I}} \quad (3.18)$$

Where  $p_u$  is the average transmitted power of each user. Then for each single user  $k$ ,

$$y_{out,k} = \sqrt{p_u} \mathbf{g}_k^H \mathbf{g}_k \tilde{\mathbf{x}} + \sqrt{p_u} \sum_{i=1, i \neq k}^K \mathbf{g}_k^H \mathbf{g}_i \mathbf{x}_i + \sigma_n^2 \mathbf{g}_k^H \tilde{\mathbf{I}} \quad (3.19)$$

Where  $\mathbf{g}_k$  is the  $k$ -th columns of the matrix  $\mathbf{G}$ . The second and third terms of above equation are interference plus noise term. They can be consider as a random variable with zero mean. And its variance:

$$\sigma_{n_i} = p_u \sum_{i=1, i \neq k}^K |\mathbf{g}_k^H \mathbf{g}_i|^2 + \|\mathbf{g}_k\|^2 \quad (3.20)$$

If we consider the interference plus noise term as additive Gaussian noise which is independent from  $\tilde{\mathbf{x}}_k$ , also based on (14)[62], the achievable uplink rate of  $k$ -th user is:

$$R_k = E[\log_2(1 + \frac{p_u \|\mathbf{g}_k\|^4}{p_u \sum_{i=1, i \neq k}^K |\mathbf{g}_k^H \mathbf{g}_i|^2 + \|\mathbf{g}_k\|^2})] \quad (3.21)$$

It is easy to find that the equation above of rate with a form of “ $\log_2(1 + \frac{1}{x})$ ” which is a convex function. By applying Jensen’s inequality, the lower bound of achievable rate is derived:

$$R_k \geq \tilde{R}_k \triangleq \log_2(1 + (E[\frac{p_u \sum_{i=1, i \neq k}^K |\mathbf{g}_k^H \mathbf{g}_i|^2 + \|\mathbf{g}_k\|^2}{p_u \|\mathbf{g}_k\|^4}])^{-1}) \quad (3.22)$$

Then it is ready to define the spectral efficiency of this Massive MIMO system as:

$$\mathcal{E} = \sum_{k=1}^K \tilde{R}_k \quad (3.23)$$

### 3.5 Numerical Results

Before we get the numerical results, how to deploy antenna array is the first thing we should consider. In [59], authors claim that for the offset configuration(sensors

are contiguous but not overlap deployed),  $2(2N_1^{(s)} + 1)N_2^{(s)}\det(\mathbf{P})$  elements can be obtained in the difference co-array. However, for Massive MIMO, we cannot make it so dense due to some physical limitation:

1. Usually the size of the antenna should be  $\frac{1}{4}\lambda$  or  $\frac{5}{8}\lambda$ .
2. The distance of antennas from each other is an integer multiple of  $\frac{1}{4}\lambda$  so that we can get good space Diversity gain.

As Massive MIMO is a promised technology which uses millimeter wave signals, we plan to generate a large array with no more than  $(2N_1^{(s)} + 1)N_2^{(s)}\det(\mathbf{P})$  elements.

Figure 3.4 shows the spectral efficiency of Massive MIMO system. Compare to the uniformly distributed antennas array, it is obvious that our nested placement method perform better spectral efficiency and as the number of antennas increasing, its spectral efficiency improves more. It will finally converge at some point due to the transmission power limit. For the same number of physical antennas, different nested array with different virtual elements could be generated, our simulation is just an example but may not be the optimal. So it is excited that nested distributed Massive MIMO still has potential in terms of spectral efficiency.

Figure 3.5 illustrates the achievable sum rate increasing as the improve of SNR. Both deployments involve same number of antennas. As the transmission power increasing, the system performance improvement with our nested distributed method is more substantial.

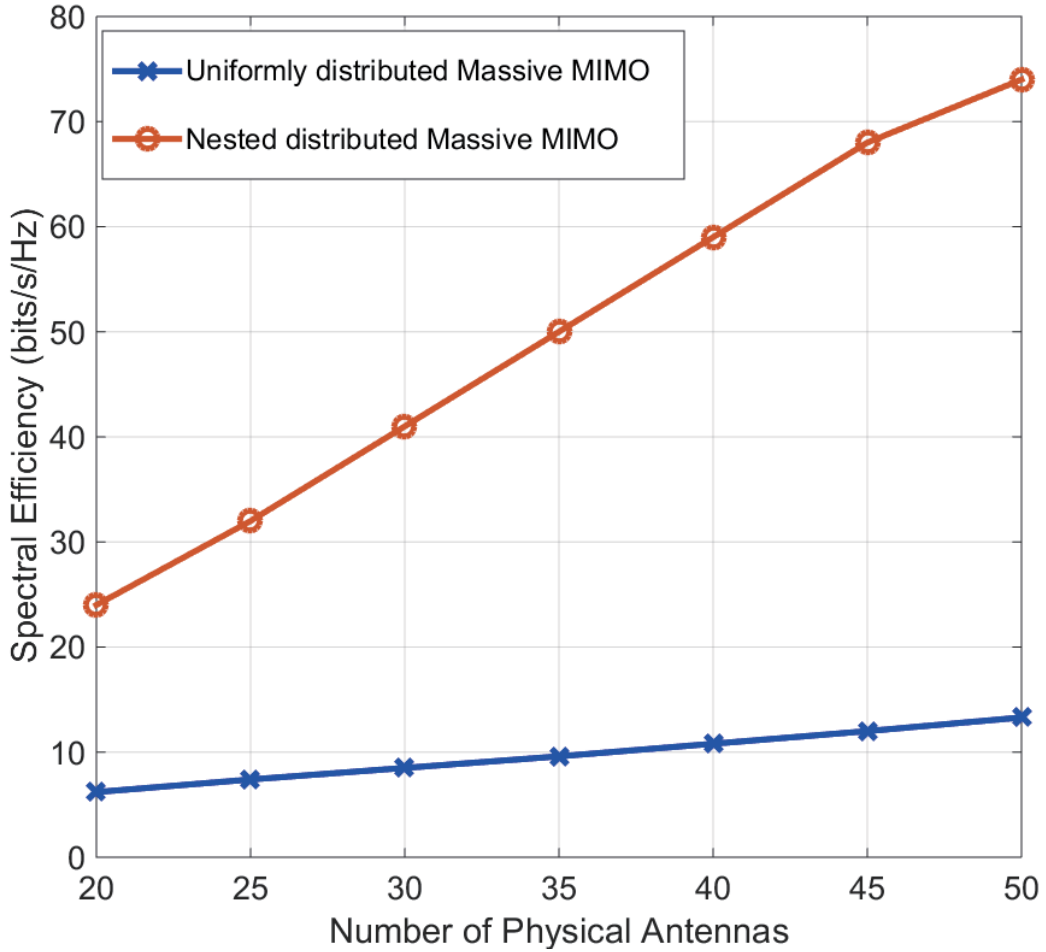


Figure 3.4. Spectral efficiency versus number of physical antennas. In this example, nested distributed antenna array could generate a large virtual array more than 800 elements with only 50 physical antennas. Here we assume 30 users are served simultaneously, SNR=2 dB.

### 3.6 Introduction of 3D Nested Distributed Massive MIMO

3D MIMO system is an important topic in 5G. Because consider the physical characteristics of 50GHz electromagnetic waves, Distributed antenna system (DAS) [63] and massive MIMO technologies could be utilized to overcome the affect of the high wallpenetration losses [64]. A 3D Massive MIMO system modeling and performance analysis was been done in [65]. And [66] proposed a a novel theoretical non-stationary three dimensional (3-D) wideband twin-cluster channel model for massive

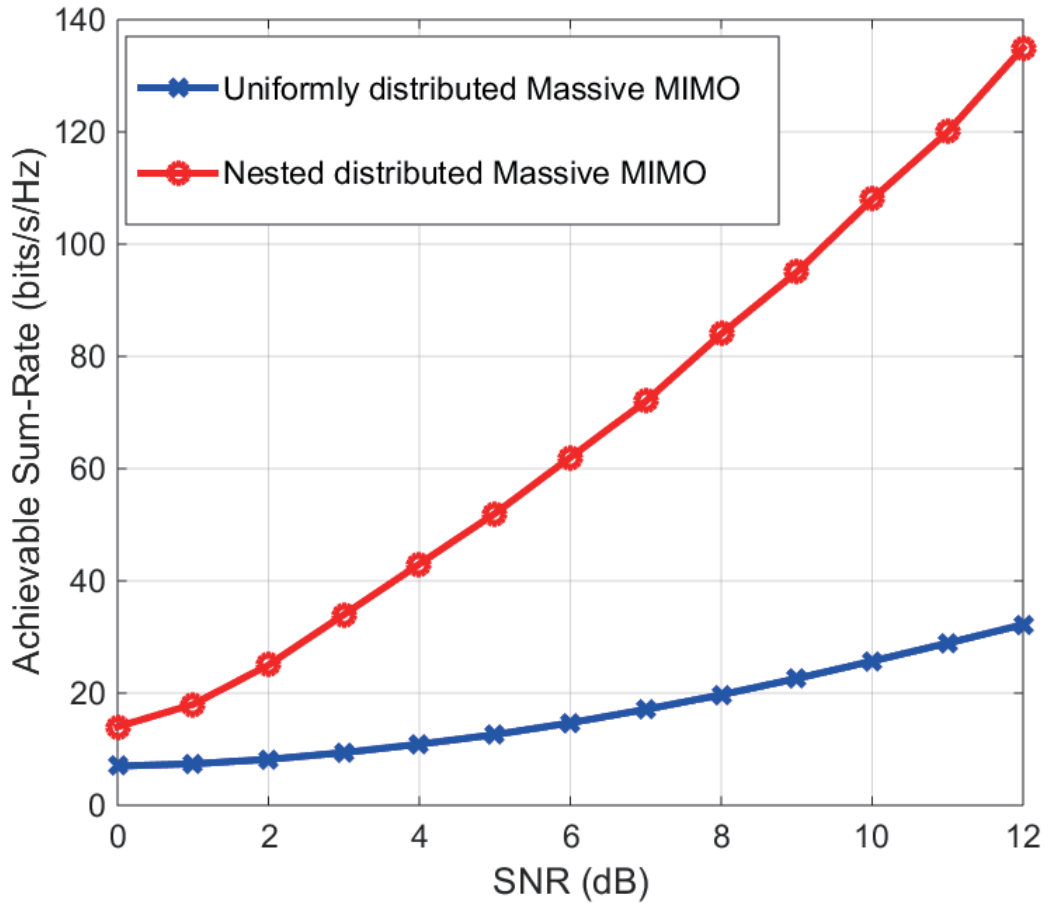


Figure 3.5. Achievable Sum-Rate versus SNR for physical antenna number fixed to 20.

MIMO. However, there are still several intrinsic problems for Massive MIMO system, particularly in three-dimensional. The densely large number of antennas may result in serious interference.

Following few sections on 3D case are organized as follows. In Section 3.8, an antenna pair with 3D cross difference co-array configuration is modeled. Section 3.9 introduced the modeling of 3D nested deployed MIMO antenna network. It also illustrates how to calculate sum rate capacity. After that, in Section 3.10 some numerical

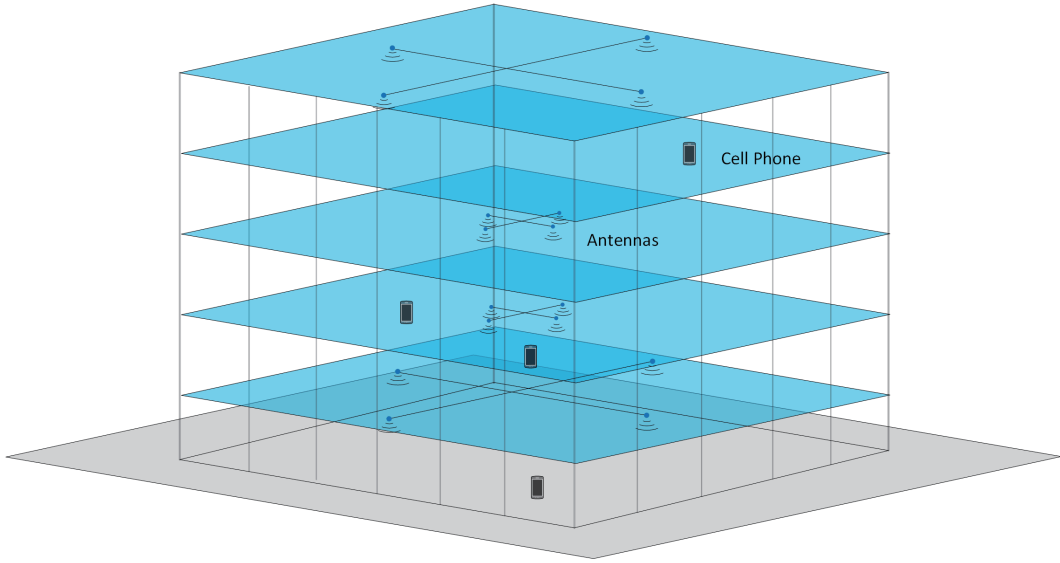


Figure 3.6. 3D Nested Distributed MIMO System in A Building.

results are provided to demonstrate accuracy of our proposed scheme. Finally, we summarize our work and make a conclusion in the last Section.

### 3.7 System and Channel Model in 3D

Based on the 2D Nested Co-array, we can easily derive the 3D Nested Co-array. First, the SFPD could be considered as a FPD shifted by a vector  $[k_1, k_2, k_3]$ . And then,  $\mathbf{N}^{(d)}$  becomes a  $3 \times 3$  non-singular matrix. An example of 3D Nested MIMO system will be illustrate in the end of next section.

**Definition 5:** (Three Dimensional Nested Array) *A  $3 \times 3$  non-singular matrix  $\mathbf{N}^{(d)}$ , an integer matrix  $\mathbf{P}$  (Expanded to  $3 \times 3$  as well) and integers  $N^{(s)}$  can be used to describe a three dimensional nested array following Definition 4.*

According to the definition of cross difference co-array and Shift FPD, virtual antennas' location could be decided by any two physical antennas. So the problem

we studying here becomes: Given physical antennas (some of them are densely deployed, some are sparsely deployed), and their location known and fixed, channels established and channel coefficients known, how to locate virtual antennas and obtain virtual channels based on Nested array.

### 3.7.0.1 Difference Co-array of Two Antennas

Consider a 3D nested antenna array with maximum  $M = 2N_1^{(s)}N_2^{(s)}N_3^{(s)} - 2$  antennas on the sparse lattice generated by  $\mathbf{N}^{(s)}$ . And  $N = \det(\mathbf{P})$  antennas on dense lattice obtained by generation matrix  $\mathbf{N}^{(d)}$ . Following definitions in previous sections, we can denoting the locations of antennas with  $\mathbf{N}^{(s)}\mathbf{n}^{(s)}$  for sparse antennas array and  $\mathbf{N}^{(d)}\mathbf{n}^{(d)}$  for dense antennas. Where  $\mathbf{n}^{(s)}$  and  $\mathbf{n}^{(d)}$  are integer vectors,  $\mathbf{n}^{(d)} \in FPD(\mathbf{P})$ . The same, we assume that there are  $K$  users in this system. Base on Definition 3, any two physical antennas can become a difference co-array pair. We take one antenna from sparse array and the other one from dense array in the following modeling. Then the signal received at one of sparse array antennas  $m$  form user  $k$  is:

$$y_m^{UL}[k] = h_{k,m}^{UL} e^{j\omega_k^m \sin\phi_k^m v_m^{\vec{}}} x^{UL}[k] + \eta_0 \quad (3.24)$$

Where,  $\omega_k^m = \frac{2\pi}{\lambda} [\cos\theta_k^m \sin\theta_k^m]$ ,  $\lambda$  is the signal wave length.  $\theta_k^m$  is the azimuthal angle from k-th users to m-th antenna.  $\phi_k^m$  is the elevation angle correspondingly.  $v_m^{\vec{}} = \mathbf{N}^{(s)}\mathbf{n}_m^{(s)}$  is the location of m-th antenna in the 3D Cartesian coordinate system.  $\mathbf{n}_m^{(s)}$  is an  $3 \times 1$  integer vector.



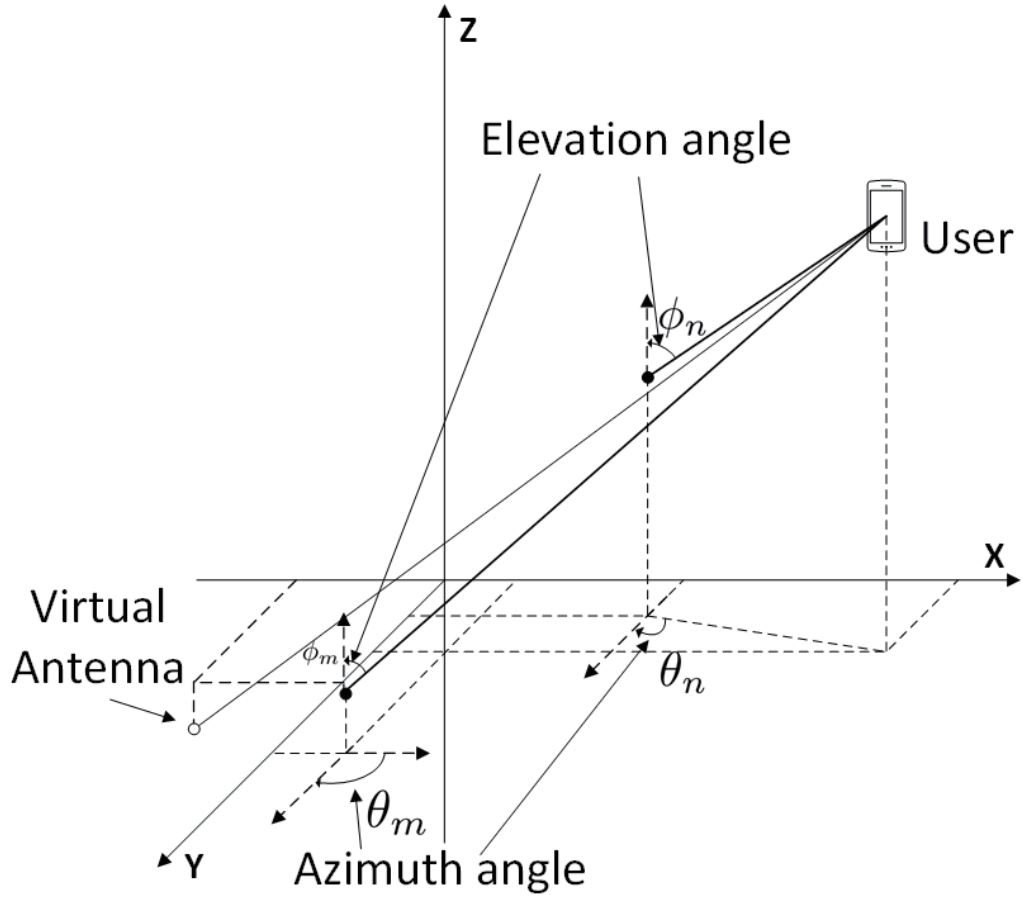


Figure 3.7. A 3D Virtual Antenna Generated by A Pair of Difference Co-Array.

Similarly, the signal received at one of dense array antennas  $n$  from the same user  $k$  can be written as:

$$y_n^{UL}[k] = h_{k,n}^{UL} e^{j\omega_k^n \sin\phi_k^n \vec{v}_n} x^{UL}[k] + \eta_0 \quad (3.25)$$

The same,  $\omega_k^n = \frac{2\pi}{\lambda} [\cos\theta_k^n \sin\theta_k^n]$ , and  $\vec{v}_n = \mathbf{N}^{(d)} \mathbf{n}_n^{(d)}$ .

Then it is ready to derive the cross correlation between the signal received at m-th and n-th antenna from the same source user  $k$ :

$$\begin{aligned}
E[y_n^{UL}[k](y_m^{UL}[k])^H] &= h_{k,n}^{UL} e^{j(\omega_k^n \vec{v}_n \sin\phi_k^n - \omega_k^m \vec{v}_m \sin\phi_k^m)} x^{UL}[k] (x^{UL}[k])^H (h_{k,m}^{UL})^H \\
&\quad + \sigma^4 \mathbf{e}_{m,n} \mathbf{e}_{m,n}^H + \sigma^2 h_{k,n}^{UL} e^{j\omega_k^n \sin\phi_k^n \vec{v}_n} x^{UL}[k] \mathbf{e}_{m,n}^H \\
&\quad + \sigma^2 \mathbf{e}_{m,n} (h_{k,m}^{UL})^H e^{j\omega_k^m \sin\phi_k^m \vec{v}_m} (x^{UL}[k])^H
\end{aligned} \tag{3.26}$$

The elements  $\omega_k^n \sin\phi_k^n \vec{v}_n - \omega_k^m \sin\phi_k^m \vec{v}_m$  here in the exponents of cross difference co-array terms behave like the signal received by a virtual antenna. The virtual antenna's location is decided by signals' arrival azimuthal angle, elevation angle and locations of physical antennas. Based on the mathematical relation above, we have:

**Proposition 1.** The possible maximum number of virtual antennas is  $N(N - 1) + 1$ , where  $N$  is the total number of physical antennas.

**Proposition 2.** If  $\vec{v} = \omega_k^n \sin\phi_k^n \vec{v}_n - \omega_k^m \sin\phi_k^m \vec{v}_m$  denotes the location of one virtual antenna, then there must be a virtual antenna locates at  $-\vec{v}$  (They are Central symmetric about  $\mathbf{0}$ ).

So it is possible to generate as many as  $N(N - 1) + 1$  virtual antennas with optimized and appropriate physical antenna placement. Since the difference co-array is symmetric about  $\mathbf{0}$ , we can design the physical antenna distribution to get desired coverage and performance.

The downlink of this system has similar form compare with the uplink. Based on equation (3.25) (3.26), we can write the signal transmit from m-th sparse array antenna to k-th user as:

$$y_m^{DL}[k] = h_{k,m}^{DL} e^{j\omega_k^m \sin\phi_k^m \vec{v}_m} x^{DL}[k] + \eta_m[k] \tag{3.27}$$

And the signal transmit from n-th dense array antenna to k-th user is:

$$y_n^{DL}[k] = h_{k,n}^{DL} e^{j\omega_k^n \sin\phi_k^n v_n^{\vec{v}}} x^{DL}[k] + \eta_n[k] \quad (3.28)$$

For the downlink, signals have experienced the different distortion from different antennas [60]. So we can derive the cross correlation between those two signals from m-th and n-th antenna as:

$$\begin{aligned} E[y_n^{DL}[k](y_m^{DL}[k])^H] &= h_{k,m}^{DL} e^{j(\omega_k^n v_n^{\vec{v}} \sin\phi_k^n - \omega_k^m v_m^{\vec{v}} \sin\phi_k^m)} x^{DL}[k] (x^{DL}[k])^H (h_{k,m}^{DL})^H \\ &\quad + \sigma_n^2 \sigma_m^2 \mathbf{e}_{m,n}^H + \sigma_n^2 h_{k,n}^{DL} e^{j\omega_k^n \sin\phi_k^n v_n^{\vec{v}}} x^{DL}[k] \mathbf{e}_{m,n}^H \\ &\quad + \sigma_m^2 \mathbf{e}_{m,n} (h_{k,m}^{DL})^H e^{j\omega_k^m \sin\phi_k^m v_m^{\vec{v}}} (x^{DL}[k])^H \end{aligned} \quad (3.29)$$

### 3.7.1 An Example of 3D Nested Massive MIMO System

An example in Fig. 3 shows a 3D nested deployed Massive MIMO system with  $\mathbf{N}^{(d)} = \begin{pmatrix} 1 & 0 & 0 \\ 0 & 1 & 0 \\ 0 & 0 & 1 \end{pmatrix}$  and  $\mathbf{P} = \begin{pmatrix} 2 & 0 & 0 \\ 0 & 2 & 0 \\ 0 & 0 & 2 \end{pmatrix}$ . According to the definitions of nested array, there are  $|\mathbf{P}| = N^{(d)} = 8$  antennas densely placed. In this case, we assume  $N_1^{(s)} = 3$ ,  $N_2^{(s)} = 3$ ,  $N_3^{(s)} = 3$ , so there are  $2N_1^{(s)}N_2^{(s)}N_3^{(s)} - 2 = 52$  antennas sparsely deployed. By applying the difference co-array, 281 virtual antennas are generated by  $8 + 52 = 60$  physical antennas.

## 3.8 Achievable Rate of 3D Nested Massive MIMO System

### 3.8.1 Channel Parameters

In a huge building, both users and distributed antennas are created across different heights (due to different floors), not just at ground level as 2D cases. If we do not consider the height of building, then the user's height  $h_{UE} = 1.6m$ . In 3D

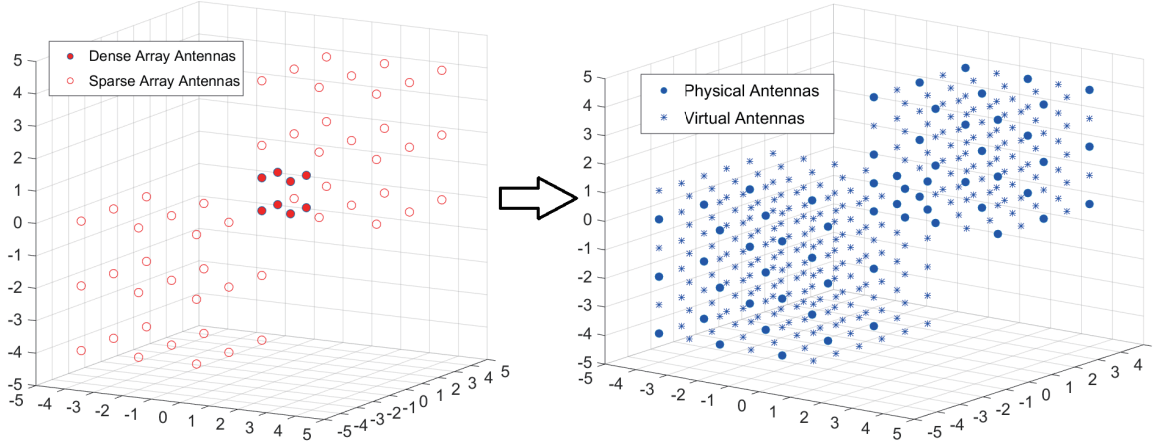


Figure 3.8. An Example of 3D nested Antenna Array.

scenario, users are randomly distributed with height  $h_{UE} = (n_{fl} - 1) \times 3 + 1.6m$ , where  $n_{fl}$  is the number of floors and we assume height of each floor is 3m. The existing Path Loss for Line of Sight(LOS) and Non-LOS models need some modifications to fit the 3D Massive MIMO scenarios. Based on [67][68], the modified Pass Loss are as follows:

If  $3m \leq d_{3D} \leq d_{BP}$

$$PL_{LOS} = 16.9 \log_{10}(d_{3D}) + 32.8 + 20 \log_{10}(f_c), \quad (3.30)$$

Otherwise,

$$PL_{LOS} = 40 \log_{10}(d_{3D}) + 28 + 20 \log_{10}(f_c) - 9 \log_{10}(d_{BP}^2 + (h_{BS} - h_{UE})^2) \quad (3.31)$$

where  $f_c$  is the central frequency given in GHz.  $d_{BP} = 2\pi h_{BS} h_{UE} \frac{f_c}{c}$  is the break point distance. For the non Line of Sight, similarly we have:

$$PL_{NLOS} = 43.3 \log_{10}(d_{3D}) + 11.5 + 20 \log_{10}(f_c) - 0.6(h_{UE} - 1.6) \quad (3.32)$$

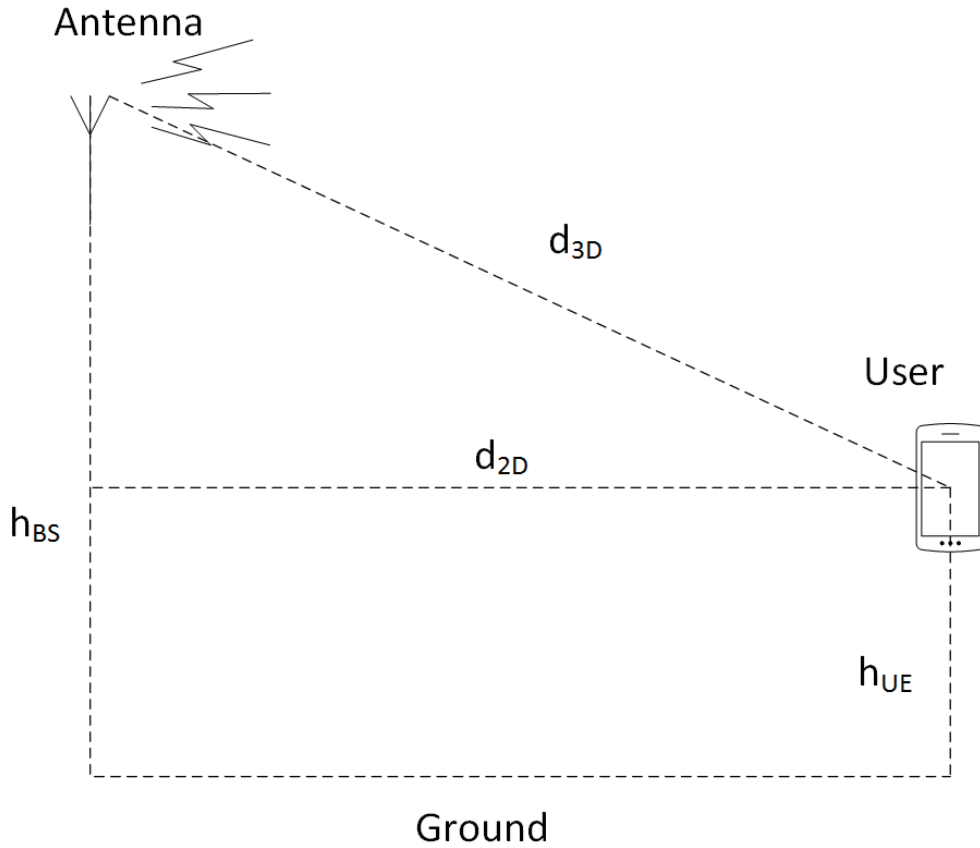


Figure 3.9. 3D Large Scale Parameters.

In addition to just consider the height of antennas and users, the elevation angles of antenna bore sight also affect the performance. This angle, we say  $\phi_{tilt}$ , usually is assumed to be fixed at  $\frac{\pi}{2}$  in 2D scenarios. However, as measured and proved in some papers [65][69][70], there are some energy propagate in the elevation which can not be ignored. Considering the azimuth angle alone here in 3D case is not accurate any more. Also if we fix the antenna bore sight, channels' degree of freedom in the elevation is wasted. In [67], ITU (International Telecommunication Union) approximates the horizontal antenna pattern as:

$$A_h(\theta) = -\min \left[ 12 \left( \frac{\theta}{\theta_{3dB}} \right)^2, A_m \right] \quad (3.33)$$

Where  $A_h(\theta)$  is the antenna gain (dB) in this direction,  $\theta \in [-\pi, \pi]$ ,  $\theta_{3dB}$  is the 3dB beam-width (Usually  $\theta_{3dB} = 70^\circ$  in practice). And  $A_m = 20dB$  is the maximum attenuation.

The vertical antenna pattern as:

$$A_e(\phi) = -\min \left[ 12 \left( \frac{\phi - \phi_{tilt}}{\phi_{3dB}} \right)^2, A_m \right] \quad (3.34)$$

Where  $A_e(\phi)$  is the antenna gain (dB) in elevation direction,  $\theta \in [-\frac{\pi}{2}, \frac{\pi}{2}]$ ,  $\phi_{tilt}$  is the tilt angle, it may be assumed that  $\phi_{3dB} = 15^\circ$ .

The combined antenna pattern at angles off the cardinal axes can be written as:

$$A_{h,e}(\theta, \phi) = -\min [-(A_h(\theta) + A_e(\phi)), A_m] \quad (3.35)$$

### 3.8.2 Model of 3D Nested MIMO System

Based on the derivation in previous sections and the 2D model, we can write the output of receiver with matrix form as:

$$\mathbf{Y}[k]_{3D} = \begin{pmatrix} \mathbf{H}_s \\ \mathbf{H}_d \end{pmatrix} \mathbf{X}[k] + \eta[k] \quad (3.36)$$

Where  $\mathbf{H}_d$  is a  $\det(\mathbf{P}) \times K$  matrix for dense array and  $\mathbf{H}_s$  is a  $(2N_1^{(s)}N_2^{(s)}N_3^{(s)} - 2) \times K$  matrix for sparse array.  $\mathbf{X}[k]$  is the source signal vector and the AWGN with power  $\sigma^2$  is represented as  $\eta[k]$ .

For  $\mathbf{H}_d$ , its elements are:

$$[\mathbf{H}_d]_{t,k} = h_{t,k} e^{j \frac{2\pi}{\lambda} \sin \phi_k^t [\cos \theta_k \sin \theta_k]^T \mathbf{N}^{(d)} \mathbf{n}_t^{(d)}} \quad (3.37)$$

Where  $k = 1, 2, \dots, K$  and  $t = 1, 2, \dots, \det(\mathbf{P})$ .

Similarly, the elements of  $\mathbf{H}_s$  are:

$$[\mathbf{H}_s]_{t,k} = h_{t,k} e^{j \frac{2\pi}{\lambda} \sin \phi_k^t [\cos \theta_k \ \sin \theta_k]^T \mathbf{N}^{(s)} \mathbf{n}_t^{(s)}} \quad (3.38)$$

Where  $k = 1, 2, \dots, K$  and  $t = 1, 2, \dots, 2N_1^{(s)} N_2^{(s)} N_3^{(s)} - 2$ .

Then it is ready to derive to auto correlation of the received signal matrix as:

$$\mathbf{R}_{YY} = E[\mathbf{Y}_{3D} \mathbf{Y}_{3D}^H] = \begin{pmatrix} \mathbf{H}_s \\ \mathbf{H}_d \end{pmatrix} \mathbf{R}_{XX} \begin{pmatrix} \mathbf{H}_s \\ \mathbf{H}_d \end{pmatrix}^H + \sigma_n^2 \mathbf{I} \quad (3.39)$$

The vectorized  $\mathbf{R}_{YY}$  is similar to 2D case as:

$$\text{Vec}(\mathbf{R}_{YY}) = \begin{pmatrix} \mathbf{H}_s \\ \mathbf{H}_d \end{pmatrix}^* \otimes \begin{pmatrix} \mathbf{H}_s \\ \mathbf{H}_d \end{pmatrix} \tilde{\mathbf{x}} + \sigma_n^2 \tilde{\mathbf{I}} \quad (3.40)$$

Here,  $\tilde{\mathbf{x}}$  is a  $K \times 1$  column vector as  $\tilde{\mathbf{x}} = [\sigma_1^2, \dots, \sigma_K^2]$ .  $\tilde{\mathbf{I}}$  is still a diagonal matrix with all 1, but it size becomes larger to  $(2N_1^{(s)} N_2^{(s)} N_3^{(s)} + \det(\mathbf{P}) - 2)^2$ . Let

$$\mathbf{H}_{3D} = \begin{pmatrix} \mathbf{H}_s \\ \mathbf{H}_d \end{pmatrix}^* \otimes \begin{pmatrix} \mathbf{H}_s \\ \mathbf{H}_d \end{pmatrix} \quad (3.41)$$

$\mathbf{H}_{3D}$  has  $K$  columns. It contains all rows  $h_{t,l}$  and  $h_{t,l}^*$  where

$$\vec{h}_{t,l} = [h_{t,l} e^{j \frac{2\pi}{\lambda} [\cos \theta_1 \ \sin \theta_1]^T (\sin \phi_1^t \mathbf{N}^{(s)} \mathbf{n}_t^{(s)} - \sin \phi_1^l \mathbf{N}^{(d)} \mathbf{n}_l^{(d)})} \dots$$

$$h_{t,l} e^{j \frac{2\pi}{\lambda} [\cos \theta_K \ \sin \theta_K]^T (\sin \phi_K^t \mathbf{N}^{(s)} \mathbf{n}_t^{(s)} - \sin \phi_K^l \mathbf{N}^{(d)} \mathbf{n}_l^{(d)})}]$$

$$t = 1, \dots, (2N_1^{(s)} N_2^{(s)} N_3^{(s)} - 2), l = 1, \dots, \det(\mathbf{P})$$

Those rows are actually generated by a pair of antennas which one from dense array, the other one from sparse array. And also rows  $h_{t,l}^{(s)}$ ,  $h_{t,l}^{*(s)}$ ,  $h_{t,l}^{(d)}$  and  $h_{t,l}^{*(d)}$  where

$$\begin{aligned} \vec{h}_{t,l}^{(s)} &= [h_{t,l} e^{j\frac{2\pi}{\lambda} [\cos\theta_1 \ \sin\theta_1]^T (\sin\phi_1^t \mathbf{N}^{(s)} \mathbf{n}_t^{(s)} - \sin\phi_1^l \mathbf{N}^{(s)} \mathbf{n}_l^{(s)})} \dots \\ &\quad h_{t,l} e^{j\frac{2\pi}{\lambda} [\cos\theta_K \ \sin\theta_K]^T (\sin\phi_K^t \mathbf{N}^{(s)} \mathbf{n}_t^{(s)} - \sin\phi_K^l \mathbf{N}^{(s)} \mathbf{n}_l^{(s)})}] \\ t, l &= 1, \dots, 2N_1^{(s)} N_2^{(s)} N_3^{(s)} - 2 \end{aligned}$$

The rows above are generated by two antennas from sparse array.

$$\begin{aligned} \vec{h}_{t,l}^{(s)} &= [h_{t,l} e^{j\frac{2\pi}{\lambda} [\cos\theta_1 \ \sin\theta_1]^T (\sin\phi_1^t \mathbf{N}^{(d)} \mathbf{n}_t^{(d)} - \sin\phi_1^l \mathbf{N}^{(d)} \mathbf{n}_l^{(d)})} \dots \\ &\quad h_{t,l} e^{j\frac{2\pi}{\lambda} [\cos\theta_K \ \sin\theta_K]^T (\sin\phi_K^t \mathbf{N}^{(d)} \mathbf{n}_t^{(d)} - \sin\phi_K^l \mathbf{N}^{(d)} \mathbf{n}_l^{(d)})}] \\ t, l &= 1, \dots, \det(\mathbf{P}) \end{aligned}$$

The rows above are generated by two antennas from dense array. These rows and their conjugates together in the matrix  $\mathbf{H}_{3D}$  behave exactly like the Massive MIMO channel based on a large 3-D nested antenna array generated by their difference co-array. Then we can write the system model as:

$$\mathbf{Y} = \mathbf{H}_{3D} \tilde{\mathbf{x}} + \sigma_n^2 \tilde{\mathbf{I}} \quad (3.42)$$

### 3.8.3 Achievable Sum Rate Analysis

As mentioned before, we suppose there are  $K$  users in this system. The channel matrix  $\mathbf{H}_{3D} = \mathbf{G}$  has  $M$  rows (means the system has  $M$  physical plus virtual antennas). And we can also assume that both  $M, K$  are large numbers and  $1 \ll K \ll M$ . Then we could derive the achievable sum rate for this nested distributed Massive MIMO system as:



$$C_{sum\ UL} = \log_2 \left| \mathbf{I}_K + \frac{p_u}{K} \mathbf{G}_u^H \mathbf{G}_u \right| \quad (3.43)$$

Considering that the system has perfect CSI, i.e.  $\mathbf{G}$  is known.  $\mathbf{g}_k$  is k-th columns which denotes the channel between k-th user and all antennas (both physical and virtual). Then the ergodic achievable Uplink rate of k-th user can be written as:

$$\begin{aligned} R_k &= E \left\{ \log_2 \left( 1 + \frac{p_u \|\mathbf{g}_k^H \mathbf{g}_k\|^2}{p_u \sum_{i=1, i \neq k}^K \|\mathbf{g}_k^H \mathbf{g}_i\|^2 + \|\mathbf{g}_k\|^2} \right) \right\} \\ &= E \left\{ \log_2 \left( 1 + \frac{p_u \|\mathbf{g}_k\|^4}{p_u \sum_{i=1, i \neq k}^K \|\mathbf{g}_k^H \mathbf{g}_i\|^2 + \|\mathbf{g}_k\|^2} \right) \right\} \end{aligned} \quad (3.44)$$

Based on equations above, we can derive the lower bound of achievable rate of 3D nested deployed Massive MIMO system as [62]:

$$\begin{aligned} R_k &\geq R_k^L \\ &= \log_2 \left( 1 + (E \left\{ \frac{p_u \sum_{i=1, i \neq k}^K \|\mathbf{g}_k^H \mathbf{g}_i\|^2 + \|\mathbf{g}_k\|^2}{p_u \|\mathbf{g}_k\|^4} \right\})^{-1} \right) \\ &\geq \tilde{R}_k^L = \log_2 \left( 1 + \frac{p_u (M-1) \beta_k(\phi_{tilt})}{p_u \sum_{i=1, i \neq k}^K \beta_i(\phi_{tilt}) + 1} \right) \\ &\stackrel{M \rightarrow \infty}{\rightarrow} \log_2(1 + \beta_k(\phi_{tilt}) E_u) \end{aligned} \quad (3.45)$$

Where  $p_u$  is the average transmitted power of each user,  $E_u = M \times p_u$ . If we assume  $G_{max}$  is the maximum antenna gain (in dB) at the antenna boresight, based on (3.34), (3.35) and [71], the antenna gain in linear scale for k-th user can be written as:

$$a_k(\phi_{tilt}) = 10^{\frac{G_{max}}{10} - 1.2 \left( \frac{\theta_k}{\theta_{3dB}} \right)^2 - 1.2 \left( \frac{\phi_k - \phi_{tilt}}{\phi_{3dB}} \right)^2} \quad (3.46)$$

$\beta_k(\phi_{tilt})$  is a function of antenna boresight angle can be defined as:

$$\beta_k(\phi_{tilt}) = \xi_k a_k(\phi_{tilt}) \cdot PL \quad (3.47)$$

Where  $\xi_k$  is the log-normal shadowing fading coefficient [72],  $PL$  can be  $PL_{LOS}$  or  $PL_{NLOS}$  which we defined before.

### 3.9 Simulation Results of 3D System

In this section, we illustrate some simulation results to support the correctness of our propositions. A typical 3D scenario in practice we considered in this simulation- in a large building with 12 floors(each floor has 3m height). Multiple users randomly distributed in this area. These assumption allows us to investigate the affect from vertical factors and examine the system performance. We fix the  $\theta_{3dB} = 70^\circ$  and  $\phi_{3dB} = 15^\circ, A_m = 20dB$ . To make it simple, a 3D nested distributed Massive MIMO is generated with 8 densely placed antennas and 14 sparsely placed antennas. Based on the definition of 3D nested array, a large system with totally 126 physical and virtual antennas created.

Since the antenna tilting angle is an important factor which not appeared in 2D case, it is necessary to investigate its affect. 3.10 shows the affect of the antenna tilting angle to spectral efficiency. In this simulation, system reach highest spectral efficiency with the tilting angle around  $10^\circ$ . And under lower SNR, the tilting angle has larger negative affect to system performance. So the dynamic adaption on tilting angles may bring some performance improvement in 3D cases.

3.11 shows the achievable sum rate with different number of antennas and placement schemes. Because we use 22 physical antennas to generate this nested antenna array with totally 126 physical plus virtual antennas, so we also simulate a system with 126 physical uniformly distributed antennas to make a comparison. According to the numerical results, with the same number of physical antennas, our scheme could extremely improve the system performance on sum-rate capacity. In other word, to reach the same achievable sum rate, our scheme uses much less antennas. But com-

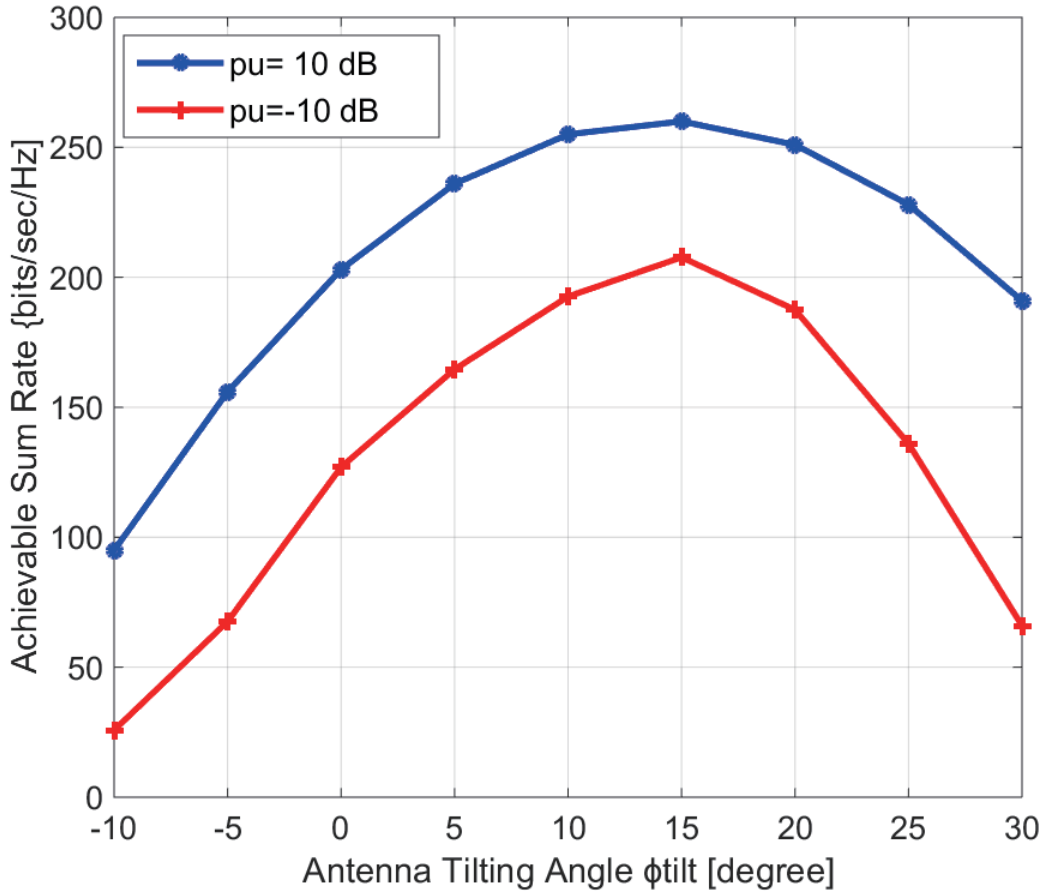


Figure 3.10. Achievable sum rate versus antenna tilting angle in different SNR.

pared to the system that the number of physical antennas equals to nested antenna array(physical+virtual), the nested Massive MIMO system cannot get a such high sum rate, due to the limitation of virtual antennas(interference, complexity, power allocation, .etc).

To capture the effect of antenna boresight angle  $\phi_{(tilt)}$  to achievable sum rate, in 3.12, first the lower bound sum rate is compared with simulated sum rate. In this simulation, we set the  $M$  equals to 22 as before with the same placement. Two typical value of tilting angle  $\phi = 6^\circ$  and  $\phi = 8^\circ$  is chosen in this experiment, it shows the correctness of another simulation in fig. 5 which is system would reach highest

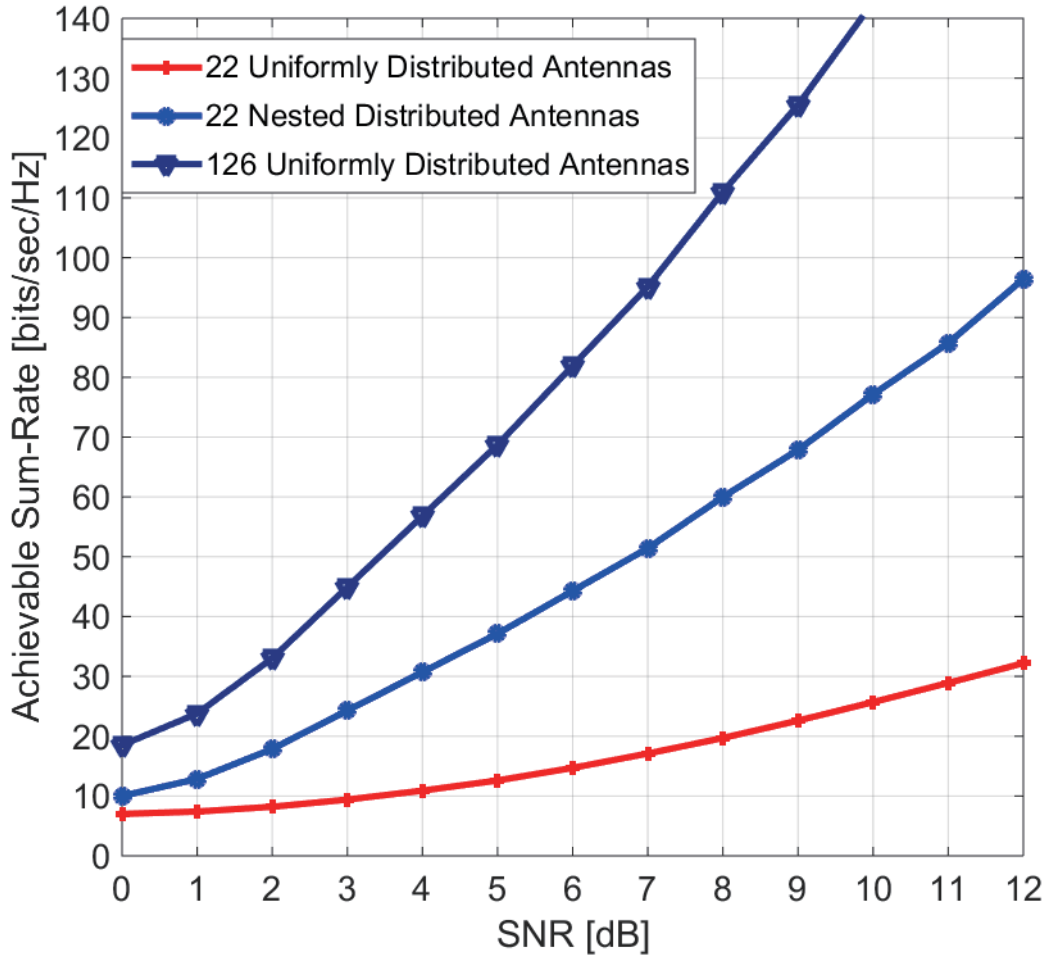


Figure 3.11. Different number of antennas and placement schemes versus SNR.

spectral efficiency as tilting angle approaching  $10^\circ$ . As the  $\|\phi_{(tilt)} - 10^\circ\|$  increasing, the system sum rate will approach the theoretical lower bound.

### 3.10 Conclusion

This chapter introduces the modeling and characteristics for nested array based Massive MIMO in the cellular communication system. The model assumes antennas been divided into two groups- sparse and dense. And any pair of antennas could

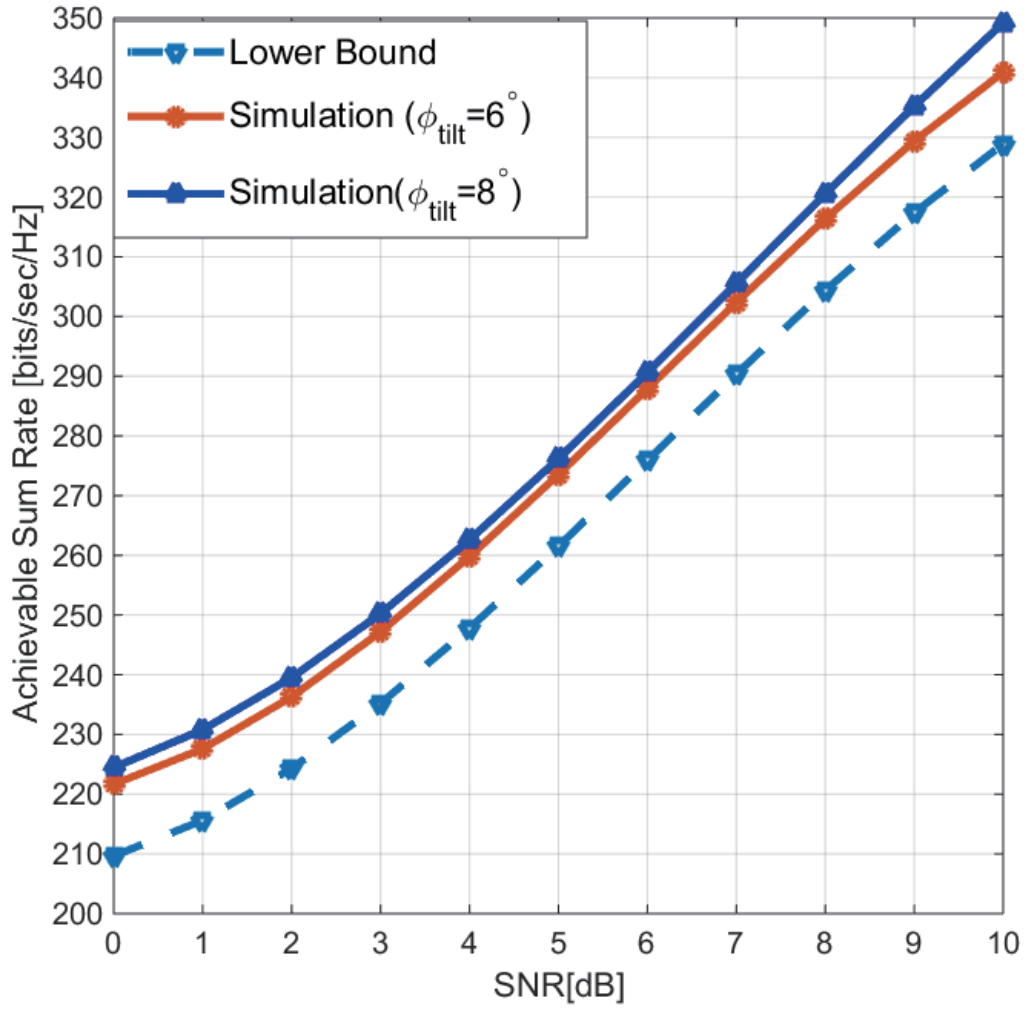


Figure 3.12. Achievable sum rate of different tilting angle and lower bound.

generate a virtual channel for uplink and downlink communication. Also the feasibility is proved in this paper. Based on Shannon Capacity, the achievable sum rate is calculated and its performance should be better than uniformly distributed Massive MIMO with less physical antennas. The spectral efficiency is given based on a zero forcing detector. Finally, simulation results are given to support the correctness.

After that it extends the dimension from 2D nested array to 3D. Linked it to the cellular communication, a three dimensional nested distributed Massive MIMO system is introduced. We also given an example in section III which use 60 physical generates a nested distributed Massive MIMO system with more than 300 elements. A 3D nested distributed Massive MIMO system model is built. By taking the characteristic of cross difference co-array, we are able to calculate the sum-rate capacity of this system. It shows that our scheme could improve the spectral efficiency and also to build a Massive MIMO system with much less antennas. The simulation results are also performed to support the correctness of the statements.

## CHAPTER 4

### Conclusions and Future Works

#### 4.1 Conclusions

As HetNets is a very important technology in 5G, Chapter 2 of this dissertation proposed an optimization method for wireless resources allocation in HetNets [73]. This is the first work which models the three layer HetNets in wireless communication as a classical cooperative game-river sharing game. Due to the complexity of this cooperative game, Backwards Induction Algorithm(BIA) was used to obtain the optimal solution. 5G considered the high user density scenario, here our proposed cooperative allocation scheme could get better performance with more subscribers. The cooperative approach get better or at least equal performance compared to the non-cooperative in bandwidth sharing problem. Since Massive MIMO is a promising technology, Chapter 3 considered a HetNets equipped with Massive MIMO at base stations. Following the idea of Chapter 2, game theory was chosen to optimize this system. Higher sum rate capacity was achieved after optimization [74],[75]. However, higher frequency band is allocated to wireless communication in 5G, which means much more densely deployed base stations. If all base stations equipped Massive MIMO, it must be a huge cost on hardware. Chapter 4 introduced a nested distributed based Massive MIMO antenna array which could achieve Massive MIMO with much less physical antennas [76]. A three dimensional nested distributed Massive MIMO system was modeled and analyzed [77].

Overall, to achieve a better performance in 5G networks, this dissertation proposed new models for HetNets and Massive MIMO. Game theoretical methods(both non-cooperative and cooperative game) were applied. Compared to traditional scheduling and resource allocation methods, game theoretical methods could achieve better performance. Based on nested array, this dissertation first ever proposed nested distributed Massive MIMO systems (both two dimensional and three dimensional). This new nested Massive MIMO model could achieve same performance with much less antennas compared to traditional uniformly distributed Massive MIMO system. All these research works could be considered as candidate technologies in 5G and contributes better performance in wireless communication.

#### 4.2 Future Works

In this work, simulation results revealed that the average sum-rate capacity significantly improved as the distance between femto cell and macro cell increasing. Because such deployment of HetNets will lead to high macro-pico/femto inter-cell interference. Sometimes it is preferable to have a UE connect to a low-power pico/femtocell node even when it has significantly lower received power as compared to a high power macro node [78]. In this situation, game theory will be very useful when we want to enable traffic off-loading to the low-power nodes and to achieve true cell-splitting gains in the network [79]. In this research, we simply consider the interference as a noise. However, if we consider the cell-splitting gains in the network, the game theoretical method could further help us to achieve a even better performance than this work. Game theoretical methods have high computational complexity. In fact, it is possible to solve the cooperative Game with non-cooperative methods which may be the best compromise between performance and computational complexity. For example, Nash bargain game, sequential bargain game and strategic



concessions game are scarcely been tried in HetNets problems.

A Massive MIMO HetNets system model was built in Chapter 3. In that model, we considered all interference signals as noise. However, for a system in full-duplex, the interference is an important issue as Downlink and Uplink antennas will receive signals that transmit by themselves. Besides, a HetNets deployment will introduce the inter-cell interference. To find an appropriate method to vanish the interference will be a big plus for system performance. For instance, to get a further improvement of our current work, the interference alignment could be applied to our model. The interference alignment is a common approach to vanish the interference in communication [39]. Some other method like eigen-beamforming [37] and Cognitive Radio [80] could also be considered as candidate methods to improve the performance based on our research. Besides the sum-rate, some other features could be investigated based on our current model, i.e. spectral efficiency, energy efficiency and beamforming. Like the first part of this manuscript, game theoretical method was applied for optimization. In the game theory, Nash Equilibrium is the optimal solution in a zero-sum game. However, in practice, resources are allocated by the Mobility Management Entity(MME) or called evolved packet core(EPC) in LTE, then a cell is possible to cooperate with its neighbors. As a results, a cooperative game could be applied to this scenario also to improve system's sum-rate capacity and spectral efficiency.

The Channel State Information at Receiver(CSIR) is assumed known in Chapter 4. But actually, how to acquire the CSI quickly and accurately is a challenge in practice. It is not easy to synchronize this system. In [81], authors were trying to increase capacity of multi-cell cooperative cellular networks with nested deployment. In the future work, we can also consider a multi-cell cooperative cellular networks

with nested deployment, and at the same time, massive MIMO antennas equipped at each cell. From the entire system point of view, the nested placement could extremely reduce the number of antennas and increase the spectral efficiency.

## REFERENCES

- [1] M. Iwamura, K. Etemad, M.-H. Fong, R. Nory, and R. Love, “Carrier aggregation framework in 3gpp lte-advanced [wimax/lte update],” *IEEE Communications Magazine*, vol. 48, no. 8, pp. 60–67, 2010.
- [2] M. Sawahashi, Y. Kishiyama, A. Morimoto, D. Nishikawa, and M. Tanno, “Coordinated multipoint transmission/reception techniques for lte-advanced [coordinated and distributed mimo],” *IEEE Wireless Communications*, vol. 17, no. 3, pp. 26–34, 2010.
- [3] V. Chandrasekhar, J. G. Andrews, T. Muharemovic, Z. Shen, and A. Gatherer, “Power control in two-tier femtocell networks,” *IEEE Transactions on Wireless Communications*, vol. 8, no. 8, pp. 4316–4328, 2009.
- [4] S.-Y. Lien, C.-C. Tseng, K.-C. Chen, and C.-W. Su, “Cognitive radio resource management for qos guarantees in autonomous femtocell networks,” in *2010 IEEE International Conference on Communications (ICC)*. IEEE, 2010, pp. 1–6.
- [5] J. Xiang, Y. Zhang, T. Skeie, and L. Xie, “Downlink spectrum sharing for cognitive radio femtocell networks,” *IEEE Systems Journal*, vol. 4, no. 4, pp. 524–534, 2010.
- [6] S.-M. Cheng, S.-Y. Lien, F.-S. Chu, and K.-C. Chen, “On exploiting cognitive radio to mitigate interference in macro/femto heterogeneous networks,” *IEEE Wireless Communications*, vol. 18, no. 3, pp. 40–47, 2011.

- [7] G. Gur, S. Bayhan, and F. Alagoz, “Cognitive femtocell networks: an overlay architecture for localized dynamic spectrum access [dynamic spectrum management],” *IEEE Wireless Communications*, vol. 4, no. 17, pp. 62–70, 2010.
- [8] A. Valcarce, D. Lopez-Perez, G. De La Roche, and J. Zhang, “Limited access to ofdma femtocells,” in *2009 IEEE 20th International Symposium on Personal, Indoor and Mobile Radio Communications*. IEEE, 2009, pp. 1–5.
- [9] D. Choi, P. Monajemi, S. Kang, and J. Villasenor, “Dealing with loud neighbors: The benefits and tradeoffs of adaptive femtocell access,” in *IEEE GLOBECOM 2008. Global Telecommunications Conference*. IEEE, 2008, pp. 1–5.
- [10] L. A. Petrosjan and V. V. Mazalov, *Game theory and applications*. Nova Publishers, 2002, vol. 8.
- [11] R. A. McCain, *Game theory: A nontechnical introduction to the analysis of strategy*. World Scientific, 2010.
- [12] R. P. Gilles, *the cooperative game theory of networks and Hierarchies*. Springer Science & Business Media, 2010, vol. 44.
- [13] Z. Ji and K. Liu, “Cognitive radios for dynamic spectrum access—dynamic spectrum sharing: A game theoretical overview,” *IEEE Communications Magazine*, vol. 45, no. 5, pp. 88–94, 2007.
- [14] Y. Wu, B. Wang, K. Liu, and T. C. Clancy, “Repeated open spectrum sharing game with cheat-proof strategies,” *IEEE Transactions on Wireless Communications*, vol. 8, no. 4, pp. 1922–1933, 2009.
- [15] J.-S. Lin and K.-T. Feng, “Femtocell access strategies in heterogeneous networks using a game theoretical framework,” *IEEE Transactions on Wireless Communications*, vol. 13, no. 3, pp. 1208–1221, 2014.
- [16] S. Ambec and Y. Sprumont, “Sharing a river,” *Journal of Economic Theory*, vol. 107, no. 2, pp. 453–462, 2002.

- [17] S. Ambec and L. Ehlers, “Sharing a river among satiable agents,” *Games and Economic Behavior*, vol. 64, no. 1, pp. 35–50, 2008.
- [18] D. Niyato and E. Hossain, “Wireless broadband access: Wimax and beyond-integration of wimax and wifi: Optimal pricing for bandwidth sharing,” *IEEE Communications Magazine*, vol. 45, no. 5, pp. 140–146, 2007.
- [19] J. Lafferty, A. McCallum, and F. C. Pereira, “Conditional random fields: Probabilistic models for segmenting and labeling sequence data,” 2001.
- [20] J. Contreras and F. F. Wu, “Coalition formation in transmission expansion planning,” *IEEE Transactions on Power Systems*, vol. 14, no. 3, pp. 1144–1152, 1999.
- [21] D. Tse and P. Viswanath, *Fundamentals of wireless communication*. Cambridge university press, 2005.
- [22] J. G. Andrews, S. Buzzi, W. Choi, S. V. Hanly, A. Lozano, A. C. Soong, and J. C. Zhang, “What will 5g be?” *IEEE Journal on Selected Areas in Communications*, vol. 32, no. 6, pp. 1065–1082, 2014.
- [23] J. Karjalainen, M. Nekovee, H. Benn, W. Kim, J. Park, and H. Sungsoo, “Challenges and opportunities of mm-wave communication in 5g networks,” in *2014 9th International Conference on Cognitive Radio Oriented Wireless Networks and Communications (CROWNCOM)*. IEEE, 2014, pp. 372–376.
- [24] Y. Zhou, D. Li, H. Wang, A. Yang, and S. Guo, “Qos-aware energy-efficient optimization for massive mimo systems in 5g,” in *2014 Sixth International Conference on Wireless Communications and Signal Processing (WCSP)*. IEEE, 2014, pp. 1–5.
- [25] P. Pirinen, “A brief overview of 5g research activities,” in *2014 1st International Conference on 5G for Ubiquitous Connectivity (5GU)*. IEEE, 2014, pp. 17–22.
- [26] M. Vehkaperä, M. A. Girnyk, T. Riihonen, R. Wichman, and L. K. Rasmussen, “On achievable rate regions at large-system limit in full-duplex wireless local

- access,” in *2013 First International Black Sea Conference on Communications and Networking (BlackSeaCom)*. IEEE, 2013, pp. 7–11.
- [27] J. Hoydis, S. Ten Brink, and M. Debbah, “Massive mimo in the ul/dl of cellular networks: How many antennas do we need?” *IEEE Journal on Selected Areas in Communications*, vol. 31, no. 2, pp. 160–171, 2013.
- [28] —, “Massive mimo: How many antennas do we need?” in *2011 49th Annual Allerton Conference on Communication, Control, and Computing (Allerton)*. IEEE, 2011, pp. 545–550.
- [29] H. Huh, G. Caire, H. C. Papadopoulos, and S. A. Ramprasad, “Achieving” massive mimo” spectral efficiency with a not-so-large number of antennas,” *IEEE Transactions on Wireless Communications*, vol. 11, no. 9, pp. 3226–3239, 2012.
- [30] J. I. Choi, M. Jain, K. Srinivasan, P. Levis, and S. Katti, “Achieving single channel, full duplex wireless communication,” in *Proceedings of the sixteenth annual International Conference on Mobile computing and networking*. ACM, 2010, pp. 1–12.
- [31] M. Duarte and A. Sabharwal, “Full-duplex wireless communications using off-the-shelf radios: Feasibility and first results,” in *2010 Conference Record of the Forty Fourth Asilomar Conference on Signals, Systems and Computers (ASILOMAR)*. IEEE, 2010, pp. 1558–1562.
- [32] Y. Hua, P. Liang, Y. Ma, A. C. Cirik, and Q. Gao, “A method for broadband full-duplex mimo radio,” *IEEE Signal Processing Letters*, vol. 19, no. 12, pp. 793–796, 2012.
- [33] M. Jain, J. I. Choi, T. Kim, D. Bharadia, S. Seth, K. Srinivasan, P. Levis, S. Katti, and P. Sinha, “Practical, real-time, full duplex wireless,” in *Proceedings of the 17th annual international conference on Mobile computing and networking*. ACM, 2011, pp. 301–312.

- [34] M. E. Knox, “Single antenna full duplex communications using a common carrier,” in *2012 IEEE 13th Annual Wireless and Microwave Technology Conference (WAMICON)*. IEEE, 2012, pp. 1–6.
- [35] T. Riihonen, S. Werner, and R. Wichman, “Mitigation of loopback self-interference in full-duplex mimo relays,” *IEEE Transactions on Signal Processing*, vol. 59, no. 12, pp. 5983–5993, 2011.
- [36] P. Lioliou, M. Viberg, M. Coldrey, and F. Athley, “Self-interference suppression in full-duplex mimo relays,” in *2010 Conference Record of the Forty Fourth Asilomar Conference on Signals, Systems and Computers (ASILOMAR)*. IEEE, 2010, pp. 658–662.
- [37] T. Riihonen, A. Balakrishnan, K. Haneda, S. Wyne, S. Werner, and R. Wichman, “Optimal eigenbeamforming for suppressing self-interference in full-duplex mimo relays,” in *2011 45th Annual Conference on Information Sciences and Systems (CISS)*. IEEE, 2011, pp. 1–6.
- [38] V. R. Cadambe and S. A. Jafar, “Interference alignment and degrees of freedom of the-user interference channel,” *IEEE Transactions on Information Theory*, vol. 54, no. 8, pp. 3425–3441, 2008.
- [39] O. El Ayach, S. W. Peters, and R. W. Heath Jr, “The feasibility of interference alignment over measured mimo-ofdm channels,” *IEEE Transactions on Vehicular Technology*, vol. 59, no. 9, pp. 4309–4321, 2010.
- [40] M. Kountouris and N. Pappas, “Hetnets and massive mimo: Modeling, potential gains, and performance analysis,” in *2013 IEEE-APS Topical Conference on Antennas and Propagation in Wireless Communications (APWC)*. IEEE, 2013, pp. 1319–1322.

- [41] K. Hosseini, J. Hoydis, S. Ten Brink, and M. Debbah, “Massive mimo and small cells: How to densify heterogeneous networks,” in *2013 IEEE International Conference on Communications (ICC)*. IEEE, 2013, pp. 5442–5447.
- [42] M. Goonewardena, X. Jin, W. Ajib, and H. Elbiaze, “Competition vs. cooperation: A game-theoretic decision analysis for mimo hetnets,” in *2014 IEEE International Conference on Communications (ICC)*. IEEE, 2014, pp. 2550–2555.
- [43] G. Scutari, D. P. Palomar, and S. Barbarossa, “Competitive design of multiuser mimo systems based on game theory: A unified view,” *IEEE Journal on Selected Areas in Communications*, vol. 26, no. 7, pp. 1089–1103, 2008.
- [44] A. C. Cirik, R. Wang, Y. Hua, and M. Latva-aho, “Weighted sum-rate maximization for full-duplex mimo interference channels,” *IEEE Transactions on Communications*, vol. 63, no. 3, pp. 801–815, 2015.
- [45] M. J. Osborne and A. Rubinstein, *A course in game theory*. MIT press, 1994.
- [46] S. U. Khan and I. Ahmad, “Non-cooperative, semi-cooperative, and cooperative games-based grid resource allocation,” in *20th International Parallel and Distributed Processing Symposium(IPDPS 2006)*. IEEE, 2006, pp. 10–pp.
- [47] A. Rapoport and A. M. Chammah, *Prisoner’s dilemma: A study in conflict and cooperation*. University of Michigan press, 1965, vol. 165.
- [48] R. Sugiura, Y. Kamamoto, N. Harada, H. Kameoka, and T. Moriya, “Optimal coding of generalized-gaussian-distributed frequency spectra for low-delay audio coder with powered all-pole spectrum estimation,” *IEEE/ACM Transactions on Audio, Speech, and Language Processing*, vol. 23, no. 8, pp. 1309–1321, 2015.
- [49] T. L. Marzetta, “Massive mimo: an introduction,” *Bell Labs Technical Journal*, vol. 20, pp. 11–22, 2015.



- [50] J. Wannstrom, “Lte-advanced,” *Third Generation Partnership Project (3GPP)*, 2012.
- [51] F. Rusek, D. Persson, B. K. Lau, E. G. Larsson, T. L. Marzetta, O. Edfors, and F. Tufvesson, “Scaling up mimo: Opportunities and challenges with very large arrays,” *IEEE Signal Processing Magazine*, vol. 30, no. 1, pp. 40–60, 2013.
- [52] B. Lee, J. Choi, J.-Y. Seol, D. J. Love, and B. Shim, “Antenna grouping based feedback compression for fdd-based massive mimo systems,” *IEEE Transactions on Communications*, vol. 63, no. 9, pp. 3261–3274, 2015.
- [53] E. Bjornson, M. Matthaiou, and M. Debbah, “Massive mimo with non-ideal arbitrary arrays: Hardware scaling laws and circuit-aware design,” *IEEE Transactions on Wireless Communications*, vol. 14, no. 8, pp. 4353–4368, 2015.
- [54] J. Park and Y. Sung, “On the pareto-optimal beam structure and design for multi-user mimo interference channels,” *IEEE Transactions on Signal Processing*, vol. 61, no. 23, pp. 5932–5946, 2013.
- [55] R. Rovatti, G. Mazzini, and C. Passerini, “Theoretic bounds to information transmission through electrical circuits,” *IEEE Transactions on Circuits and Systems I: Regular Papers*, vol. 60, no. 9, pp. 2474–2487, 2013.
- [56] S. Wang, Y. Li, M. Zhao, and J. Wang, “Energy-efficient and low-complexity uplink transceiver for massive spatial modulation mimo,” *IEEE Transactions on Vehicular Technology*, vol. 64, no. 10, pp. 4617–4632, 2015.
- [57] A. Lozano, R. W. Heath, and J. G. Andrews, “Fundamental limits of cooperation,” *IEEE Transactions on Information Theory*, vol. 59, no. 9, pp. 5213–5226, 2013.
- [58] P. Pal and P. Vaidyanathan, “Nested arrays: a novel approach to array processing with enhanced degrees of freedom,” *IEEE Transactions on Signal Processing*, vol. 58, no. 8, pp. 4167–4181, 2010.

- [59] —, “Nested arrays in two dimensions, part i: geometrical considerations,” *IEEE Transactions on Signal Processing*, vol. 60, no. 9, pp. 4694–4705, 2012.
- [60] A. Goldsmith, *Wireless communications*. Cambridge university press, 2005.
- [61] T. L. Marzetta, “Noncooperative cellular wireless with unlimited numbers of base station antennas,” *IEEE Transactions on Wireless Communications*, vol. 9, no. 11, pp. 3590–3600, 2010.
- [62] H. Q. Ngo, E. G. Larsson, and T. L. Marzetta, “Energy and spectral efficiency of very large multiuser mimo systems,” *IEEE Transactions on Communications*, vol. 61, no. 4, pp. 1436–1449, 2013.
- [63] L. Dai, “An uplink capacity analysis of the distributed antenna system (das): from cellular das to das with virtual cells,” *IEEE Transactions on Wireless Communications*, vol. 13, no. 5, pp. 2717–2731, 2014.
- [64] C.-X. Wang, F. Haider, X. Gao, X.-H. You, Y. Yang, D. Yuan, H. Aggoune, H. Haas, S. Fletcher, and E. Hepsaydir, “Cellular architecture and key technologies for 5g wireless communication networks,” *IEEE Communications Magazine*, vol. 52, no. 2, pp. 122–130, 2014.
- [65] Q.-U.-A. Nadeem, A. Kammoun, M. Debbah, and M.-S. Alouini, “3d massive mimo systems: modeling and performance analysis,” *IEEE Transactions on Wireless Communications*, vol. 14, no. 12, pp. 6926–6939, 2015.
- [66] S. Wu, C.-X. Wang, E.-H. M. Aggoune, M. M. Alwakeel, and Y. He, “A non-stationary 3-d wideband twin-cluster model for 5g massive mimo channels,” *IEEE Journal on Selected Areas in Communications*, vol. 32, no. 6, pp. 1207–1218, 2014.
- [67] R. Itu, “{ITU-R M. 2135: Guidelines for evaluation of radio interface technologies for IMT-Advanced},” 2008.

- [68] A. Jassal, H. Khanfir, and S. Martinez Lopez, “Preliminary system-level simulation results for the 3gpp 3d mimo channel model,” in *2014 IEEE 80th Vehicular Technology Conference (VTC Fall)*. IEEE, 2014, pp. 1–5.
- [69] A. Kuchar, J.-P. Rossi, and E. Bonek, “Directional macro-cell channel characterization from urban measurements,” *IEEE Transactions on Antennas and Propagation*, vol. 48, no. 2, pp. 137–146, 2000.
- [70] J. Fuhl, J.-P. Rossi, and E. Bonek, “High-resolution 3-d direction-of-arrival determination for urban mobile radio,” *IEEE Transactions on Antennas and Propagation*, vol. 45, no. 4, pp. 672–682, 1997.
- [71] X. Li, L. Li, and L. Xie, “Achievable sum rate analysis of zf receivers in 3d mimo systems.” *THIS*, vol. 8, no. 4, pp. 1368–1389, 2014.
- [72] M. Matthaiou, C. Zhong, M. R. McKay, and T. Ratnarajah, “Sum rate analysis of zf receivers in distributed mimo systems,” *IEEE Journal on Selected Areas in Communications*, vol. 31, no. 2, pp. 180–191, 2013.
- [73] S. Yuan and Q. Liang, “Cooperative bandwidth sharing for 5g heterogeneous network using game theory,” in *(submitted to )11th IEEE International Conference on Networking, Architecture, and Storage (NAS 2016)*. IEEE, 2016.
- [74] —, “Game theoretical method for sum-rate maximization in full-duplex massive mimo heterogeneous networks,” in *2015 IEEE 12th International Conference on Mobile Ad Hoc and Sensor Systems (MASS)*. IEEE, 2015, pp. 610–615.
- [75] —, “Game theoretical method for sum-rate maximization in full-duplex massive mimo heterogeneous networks,” in *(accepted by )Signal Processing*, 2016.
- [76] —, “To achieve massive mimo with much less antennas by nested placement,” in *(accepted by )IEEE INFOCOM 2016, 5G Workshop*. IEEE, 2016.

- [77] —, “3d nested distributed massive mimo: modeling and performance analysis,” in *(submitted to )Ad Hoc Networks Special Issue on Hybrid Wireless Networks*. Elsevier, 2016.
- [78] M. Huang and W. Xu, “Macro-femto inter-cell interference mitigation for 3gpp lte-a downlink,” in *2012 IEEE Wireless Communications and Networking Conference Workshops (WCNCW)*. IEEE, 2012, pp. 75–80.
- [79] Q. Inc., *Importance of serving cell selection in heterogeneous networks*. 3GPP, Jan. 2010.
- [80] M. Cui, B.-J. Hu, X. Li, and H. Chen, “A novel power control algorithm for massive mimo cognitive radio systems based on game theory,” in *2015 IEEE 81st Vehicular Technology Conference (VTC Spring)*. IEEE, 2015, pp. 1–5.
- [81] Q. Wu and Q. Liang, “Increasing capacity of multi-cell cooperative cellular networks with nested deployment,” in *2015 IEEE International Conference on Communications (ICC)*. IEEE, 2015, pp. 4647–4652.

## BIOGRAPHICAL STATEMENT

Shitong Yuan was born in ChangSha, China, in 1990. He received his B.S. degree from University of Electrical Science and Technology of China, in 2012, his Ph.D. degrees from The University of Texas at Arlington in 2016, respectively, all in Electrical Engineering. From 2014 to 2016, he was with the department of Electrical Engineering, University of Texas at Arlington as a Teaching Assistant for several courses. In 2013, he joined Broadcom Crop. as an internship for the LTE testing. His current research interest is in the area of optimization in wireless communication and 5-th generation cellular system.